PB85-114023

Ultraviolet Disinfection of a Secondary Effluent: Measurement of Dose and Effects of Filtration

North Carolina Univ. at Chapel Hill

Prepared for

Municipal Environmental Research Lab.
Cincinnati, OH

Oct 84

U.S. Department of Commerce
National Technical Information Service
NTIS

PB85-114023

EPA-600/2-84-160
October 1984

ULTRAVIOLET DISINFECTION OF A SECONDARY EFFLUENT

Measurement of Dose and Effects of Filtration

by

J. Donald Johnson
Robert G. Qualls
University of North Carolina
Chapel Hill, North Carolina 27514

6 1/2"
9-1/8"

Grant No. R 804770010

Project Officer

Albert D. Venosa
Wastewater Research Division
Municipal Environmental Research Laboratory
Cincinnati, Ohio 45268

MUNICIPAL ENVIRONMENTAL RESEARCH LABORATORY
OFFICE OF RESEARCH AND DEVELOPMENT
U.S. ENVIRONMENTAL PROTECTION AGENCY
CINCINNATI, OHIO 45268

BEGIN LAST LINE OF TEXT
3/8"
BOTTOM OF IMAGE AREA OUTSIDE DIMENSION FOR TABLES AND ILLUSTRATIONS
PAGE NUMBER
EPA Form 2350-6 (4-80)
(PREVIOUSLY CIN. EPA FORM 237)
© U.S. GOVERNMENT PRINTING OFFICE: 1980-660-730
TYPING GUIDE SHEET

REPRODUCED BY
NATIONAL TECHNICAL
INFORMATION SERVICE
U.S. DEPARTMENT OF COMMERCE
SPRINGFIELD, VA. 22161

TECHNICAL REPORT DATA

(Please read Instructions on the reverse before completing)

1. REPORT NO. EPA-600/2-84-160	2.	3. RECIPIENT'S ACCESSION NO. PB85 114023
4. TITLE AND SUBTITLE "Ultraviolet Disinfection of A Secondary Effluent: Measurement of Dose and Effects of Filtration"		5. REPORT DATE October 1984 6. PERFORMING ORGANIZATION CODE
7. AUTHOR(S) J. D. Johnson and R. G. Qualls		8. PERFORMING ORGANIZATION REPORT NO.
9. PERFORMING ORGANIZATION NAME AND ADDRESS University of North Carolina Environmental Science and Engineering Department Chapel Hill, North Carolina 27514		10. PROGRAM ELEMENT NO. CAZB1B 11. CONTRACT/GRANT NO. R 804770
12. SPONSORING AGENCY NAME AND ADDRESS Municipal Environmental Research Laboratory--Cin.,OH Office of Research and Development U.S. Environmental Protection Agency Cincinnati, Ohio 45268		13. TYPE OF REPORT AND PERIOD COVERED Final 14. SPONSORING AGENCY CODE EPA/600/14

15. SUPPLEMENTARY NOTES

Project Officer: A. D. Venosa (513) 684-7668

16. ABSTRACT

Ultraviolet (UV) disinfection of wastewater secondary effluent was investigated in a two-phase study to develop methods for measuring UV dose and to determine the effects of filtraton on UV disinfection. The first phase of this study involved a pilot plant study comparing filtration, water quality parameters, and two reactors. The pilot plant study led to laboratory experiments involving: (1) the development of a method for in situ measurement of intensity using a calibrated bioassay, (2) experimental verification of a method for calculating intensities, (3) evaluation of the role of lamp spacing in dose efficiency, and (4) simulation of UV disinfection in continuous flow.

A bioassay method was developed to measure average dose rate (i.e., intensity) within a UV reactor. The survival of Bacillus subtilis spores was determined as a function of UV dose to calibrate the sensitivity of the spores. Spores were added to unknown systems, and the survival used to determine the average dose rate. Results from the pilot experiments showed spectrophotometric measurements significantly overestimated the UV absorbance in wastewater because of scattering. A method to correct for scattering was tested. A method for simulating survival in complex flowthrough reactors was presented, and a simulation of pilot plant runs corresponds reasonably well with the observed survival. Mixed media filtration significantly improved disinfection in pilot plant experiments. A laboratory experiment showed that a relatively small number of coliforms were protected inside particles, but they were the factor limiting disinfection at -3 or -4 logs of survival.

17. KEY WORDS AND DOCUMENT ANALYSIS

a. DESCRIPTORS	b. IDENTIFIERS/OPEN ENDED TERMS	c. COSATI Field/Group

18. DISTRIBUTION STATEMENT RELEASE TO PUBLIC	19. SECURITY CLASS *(This Report)* UNCLASSIFIED	21. NO. OF PAGES 126
	20. SECURITY CLASS *(This page)* UNCLASSIFIED	22. PRICE

EPA Form 2220-1 (Rev. 4-77) PREVIOUS EDITION IS OBSOLETE

DISCLAIMER

Although the information described in this document has been funded wholly or in part by the United States Environmental Protection Agency through assistance agreement number R-804770 to the University of North Carolina, Chapel Hill, it has not been subjected to the Agency's required peer and administrative review and therefore does not necessarily reflect the views of the Agency and no official endorsement should be inferred.

6-1/2"
9-1/8"
BEGIN LAST LINE OF TEXT
3/8"
BOTTOM OF IMAGE AREA: OUTSIDE DIMENSION FOR TABLES AND ILLUSTRATIONS

FOREWORD

The U. S. Environmental Protection Agency was created because of increasing public and government concern about the dangers of pollution to the health and welfare of the American people. Noxious air, foul water, and spoiled land are tragic testimonies to the deterioration of our natural environment. The complexity of that environment and the interplay of its components require a concentrated and integrated attack on the problem.

Research and development is that necessary first step in problem solution; it involves defining the problem, measuring its impact, and searching for solutions. The Municipal Environmental Research Laboratory develops new and improved technology and systems to prevent, treat, and manage wastewater and solid and hazardous waste pollutant discharges from municipal and community sources, to preserve and treat public drinking water supplies, and to minimize the adverse economic, social, health, and aesthetic effects of pollution. This publication is one of the products of that research and provides a most vital communications link between the researcher and the user community.

This report reflects concern over the environmental effects of chlorination disinfection of wastewater. Evidence that chlorine residuals or by-products are toxic to aquatic life and may result in formation of carcinogenic compounds has prompted this research into economical alternatives for disinfection.

Francis T. Mayo, Director
Municipal Environmental Research
Laboratory

BEGIN LAST LINE OF TEXT
BOTTOM OF IMAGE AREA OUTSIDE DIMENSION FOR TABLES AND ILLUSTRATIONS
3/8"

ABSTRACT

The first phase of this study involved an ultraviolet (UV) disinfection pilot plant study comparing: filtration, water quality parameters, and two reactors. The pilot plant study directed us to laboratory experiments involving: (1) the development of a method for *in situ* measurement of dose rate using a calibrated bioassay, (2) experimental verification of a method for calculating dose rates, (3) evaluation of the role of lamp spacing in dose efficiency, and (4) simulation of UV disinfection.

A bioassay method was developed to measure average dose rate (i.e., intensity) within a UV reactor. The survival of spores of *Bacillus subtilus* was determined as a function of UV dose in order to "calibrate" the sensitivity of the spores. Spores were added to unknown systems and the survival could be used to determine the average dose rate. A modification was used for flowthrough reactors, in which spores were injected as a spike and collected at a known time from injection.

Spectrophotometric measurements were found to significantly overestimate the UV absorbance in wastewater because of scattering. A method to correct for scattering was tested. A point-source summation method for calculation of dose rate was verified by bioassay measurements in a simple cylinder. This calculation method was also applied to multiple lamp reactors. A method for simulating survival in complex flowthrough reactors was presented and a simulation of our pilot plant runs corresponded reasonably well with the observed survival. Mixed media filtration significantly improved disinfection in pilot plant media experiments. A laboratory experiment showed that a relatively small number of coliforms were protected inside particles, but they were the factor limiting disinfection at -3 or -4 logs survival.

This report was submitted in fulfillment of Grant No. R 804770 by the University of North Carolina under the sponsorship of the U. S. Environmental Protection Agency. This report covers the period January 1977 to March 1980 and work was completed as of March 1980.

TABLE OF CONTENTS

Page

Foreword iii
Abstract iv
Figures viii
Tables xi
Acknowledgements xiii
1. Introduction 1
2. Conclusions. 2
3. Recommendations for Further Research 4

4. Literature Review

Inactivation of Microorganisms by Ultraviolet Light. 6
Kinetics of Inactivation 8

Measurement of UV Dosage

Measurement of output and incident intensity (I_o) 10
Dose rate distribution around a linear source 12
Flow characteristics and dose 14
Lamp spacing and dose 16
Absorbance and Scattering. 16

Disinfection of Water and Wastewater

Disinfection of natural water 22
Disinfection of wastewater effluents. 23
Photoreactivation. 25

5. Materials and Methods

Pilot Plant Experiments

Pilot plant design. 26
The disinfection units. 26
Pilot plant methods 28
Analysis of samples 29
Virus seeding experiments 30
Photoreactivation 30
Flow distribution studies 30
Potassium ferrioxalate actinometry. 31

BEGIN FIRST LINE OF TEXT HERE
CENTER OF PAGE
TOP OF IMAGE AREA
DROPPED HEAD. BEGIN SECTIONS HERE
6-1/2"
9-1/8"
BEGIN LAST LINE OF TEXT
BOTTOM OF IMAGE AREA OUTSIDE DIMENSION FOR TABLES AND ILLUSTRATIONS
3/8"
PAGE NUMBER
EPA Form 2350-4 (4-80)
(PREVIOUSLY CIN. EPA FORM 267)
☆ U.S. GOVERNMENT PRINTING OFFICE 1980-660-639
TYPING GUIDE SHEET

Growth of E. coli cultures 31
Irradiation of E. coli in tap water in the UV reactors 32

Experimental Work

Measurements of UV output at 254 nm. 33
Collimated beam irradiation apparatus. 34
Bacillus subtilis spore preparation. 35
Calibration of Bacillus subtilus as a bioassay for UV dose . . 37
Fulvic acid as an absorber 37
Cylindrical irradiation apparatus. 38
Flowthrough irradiation experiments. 40

6. Results and Discussion

Pilot Plant Results and Discussion

Summary of pilot plant results 41
Effects of filtration on disinfection and UV absorbance. . . . 41
Effects of water quality parameters on coliform survival . . . 43
Prediction of spectrophotometric UV absorbance from water quality parameters 47
Poliovirus inoculation results 49
Photoreactivation results. 49

Estimation of Dose in Pilot Plant Experiments

Summary. 52
Dye studies of retention time. 52
In situ estimations of UV output and dose. 55

Laboratory Experimental Results and Discussion

Separating effects of absorbance and scattering. 61
Summary. 61
Results. 62

Calculation and Measurement of Dose Rate around a Cylindrical Source

Summary. 74
Results. 74

Effects of Fluid Depth and Lamp Spacing on Efficient Use of UV Light

Summary. 80
Results. 81
Interference by neighboring lamps. 83

7. Summary Discussion

Dose Rate Measurement

Bioassay method. 90
Low absorbance actinometry 90
Separating Effects of Absorbance and Scattering of UV Light . . . 91

Calculation and Simulation of Dose

Point source summation technique 92
Comparison to other methods of calculation used in other studies. 93
Multiple lamp systems. 94
Exposure time and non-ideal flow 95

BEGIN FIRST LINE OF TEXT HERE
CENTER OF PAGE
TOP OF IMAGE AREA
DROPPED HEAD; BEGIN SECTIONS HERE
BEGIN LAST LINE OF TEXT
BOTTOM OF IMAGE AREA; OUTSIDE DIMENSION FOR TABLES AND ILLUSTRATIONS
3/8"
PAGE NUMBER
EPA Form 2360-4 (4-80)
(PREVIOUSLY CIN. EPA FORM 287)
U.S. GOVERNMENT PRINTING OFFICE 1980-660-738
TYPING GUIDE SHEET

Lamp Spacing and Efficient Use of UV Light 97
Protection of Coliforms by Particles of Various Sizes and the Effects of Filtration. 98
    Simulation of average survival in a flowthrough reactor 102
    Recommendations 102
8. Literature Cited 106

6-1/2"
9-1/8"
BEGIN LAST LINE OF TEXT
3/8"
BOTTOM OF IMAGE AREA; OUTSIDE DIMENSION FOR TABLES AND ILLUSTRATIONS

FIGURES

Number — Page

1 Relative comparison of UV and chlorine disinfection requirements for indicator bacteria and pathogens (from Yip and Konasewitch, 1972). 7

2 Selected dose-survival curves from various sources. 9

3 Diagram illustration of the differences in planar energy flux density and 3-dimension energy flux density through a cross-section for an inactivation reaction. 11

4 Cylindrical reactor geometry for point source summation calculation. Modified from Jacob and Dranoff (1970) 13

5 Relative scattering from small and large particles as a function of angle. From Black and Hannah (1965). 18

6 Extrapolation method for separating true absorbance and scattering components. Autoclaved E. coli 20NTU solution shown as example. 20

7 The "specific correction method" for separating true absorance and scattering components using opalescent plate cuvettes . . . 21

8 The Aquafine unit 27

9 The Pure Water Systems unit 28

10 Method for determining UV output of tubular lamp. 34

11 Collimated beam apparatus 35

12 Cylindrical batch irradiation apparatus. 39

13 Δ turbidity (unfiltered-filtered) vs. Δ absorbance for only paired samples in pilot study of dual media filtration. 50

14 Photoreactivation; log survival of UV irradiated effluent total coliform exposed to 75 minutes of sunlight shown vs. log survival of the dark controls. 51

15 Aquafine unit dye studies at flow rate of 2.87 and 0.56 l/sec. . 53

9-1/8"
BEGIN LAST LINE OF TEXT
BOTTOM OF IMAGE AREA; OUTSIDE DIMENSION FOR TABLES AND ILLUSTRATIONS
3/8"

PAGE NUMBER
EPA-287 (Cin.)
(4-76)

Number | Page
16 PWS unit dye studies at flow rates of 2.04 and 0.56 l/sec . . . 54
17 Aquafine unit actinometry dosages vs. a) UV intensity at reactor wall and b) theoretical retention time. 56
18 Pure water systems unit actinometry dosages vs. a) UV intensity at reactor wall and b) theoretical retention time 57
19 Log reductions of *E. coli* vs. conventional dose 59
20 Log reductions of *E. coli* vs. actinometry dose. 60
21 *E. coli* B calibration curve, log survival vs. dose in collimated beam. 64
22 Log survival of *Bacillus subtilis* spores vs. UV dose in a collimated beam of known dose rate 65
23 *E. coli* B log survival in solutions of various turbidities (NTU) and depths in a collimated beam. Dose is calculated using the spectrophotometric absorbance 66
24 *E. coli* B log survival in solutions of various turbidities (NTU) and depths in a collimated beam. Dose calculated using extrapolation method to estimate true absorbance. 67
25 Absorption spectra of unfiltered (solid symbols) and .45 μ filtered (open symbols) Chapel Hill tertiary effluent measured in a Cary spectrophotometer. Spectra were measured in regular cells (circles) and in "opalescent plate" cells (triangles) which correct for forward scattering. 69
26 Spectrophotometric absorbance vs. absorbance measured by the bioassay method for a Chapel Hill tertiary effluent sample. . . 71
27 Effect of filtration on survival of total coliforms in Sandy Creek effluent 73
28 Dose rate at reactor mid-length vs. radial distance from the lamp axis 76
29 Average dose rate within a cylinder of radius R 77
30 Assay of average dose rate in 1.32 cm radius flowthrough tube by injection of spores and collection of separate fractions over time after injection. 79
31 Effectiveness of various fluid depths in cylinders of radius r around UV lamps 83

6-1/2"
BEGIN LAST LINE OF TEXT
BOTTOM OF IMAGE AREA, OUTSIDE DIMENSION FOR TABLES AND ILLUSTRATIONS
3/8"

PAGE NUMBER
EPA-287 (Cin.)
(4-76)

Number

Number		Page
32	Average seconds exposure per liter of fluid treated in cylinders of radius r needed to produce a log survival of -3 using *Bacillus* spores (ave. dose of 23.8 mW-sec/cm^2) for fluids of absorbances 0, .16 and .32.	85
33	Setup for approximate UV% transmission of lamp A through lamp B.	88
34	Comparison of methods for calculation dose rate profiles. . . .	99
35	Simulated average dose rate in Aquafine reactor as a function of absorbance of fluid.	103
36	Dose-survival curve for total coliforms in unfiltered Sandy Creek secondary effluent in a collimated beam	104

DROPPED HEAD. BEGIN SECTIONS HERE
6-1/2"
9-1/8"
BEGIN LAST LINE OF TEXT
BOTTOM OF IMAGE AREA; OUTSIDE DIMENSION FOR TABLES AND ILLUSTRATIONS
3/8"
PAGE NUMBER
EPA-287 (Cin.)
(4-76)

TABLES

Number

Number Page

1 Methods used for calculations of average dose rate in several studies. 15

2 Mean log total and fecal coliform MPN/100 ml in UV effluent for each treatment broken down by filtration status, disinfection unit, flow rate and applied voltage 42

3 Inactivation shown as mean -log survival of total and fecal coliforms in unfiltered and filtered secondary effluent, broken down by filtration status, disinfection unit, applied voltage, and flow rate. 43

4 The importance of independent variables in explaining variation in log survival of total and fecal coliforms; results of stepwise multiple regression 44

5 Correlations among water quality variables for the filtered and the unfiltered effluent. 45

6 Effects of filtration on mean water quality parameters and log survival of fecal coliforms in pilot plant study 46

7 Stepwise multiple regression of the effects of selected randomly varying water quality parameters on the UV absorbance (spectrophotometric) for unfiltered and filtered treatments. . 48

8 Survival of poliovirus (plaque forming units) inoculated into secondary effluent 50

9 Spectrophotometric absorbance of various fractions of Sandy Creek secondary effluent at 254 nm 62

10 Effect of .45 μ filtration on UV absorbance of synthetic turbidity standards 68

11 Separation of the soluble and particulate absorbance fractions and bioassayed absorbances by varying the particulate component and keeping a constant soluble fraction 70

12 Comparison of methods of measuring the true absorbance of a turbid 3° effluent (14 NTU) and the same sample 45 μ filtered (0.67 NTU) 72

BEGIN LAST LINE OF TEXT
3/8"
BOTTOM OF IMAGE AREA; OUTSIDE DIMENSION FOR TABLES AND ILLUSTRATIONS

Number Page

13 Test of adherence to Bunsen-Roscoe Law (reciprocity of time and intensity) in calculating dose in the time frame of the petri dish and cylinder experiments. 75

14 Effects of scattering and absorbance in a cylindrical reactor (3.82 cm radius) using the bioassay of average dose rate in a filtered and unfiltered (14 NTU) effluent sample. . . . 81

15 Effectiveness of various fluid depths in a collimated UV beam 82

16 Effectiveness of various fluid depths in cylinders surrounding UV lamps 84

17 Average seconds exposure needed per liter to treat fluid in cylinders of various radii 86

18 Effect of expanding lamp spacing and total volume of lamp array on the simulated dose at a constant flow rate using Pure Water Systems' design (from Scheible and Bassel (1981)) 87

19 Relative costs of designs using different lamp spacing (and total volume of unit) based on the Bergen County design. . . 89

20 Comparison of Aquafine and Pure Water Systems units. 100

21 Observed vs. simulated survival(s) of total coliforms in a Sandy Creek secondary effluent in a collimated beam. 104

BEGIN LAST LINE OF TEXT
3/8"
BOTTOM OF IMAGE AREA; OUTSIDE DIMENSION FOR TABLES AND ILLUSTRATIONS

PAGE NUMBER
EPA-287 (Cin.)
(4-76)

ACKNOWLEDGEMENTS

We appreciate the collaboration of Dr. Donald E. Francisco on the pilot plant phase of this project. Kent H. Aldrich and Thomas S. Wolfe collected much of the pilot plant data. The following three people contributed work as part of Master's theses. Kent Aldrich contributed the work on *in situ* use of actinometry. Michael P. Flynn did the work on use of *E. coli* to assay the effects of UV scattering. Marion E. Elliot did the work on photoreactivation. Others who contributed advice and assistance were Dr. D. Gordon Sharp , Douglas Van Osdell, Dr. John H. Jagger, and the staff of the Sandy Creek Treatment Plant in Durham, N. C. Special thanks go to Judy Via and Maggie Schimert for typing. We are indebted to the project officer Albert D. Venosa for his valuable support, advice and reviews.

SECTION 1

INTRODUCTION

Disinfection of wastewater effluents by chlorination is cheap and effective, but it has been shown to cause several environmental problems. Residuals and by-products can be toxic to aquatic life in receiving waters (Ward and DeGraeve 1978). They may result in formation of carcinogenic compounds (Piecuch 1974). In addition chlorination is much less effective at killing viruses than at killing bacteria (Cramer, et al. 1976). Two alternatives to chlorination for wastewater disinfection are ozone and ultraviolet light.

While pilot studies of UV disinfection have generally met disinfection goals, comparisons between studies are limited because there is no direct method of measuring ultraviolet doses, nor is there a substantiated method of calculating doses in the complicated geometries used. In addition, lack of dose measurement methods confounds the controlled evaluation of the effects of variables such as UV absorbance of the water, filtration and lamp spacing.

The first phase of this study involved a pilot plant study comparing: (1) two ultraviolet disinfection units employing different lamp spacing ("film depth"), (2) the effects of mixed media filtration, and (3) the effects of randomly varying water quality parameters. Experience from the pilot plant study directed us to the second laboratory experimental phase involving: (1) verification of the effects of filtration, (2) separation of the effects of absorbed and scattered light and its relation to spectrophotometrically measured absorbance, (3) evaluation of a method for calculating dosages, (4) methods for in situ measurement of UV dosages, and (5) evaluation of the role of film depth on efficiency of dosage.

SECTION 2

CONCLUSIONS

1. The Aquafine unit generally achieved levels of disinfection better than 200/100 ml fecal coliform. However, the Pure Water Systems unit performed poorly due to serious short circuiting of flow.

2. Dual media filtration resulted in significantly better disinfection at the higher levels of disinfection in the pilot plant studies. Lab experiments confirmed that at the higher levels of disinfection, most survivors are associated with particles and are protected, showing relatively little response to increased UV doses. Thus at high levels of disinfection, further disinfection is limited mainly by the number of particle protected organisms.

3. Because of the non-linear relationship between survival and dose, dispersion of flow severely limits dinfection efficiency. Poor flow characteristics proved more important in the pilot plant commercial UV units than did changes in flow rate and UV intensity (dose rate).

4. Water quality parameters did not give consistently significant prediction of coliform survivals in the pilot plant studies because of (a) a relatively narrow range of variation in UV absorbance and (b) the relatively low dose response due to the protected survivors and poor flow characteristics.

5. In pilot plant studies, spectrophotometric UV absorbances were predicted best by coliform titers, or if these were not considered, by COD, turbidity and suspended solids.

6. Intensity measurements taken with a UV detector at the wall of the unit were of little value in determining UV dose.

7. Ferrioxalate actinometry overestimated UV output in *in situ* flowthrough measurements. A low absorbance modification of this method proved impractical.

8. Both *E.coli* B and a radiation resistant strain, B/r, proved too sensitive to provide an *in situ* assay of UV dose. However, *Bacillus subtilis* spores proved to be excellent organisms for a bioassay of UV dose when calibrated in a collimated UV beam of known intensity (dose rate). In batch studies, they showed approximate Chick's Law behavior.

9. The UV output of a lamp may be measured by a spherical integration of intensities measured at least two lamp lengths away. The biologically effective intensity (dose rate) cannot be measured with the common radiometer near the lamp surface because it does not measure the 3-dimensional dose rate. The UV rays which come in from angles are underestimated by a planar detector even if it is cosine corrected.

10. Bioassay studies in autoclaved *E. coli* turbid suspensions showed that scattered UV light continued to be an effective germicidal agent. Spectrophotometrically measured absorbance thus overestimates the attenuation of UV intensity with depth in turbid effluents because it includes both light removed by true absorption and light scattered away from the detector.

11. A point source summation model for calculation of dose rate (i.e., intensity) around a tubular UV lamp was verified by bioassay experiments. Calculations must include radial spreading and true absorbance of light from each segment of lamp along the lamp length separately. Previous attempts to calculate dose rate have not incorporated one or more of the above factors. Methods are presented for calculation of average dose rate in a multiple lamp reactor.

12. A successful bioassay method was developed for doses of up to 30 mW-sec/cm^2 in a flowthrough UV reactor. This method can be used to measure average dose rate when the retention time is known.

13. The trade-off between lower average dose rate (i.e., intensity) and greater volume with increased fluid depth favors "thick film" lamp configurations. However, flow dispersion characteristics must be considered in this trade off.

14. Neighboring lamps were shown to absorb most of the UV light striking them, thus decreasing the efficient use of light in closely spaced lamp configurations. This decreased efficiency of the thin film systems was simulated for the N. W. Bergen County, N. J. reactor design. Lamp spacings two to three times the 3.55 cm spacing used in the Bergen County design would be optimum depending on relative lamp costs if flow dispersion characteristics were constant.

BEGIN LAST LINE OF TEXT
3/8"
BOTTOM OF IMAGE AREA; OUTSIDE DIMENSION FOR TABLES AND ILLUSTRATIONS

4

SECTION 3

RECOMMENDATIONS FOR FURTHER RESEARCH

Three areas on a practical engineering level have prevented the efficient application of UV disinfection to water and wastewater in a wide range of conditions.

a) Insufficient and/or incorrect methods of evaluating UV dose by calculation or measurement under conditions of non-ideal flow in absorbing solutions make literature data difficult to interpret.

b) Inadequate design criteria and parameters, and their interaction, have hampered the development of efficient reactors.

c) Lack of dose response data under conditions of accurately known dosages has prevented prediction or control of disinfection as a function of dose rate (intensity), flow rate and flow non-ideality, effects of water quality parameters on dose rate, and organism type and degree of protection.

This report has developed methods and tested them in simple laboratory reactors for measuring and computing dose rate in adsorbing solutions, distributed retention times and developed a model for the calculation of true dose-survival curves.

The following additional work is needed to provide a rational basis for UV application in water and wastewater disinfection.

1. Determination of UV dose-survival data for coliform indicator and other important bacteria and viruses in equipment where dose can be accurately measured (such as in the calibrated collimated beam apparatus) and in natural effluent suspensions.

2. Development and testing of a very small radiometer detector with an opalescent plate which measures 3 dimensional dose rate for a hemispherical field in practical reactors.

3. Tests of the effects of lamp and reactor configurations on flow dispersion, dose rate-volume product and the trade-offs between these configurations, especially as a function of lamp spacing and fluid absorbance.

4. Test the point source summation model with the spore bioassay method in multiple lamp units first in smaller batch systems where non-ideal flow is not a problem and then in larger reactors using various designs and flow characteristics.

5. Measurement of the effects of particle protection for coliforms in effluents as a function of particle size so as to evaluate the importance of filtration and the level of filtration required.

6. Determination of UV and visible light dose-response data for photoreactivation in a wide variety of effluents and in receiving streams.

7. Comparison of MPN and membrane filtration techniques, with and without enrichment, for fecal and total coliform irradiated survivors.

BEGIN FIRST LINE OF TEXT HERE
CENTER OF PAGE
TOP OF IMAGE AREA
DROPPED HEAD; BEGIN SECTIONS HERE
6-1/2"
9-1/8"
BEGIN LAST LINE OF TEXT
3/8"
BOTTOM OF IMAGE AREA OUTSIDE DIMENSION FOR TABLES AND ILLUSTRATIONS
PAGE NUMBER
EPA Form 2350-4 (4-80)
(PREVIOUSLY CIR. EPA FORM 667)
☆ U.S. GOVERNMENT PRINTING OFFICE 1980-660-638
TYPING GUIDE SHEET

SECTION 4

LITERATURE REVIEW

INACTIVATION OF MICROORGANISMS BY ULTRAVIOLET LIGHT

Most microorganisms are inactivated by ultraviolet light, particularly between the wavelengths of 240 to 290 nm with peak activity around 265 nm (Gates 1930). This action spectrum corresponds closely with the absorption spectrum of deoxyribonucleic acid (DNA) and ribonucleic acid (RNA). The primary mechanism for inactivation is the dimerization of the pyrimidine bases, which blocks subsequent cell division or normal function (Setlow and Setlow 1962). Under some conditions this genetic damage may be undone, chiefly by two processes: (1) "dark repair", the enzymatic excision of the damaged area on the DNA strand, and (2) photoreactivation, the enzyme mediated reversal or prevention of the dimerization damage by light of longer wavelengths (Jagger 1958, 1967).

The sensitivity to UV inactivation may vary with the growth stage of the individual cell as well as certain other environmental conditions and among different species. Morton and Haynes (1969), using a radiation resistant strain of *Escherichia coli* B/r, found a high sensitivity to UV in the log phase of growth, an even higher sensitivity in the transition to stationary phase, and a relatively low sensitivity in the stationary phase. They explained this pattern of sensitivity in terms of the presence of repair enzymes and the effects of depletion of the medium on the repair capacity. Grunau (1978) explained sensitivity of rapidly growing bacteria in terms of the presence of active membrane-attached replication forks which could be unusually susceptible to damage. The nature of the medium on which the irradiated cells are plated can affect the number of damaged cells which survive and hence the apparent sensitivity. Irradiated cells held in non-nutritive liquid for several hours before plating may show greater survival rates because they have time to carry on dark repair before the chromosomes are stimulated to begin replication (Charles and Zimmerman 1956).

Variations in UV sensitivity may occur between species. The most important question from species comparisons is whether *Escherichia coli* is a useful indicator of the survival of pathogenic microorganisms. One advantage of UV over chlorine disinfection is the sensitivity of viruses to UV. The relative resistances of several species of microorganisms to UV and chlorine are summarized from several sources by Yip and Konasewich (1972) (Figure 1). Bacterial spores may be particularly resistant (Sharp 1938).

BEGIN FIRST LINE OF TEXT HERE
CENTER OF PAGE
TOP OF IMAGE AREA
DROPPED HEAD; BEGIN SECTIONS HERE
BEGIN LAST LINE OF TEXT
3/8"
PAGE NUMBER
BOTTOM OF IMAGE AREA; OUTSIDE DIMENSION FOR TABLES AND ILLUSTRATIONS
EPA Form 2350-4 (4-80)
(PREVIOUSLY CIN. EPA FORM 437)
U.S. GOVERNMENT PRINTING OFFICE: 1980-660-639
TYPING GUIDE SHEET

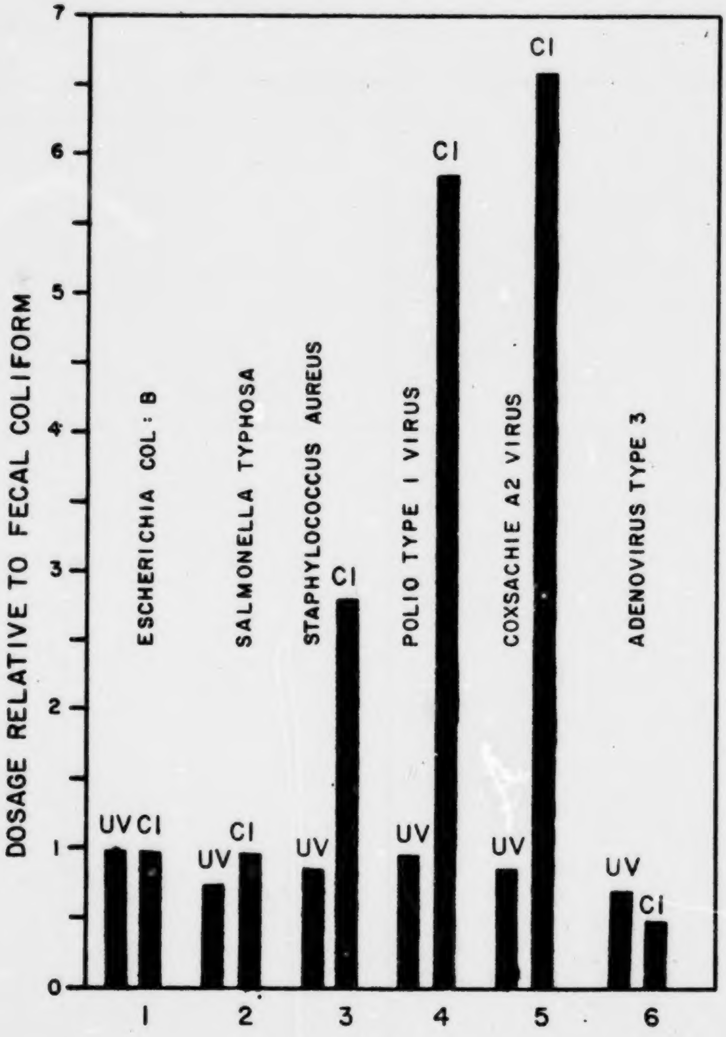

Fig. 1. Relative comparison of UV and chlorine disinfection requirements for indicator bacteria and pathogens (from Yip and Konasewitch, 1972).

BEGIN LAST LINE OF TEXT
3/8"
BOTTOM OF IMAGE AREA; OUTSIDE DIMENSION FOR TABLES AND ILLUSTRATIONS
PAGE NUMBER
EPA-287 (Cin.)
(4-76)

KINETICS OF INACTIVATION

As a first approximation, the number of organisms inactivated per unit of energy dose is proportional to the number remaining alive (Sharp 1938). This relationship may be expressed in the linear form:

$$1) \qquad \log \frac{N}{N_o} = -(k)\ (\mathrm{Dose})$$

where N_o is the density of organisms at time 0, N is the density of survivors, and k is a constant. The dose is the amount of energy striking a unit area of the object (e.g. cell) (Jagger 1967) and may be expressed with the indicated units

$$2) \qquad \mathrm{dose}\ (\mathrm{mW\text{-}sec/cm^2}) = \mathrm{intensity}\ (\mathrm{mW/cm^2}) \times \mathrm{time}\ (\mathrm{sec})$$

(where mW = 10^{-3} Watt). To avoid some ambiguities, the term dose rate is sometimes substituted for intensity (Jagger 1967). The reciprocity of time and dose rate in determining the inactivation response generally holds true but some exceptions have been found. Gates (1929) found that a very low dose rate (.056 mW/cm^2) yielded slightly less inactivation than a higher dose rate at a proportionally shorter exposure time for *S. aureus*. Powers, *et al*. (1973), using *B. megaterium* spores, showed a "dose rate dependence" only at dose rates below .03 mW/cm^2. These exceptions at long exposure times are regarded as the results of repair or photoreactivation occurring simultaneously with inactivation. No dose rate dependences have been reported at the relatively high dose rates likely in practical disinfection. Oliver and Cosgrove (1975), using effluent samples, found no dose-rate dependences when 1-200 mW/cm^2 dose rates were used.

While the linear dose-response curve may hold for a uniformly sensitive population inactivated by a "single hit", departures from linearity are frequent (Jagger 1967). Curves frequently show: (1) a "shoulder" in the initial (less than 1 or 2 log inactivation) part of the curve, usually attributed to the "multiple-hit" requirement for inactivation and subsequent repair of single lesions (Jagger 1967), and (2) a leveling off of response at relatively higher doses, usually attributed to the presence of a small number of more resistant (Jagger 1967) or protected cells (Oliver and Cosgrove 1975). Although the clearest way to plot dose-response curves is a semi-log plot, the leveling out of the curves for wastewater effluents has prompted Severin (1978) to use an empirical power transformation of the dose axis and Scheible and Bassel (1981) to use a log transformation in attempt to linearize their dose-response data. These authors wanted to linearize their data for predictive purposes and it should be realized that for the heterogenous wastewater microorganisms the underlying model is more likely to be a continuum of negative exponential processes, each having a different rate constant, k (equation 1).

Several dose-response curves from various studies are shown in Figure 2. These dose-response curves are impossible to compare strictly because the

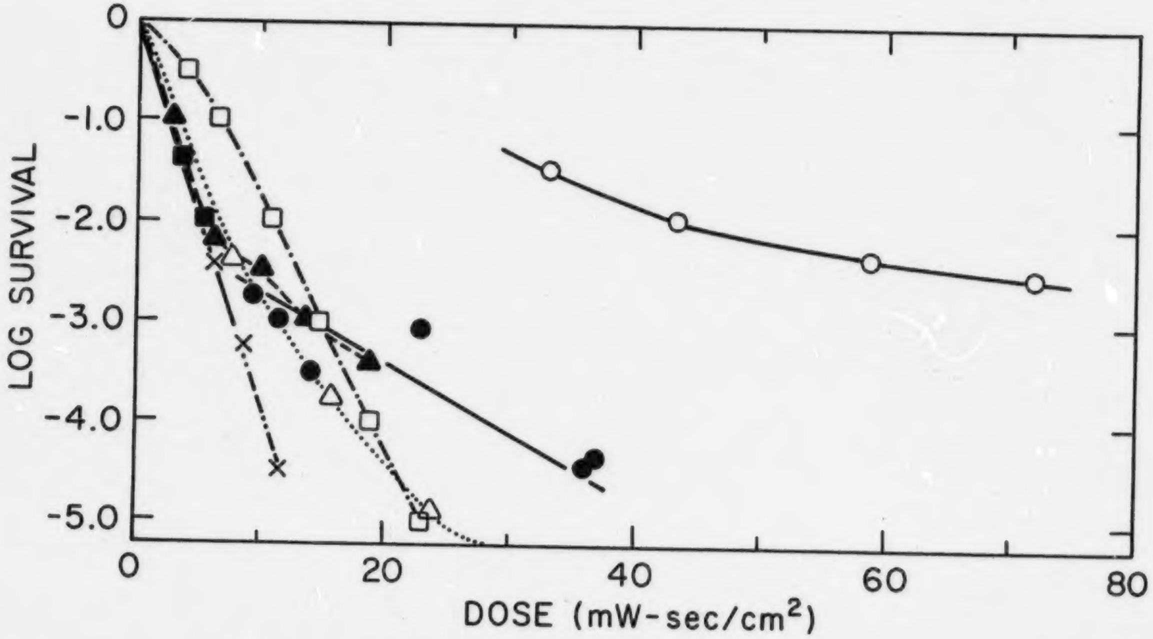

Fig. 2. Selected dose-survival curves from various sources

-o- Scheible and Bassel (1981), total coliforms, from regression line
-●- Petrasek, et al.(1981), total coliforms
.△. Roeber and Hoot (1975), coliforms, activated sludge effluent
-▲- This study, total coliforms, Sandy Creek 2° effluent
-·□-· Luckiesh and Holladay (1944), cultured *E. coli*
-■- Sharp (1938), *E. coli*
---·X---· This study, *E. coli* B/r

dose rates were measured or estimated in various ways. Similarities or differences may simply be artifacts of the method of dose estimation.

MEASUREMENT OF UV DOSAGE

Measurement of output and incident intensity (I_0)

The germicidal lamps used for disinfection are generally low pressure mercury vapor lamps in the form of long tubes. Approximately 33% of the energy input is emitted as light. About 80% of this is at the 254 nm wavelength and about 1% at other germicidal wavelengths. Other major lines occur at 313, 365, 405, 436 and 546 nm. The output at 254 nm varies with lamp age and temperature. Submerged lamps are surrounded with quartz tubes ("sleeves") to keep the temperature closer to optimum. Measurements of germicidal output should be made with a meter which measures a narrow band around the 254 wavelength,or a correction factor must be determined under known operating conditions since the 254 nm output is a variable fraction of the total light output (Jagger 1967).

"Cosine-corrected" radiometers measure planar energy flux density, i.e. the energy flux striking a flat surface of a given area (Figure 3). This surface will intercept a smaller amount of light coming in at an angle than if it were oriented normally to the rays. When the source rays are not collimated, as with the germicidal lamp, the appropriate measure of intensity for disinfection dosages is the energy flux density, i.e. three-dimensional energy flux density. For any population of randomly oriented particles, the cross section has an equal probability of being oriented in any direction (Roesch and Attix 1968). Thus in Figure 3 the light flux coming from the ends of the linear lamp is under-represented by the planar cross section oriented parallel to the lamp axis. It is unclear in most disinfection studies whether the incident intensity measured was 3-dimensional intensity or whether the planar intensity was measured. Using a detector measuring planar intensity near a germicidal lamp will lead to a large underestimation of the dose rate. To avoid this ambiguity, we shall use the term dose rate rather than intensity when three-dimensional energy flux density is intended.

The most direct way to measure total output of a cylindrical lamp is by integration of the intensity over a sphere centered on the lamp's midpoint (Barrows, 1951) (described in Methods). By measuring planar intensity far from the lamp the total energy flux density is approximated.

Another method of determining the output of the lamp is by potassium ferrioxalate actinometry (Hatchard and Parker 1956). When acid solutions of 0.006 M ferrioxalate are irradiated by light below about 577 nm wavelength the light is completely absorbed within a few millimeters and iron is reduced quantitatively to the Fe^{2+} ion while oxalate is oxidized. The quantum yield, the moles of Fe^{2+} per mole of photons absorbed by the solution, is so high (about 1.25 at 254 nm) that large quantities of Fe^{2+} are released with relatively small doses of light. The Fe^{2+} may then be analyzed spectrophotometrically by the phenanthroline (ibid.) or

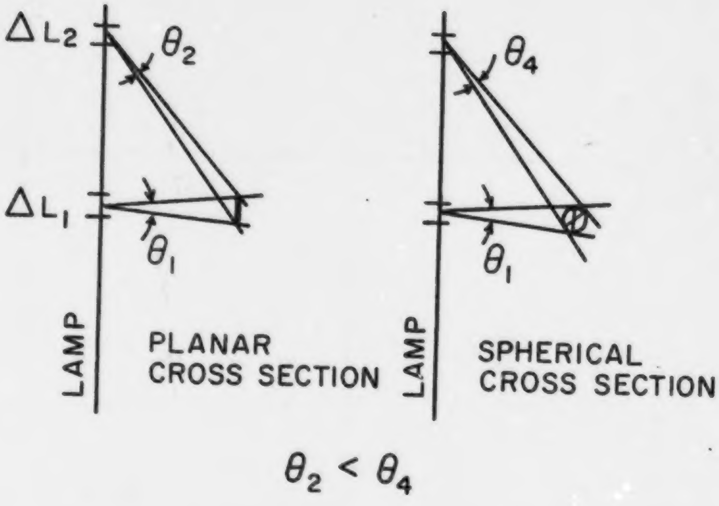

Fig. 3. Diagram illustration of the differences in planar energy flux density and 3-dimensional energy flux density through a cross-section for an inactivation reaction (eg. a nucleus, a locus) when the source is not collimated.

bathophenantroline (Knapp 1959) methods. The number of moles of Fe^{2+} may be converted to the energy absorbed by the solution,providing the wavelength distribution is known. In order to measure only the 254 nm output some correction factor must be determined for the other wavelengths (approximately 18% on a quantum basis,but variable). To measure output,the solution must surround the lamps.

The incident intensity, I_0, is the intensity at the surface of the solution of interest, in the case of most disinfection schemes, the outer surface of the quartz sleeve. In a collimated beam,a radiometer or a ferrioxalate solution may be used to measure I_0 (Jagger 1967). Scheible and Bassel (1981) calculated the I_0 at the surface of the quartz sleeve by dividing the output (W) by the surface area of the outside of the quartz sleeve (cm^2), yielding W/cm^2. This calculation yields an intensity related to the planar energy flux density since the surface area is oriented parallel to the lamp axis. We believe it yields an underestimate of the true dose rate at the surface of the quartz sleeve. I_0 may also be calculated by the more general technique of point source summation presented below.

Because of the problems of using planar detectors,no direct radiometric technique can measure dose rate distributions in an enclosed UV reactor. Calculation of the average dose rate in a stirred,absorbing, non-scattering

BEGIN LAST LINE OF TEXT
3/8"
PAGE NUMBER
BOTTOM OF IMAGE AREA, OUTSIDE DIMENSION FOR TABLES AND ILLUSTRATIONS
EPA Form 2350-4 (4-80)
(PREVIOUSLY CIN. EPA FORM 287)
U.S. GOVERNMENT PRINTING OFFICE 1980-
TYPING GUIDE SHEET

solution in a collimated beam is, however, a straightforward integration of the Beer-Lambert law over the depth of the liquid (Morowitz 1950):

3) $$I_{ave} = I_o \frac{1 - \exp(-a_e L)}{a_e L}$$

where I_{ave} is the average dose rate, I_o is the incident dose rate, a_e is the absorbance per cm (base e), and L is the path length (depth).

Dose rate distribution around a linear source

Given an infinitely long linear light source in a non-absorbing medium, the dose rate (I) is inversely proportional to the perpendicular (radial) distance R to the source. Thus,if the dose rate (I_1) at R_1 is known, the dose rate at R_2 may be calculated:

4) $$I_2 = I_1 \frac{R_2}{R_1}$$

The dose rate distribution around an ideal linear light source of finite length may be calculated by assuming the line segment consists of many point sources and the contribution from each may be summed over the length of the source. The technique of point source summation was presented in Rockwell (1956), and Kase and Nelson (1978), and was evaluated for light intensity profiles in a perfectly mixed photoreactor by Jacob and Dranoff (1970). We can consider a cylindrical coordinate system around a linear light source surrounded by a quartz sleeve (Fig. 4). The linear source of output OPT is divided into N point sources each of which has strength S (units in Watts).

5) $$S = OPT/N$$

The energy flux density at a point at distance Z_C along the cylinder and at radius R from the lamp due to a point source at distance Z_L along the lamp is a function of the spherical spreading of the rays over path P and the attenuation over path ($P-P_1$) due to absorbing medium.

6) $$I_{(Z_L),(R,Z_C)} = \frac{S}{4\pi P^2} e^{-a(P-P_1)}$$

The path length P may be put in terms of the coordinate system:

7) $$P^2 = R^2 + Z_{LC}^2 \quad \text{where } Z_{LC} = Z_L - Z_C$$

Using similar triangles,

8) $$P - P_1 = (R - R_1)\frac{P}{R}$$

BEGIN FIRST LINE OF TEXT HERE
CENTER OF PAGE
TOP OF IMAGE AREA
DROPPED HEAD; BEGIN SECTIONS HERE
6-1/2"
BEGIN LAST LINE OF TEXT
3/8"
BOTTOM OF IMAGE AREA; OUTSIDE DIMENSION FOR TABLES AND ILLUSTRATIONS
PAGE NUMBER
EPA Form 2350-4 (4-80)
(PREVIOUSLY CIN. EPA FORM 287)
☆ U.S. GOVERNMENT PRINTING OFFICE 1980-660-839
TYPING GUIDE SHEET

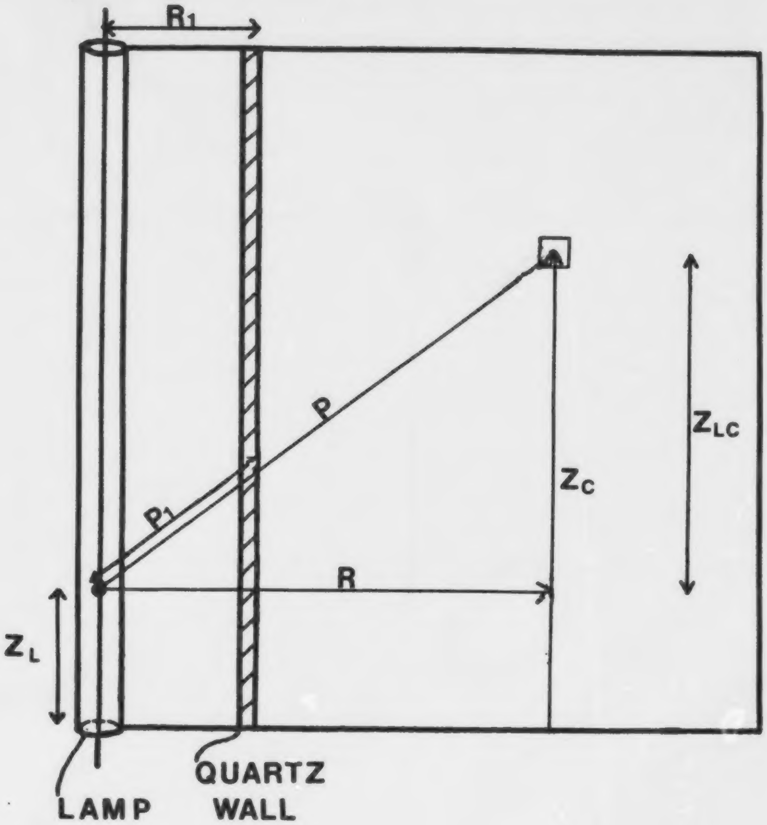

Fig. 4. Cylindrical reactor geometry for point source summation calculation. Modified from Jacob and Dranoff (1970).

The total energy flux density at point (Z_C, R) is the sum of the contributions of each point source at each Z_L over the source length:

$$I_{(R,\ Z_C)} = \sum_{Z_{L_N}}^{Z_{L_O}} I_{(Z_L),(R,\ Z_C)} \qquad (9)$$

Jacob and Dranoff also introduced an expression in the exponent of equation 6 to account for absorption in the glass wall separating the liquid from the air space. Reflection, refraction, and the finite diameter of the source lamp are ignored by this technique.

Some authors have used a combination of equation 4 and an assumption that the rays reaching a point in an absorbing solution undergo attenuation along a path length strictly perpendicular to the axis of the lamp ("radial light model") (Severin 1978; Scheible and Bassel 1979). The point source summation method takes into account the fact that light reaching a point in the solution is coming from various angles with different path lengths through the absorbing medium. Jacob and Dranoff, using a specially designed detector, compared the predictions of the point source summation and the radial light model and measurements of "intensity" profiles in an annular reactor with a lamp at the axis. The measurements of the intensity profiles deviated from both models at the mid-length of the reactor, but near the end of the reactor the point source summation was much closer to the measurements than the radial light model predictions in water. An empirical correction factor was applied which made the point source model predictions fit the data when an absorbing solution was added. The deviations were attributed to the finite size of the light source and the effects of refraction and reflection. The measurements were made with a very small probe using a photocell mounted beneath a quartz window. The intensity measured by this small probe was likely to have been planar energy flux density rather than energy flux density. Normally, probes must be fitted with a diffuser above the photocell to correct for the bias of the orientation of the cell surface (Westlake 1968). If the measurements were biased by the orientation of the cell the deviations may have been due to this factor.

The average dose rate within a submerged multiple lamp unit has been calculated by mapping the dose rate at various points on a cross section of the reactor and averaging the dose rates over the area outside the quartz sleeves (Petrasek, *et al*. 1980; Scheible and Bassel 1981). The dose rate at any one point was assumed to be the sum of the dose rate due to each lamp calculated by one of the previous methods. The effects of reflection off of walls and glass, and refraction were not considered. The shadowing effects of adjacent lamps and quartz sleeves may be taken into account.

The methods of calculation of the average dose rate used in several studies are summarized in Table 1. The calculation has been broken down into four steps: (1) the output of the sources, (2) the incident intensity, (3) the dose rate at one point due to one lamp, and (4) the average dose rate over the volume of the unit. In general these authors recognized the drawbacks of these methods and noted the need for an accurate method of calculation of dose rate.

Flow characteristics and dose

The flow characteristics of a given unit may affect both the exposure time and the dose rate to which various flow fractions are subjected. Dose rate gradients will exist in any unit and, ideally, the microorganisms should be well mixed across these gradients (usually perpendicular to the flow). Cortelyou, *et al*. (1954) found an increase in disinfection efficiency in one unit as baffles were added to increase mixing. On the other hand, longitudinal dispersion or short circuiting of the flow will decrease the disinfection efficiency since some flow fractions will receive less than the volumetric exposure time. Since the number of surviving organisms in the effluent is logarithmically related to the dose received, the effluent titer will be more or less limited by the first significant flow fraction to pass the unit when 4 or 5 logs of inactivation are desired. If a volume of water is able to traverse the disinfection unit in an area of low dose rate, the effluent titer will similarly be limited.

BEGIN FIRST LINE OF TEXT HERE
CENTER OF PAGE
TOP OF IMAGE AREA
DROPPED HEAD; BEGIN SECTIONS HERE
6-1/2"
9-1/8"

Table 1. Methods used for calculations of average dose rate in several studies.

Steps in Calculation of Dose Rate	Methods Used for Dose Rate Calculations
1. Output of source	1. a) rated output b) integration over sphere
2. Incident intensity	2. a) meter measurement b) output/surface area c) actinometry d) output and point source summation
3. Dose rate at a point due to one lamp	3. a) meter b) $I_1=I_o(R_1/R_o)$ c) attenuation of radial or parallel ray paths d) point source summation
4. Average dose rate in volume	4. a) integration of Beer-Lambert law over depth b) total I=sum I from each lamp c) map I at points on cross section d) assume it's same as incident intensity
5. Type of unit	5. a) suspended over liquid b) submerged

	Methods				
Authors	1*	2	3	4	5
Oliver and Cosgrove	-	c	-	d	a
Roeber and Hoot	-	a	a	a	a
Severin	-	-	b,c	-	b
Petrasek, *et al.*	-	a	b	b,c	b
Scheible and Bassel	a	b	b,c	b,c	b
This study	b	c,d	d	b,c	b

* Numbers correspond to the numbers in the section "Steps in Calculation of Dose Rate" above.

BEGIN LAST LINE OF TEXT
3/8"
BOTTOM OF IMAGE AREA; OUTSIDE DIMENSION FOR TABLES AND ILLUSTRATIONS

PAGE NUMBER
EPA Form 2350-4 (4-80)
(PREVIOUSLY EIN. EPA FORM 287)
☆ U.S. GOVERNMENT PRINTING OFFICE 1980-660-629
TYPING GUIDE SHEET

Lamp spacing and dose

In order to minimize the dose rate gradients in disinfection units in which highly absorbing liquids are flowing, some authors and designers have suggested placing the lamps close together and close to the wall. This scheme is sometimes referred to as the "thin film" design. This design produces high dose rates and allows for short exposure times. The alternative strategy "thick film" uses low dose rate and long exposure times. For a given number of lamps applied to a given flow rate of fluid, the close lamp spacing will occupy less volume and thus give shorter retention times than greater lamp spacing would allow. Opinions vary on the relative tradeoffs between these two design strategies. Oliver and Cary (1976) advocated a thin film system in which lamps were suspended over a flat weir. This strategy, however, was based on the dose rate of light in the bottom most layer of water passing over the weir. Thus, it was assumed that flow was stratified. Severin (1976) suggested that the expression he used for light intensity at various distances from the light source implies that the optimum design of UV disinfection units for wastewater effluents would utilize the thin film design. Severin's reasoning, however, ignored the fact that greater volumes of water occur in each radial increment as distance from the lamp increases, as well as the effects of mixing on the average dose rate within that volume. On the other hand, Luckiesh and Holladay (1944) pointed out: "Whenever practicable,the depth of water should be great enough so that most of the germicidal energy is absorbed in the water. Otherwise much of it is lost by absorption of the walls of the container. Few surfaces efficiently reflect the shortwave germicidal energy in the region of 2537 A°." They added that even otherwise efficient reflectors will accumulate deposits under use. Hoather (1955), speaking of relatively clear water, also noted that using a submerged lamp system,a "thick film" would be more efficient for these reasons if flow were well distributed. He pointed out that the product of intensity of radiation times volume at any moment would be much greater using a 6-inch space rather than a 1-inch space. Haas and Sakellaroupoulos (1979) derived a series of equations modeling intensity distributions and flow distributions in cylindrical UV reactors. Their derived results showed that even for typical absorption coefficients of wastewater, the thicker film design is more efficient when light is lost on the walls. The Bergen County reactor (Scheible and Bassel 1979) used a close lamp spacing but minimized loss to the walls by making the array of lamps large. In this sort of design the loss to the walls is minimized,but loss by absorption by neighboring lamps is important. The mercury vapor in neighboring lamps strongly absorbs the 254 nm light.

ABSORBANCE AND SCATTERING

Calculation of the average intensity requires the proper measure of absorption of the germicidal light. Most precision spectrophotometers exclude light scattered at more than a few degrees as the collimated beam passes through the sample. Thus, in solutions where scattering occurs, the measured spectrophotometric absorption is actually the sum of true absorption and scattering of light from the beam. Scattered light may remain as an effective germicidal agent in a practical disinfection unit, so it is essential to evaluate true absorption and scattering separately when spectrophotometric data are used to calculate intensities. This has not been generally recognized in the UV water treatment literature.

Compounds containing double bonds, especially conjugated double bonds, are the most important absorbers in the germicidal wavelengths. Among these are compounds containing benzene or heterocyclic rings. Both the aromatic amino acids and to a minor extent, the peptide bonds in proteins absorb in the far UV. Proteins show an absorption peak near 280 nm. Nucleic acid bases are very strong absorbers and in the germicidal region absorb 10 to 20 times as much as equal weights of protein. Since bacterial cells may contain about 20% nucleic acids and 70% protein dry weight, most of their absorption is usually due to nucleic acids. Humic acids also absorb strongly in the germicidal wavelengths. Most common inorganic materials likely to occur in wastewater are relatively unimportant (Jagger 1967). Iron salts may absorb at 254 nm but Huff(1965) found that concentrations up to 3 or 4 mg/l did not affect disinfection efficiencies. Huff also tested the effects of added color as tea and leaf extract. These interfered with transmission and disinfection at color levels above about 7 units.

We have not found any direct data on which compounds contribute the most to absorbance at 254 nm in wastewater effluents. There are data, however, on the composition of wastewater effluents. Bunch et al. (1961) defined about 35% of the soluble organics in several types of effluents. The fractions were defined as ether extractables, proteins, carbohydrates, polysaccharides, tannins and lignins, and alkyl benzene sulfonates. Rebhun and Manka (1974) classified the soluble organic content of a trickling filter plant secondary effluent. Among other fractions,they classified about 40-50% as humic substances and 11.7% as proteins (as a percentage of COD). Most of the humic fraction was classified as fulvic acids and most had molecular weights of less than 5000. Whether free nucleic acids or fragments occur in wastewater effluents in high enough concentrations to contribute to the absorbance at 254 nm is a question which needs attention.

The particulate and colloidal matter in wastewater effluents may be expected to both absorb and scatter germicidal light. The scattering and absorption of germicidal light in turbid cell suspensions has been reviewed by Jagger (1967). Rickert and Hunter (1972), and Dean et al.(1967) have shown that most of the colloidal and supracolloidal (solids of size 1-11 μ) matter in activated sludge effluent consists of bacterial flocs, cells, and fragments of cell walls. Thus,the scattering properties of cell suspensions may have much in common with that of wastewater effluents. A suspension of bacteria scatters light by several mechanisms: small particle (Rayleigh) scattering, large particle scattering, fluorescence and refraction. Much more light is scattered in the forward (away from source) direction. Figure 5 (Black and Hannah 1965) illustrates the scattering intensities from small and large particles as a function of angle. The angular distribution of scattered light is important in disinfection applications because it influences the proportion of scattered light detected by a spectrophotometer and the path length the scattered light travels through the absorbing solution.

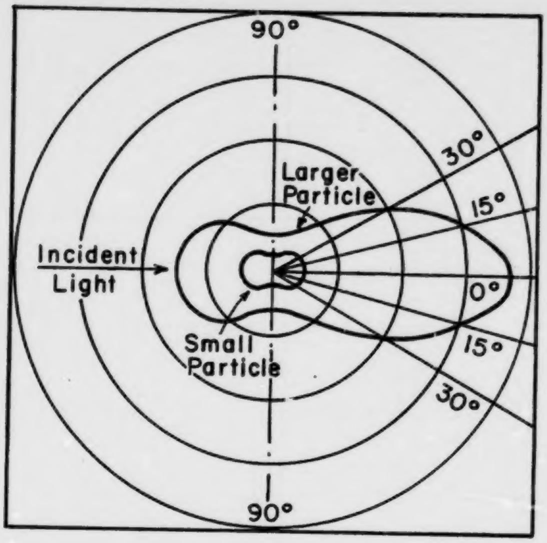

Fig. 5. Relative scattering from small and large particles as a function of angle. From Black and Hannah (1965).

Several methods have been presented for separating absorption from scattering in turbid suspensions (summarized by Jagger 1967): (1) summing of intensity distributions around a sample, (2) the extrapolation method, (3) using a detector which intercepts a wide angle in a spectrophotometer beam, and (4) the opalescent-plate and specific-correction technique. The first method is the most direct but is very difficult. Calkins (1965) used a specially assembled device to measure the absorption and scattering of visible and UV light by suspensions of protozoa. He realized that the light scattered from the beam would still contribute to the germicidal dose. He measured the transmission of a collimated beam through a small quartz cylinder containing the sample at several angles around the cuvette. Water surrounded the cuvette to minimize refraction effects. Scatter appeared to account for the loss of light from the direct beam at visible wavelengths but true absorption became more important in the germicidal region.

The extrapolation method requires an absorbance scan with a spectrophotometer from a wavelength region where it is known that there is no true absorption into and below the germicidal wavelengths. The spectrophotometric absorbance is treated as the sum of a true absorbance component and a scattering component. The scattering coefficient (p) is assumed to vary as an inverse power of the wavelength:

11) $p = K\lambda^{-n}$

where n and K are constants. The log of the spectrophotometer absorbance

BEGIN LAST LINE OF TEXT
3/8"
BOTTOM OF IMAGE AREA: OUTSIDE DIMENSION FOR TABLES AND ILLUSTRATIONS

is plotted against the log of the wavelength. The line in the region where only scatter is important is extrapolated (Fig. 6). The spectrophotometric absorbance at the point where the line crosses the desired wavelength is regarded as the scattering component and the remainder as the true absorbance (Jagger 1967). Jagger warns that this method is "at best" a rough correction. It makes several assumptions which are difficult to verify. Koch (1961) found that the log-log plot of absorbance vs. wavelength was linear between wavelengths 350 and 800 nm for a suspension of _E. coli_. Bitton _et al_. (1972) used this method to separate absorption and scattering to compare the relative doses to _Klebsiella aerogenes_ exposed to 254 nm light in suspensions of clays and a humic acid solution. They found the survival to be correlated with the "specific absorbance" (corrected for scattering) rather than the spectrophotometer absorbance for the clay suspensions. The method was not used for the humic acid solution. Several of the clays showed mainly scattering and very little specific absorbance at 254 nm.

Jagger _et al_. (1975) compared the "effective optical density" of solutions of _E. coli_ B/r to values for average dose calculated from the absorbance measured on a narrow slit (Cary 14) spectrophotometer and an Aminco-Chance Duochrometer in which a wide angle of the transmitted light is intercepted by the detector. The "effective optical density" was determined from survival of the bacteria over a range of cell concentrations and calculating the absorbance which would yield that survival using the Morowitz equation (see equation 3). The narrow beam spectrophotometer absorbance was about 3 times higher than the "effective optical density" while the Duochrometer yielded values very close to the effective optical density. The technique of using a detector which intercepts a large angle of the transmitted beam corrects only for forward scatter and does not account for wide angle scatter which misses the detector. The relative germicidal importance of the wide angle scattered light will depend on the geometry of the container.

Another method for including scattered light in measurements of transmitted light was suggested by Shibata _et al_. (1954) and used by Latimer and Eubanks (1962). It involves placing an opalescent plate, e.g. quartz ground so as to be translucent but not transparent, behind the sample in an ordinary spectrophotometer. Light scattered in the sample which strikes the back plate is then scattered again in the plate. This scattered light then has as much chance to pass the slit and be detected as light directly transmitted through the solution. Thus, when an opalescent surface is used with both the reference and sample cells the transmittance is "corrected" for _forward_ scatter. A modification of this method was used to correct for total scatter, the "specific correction method". A complete absorbance spectrum was run using both the normal cuvettes and the opalescent plate cuvettes (Fig. 7). A region of the spectrum was chosen in which there is no true absorption, only scattering(λ_0). There,the absorbance of the opalescent plate sample should be entirely due to wide angle scatter and the difference between the two curves is due to the forward scatter. A scattering correction (s) is calculated:

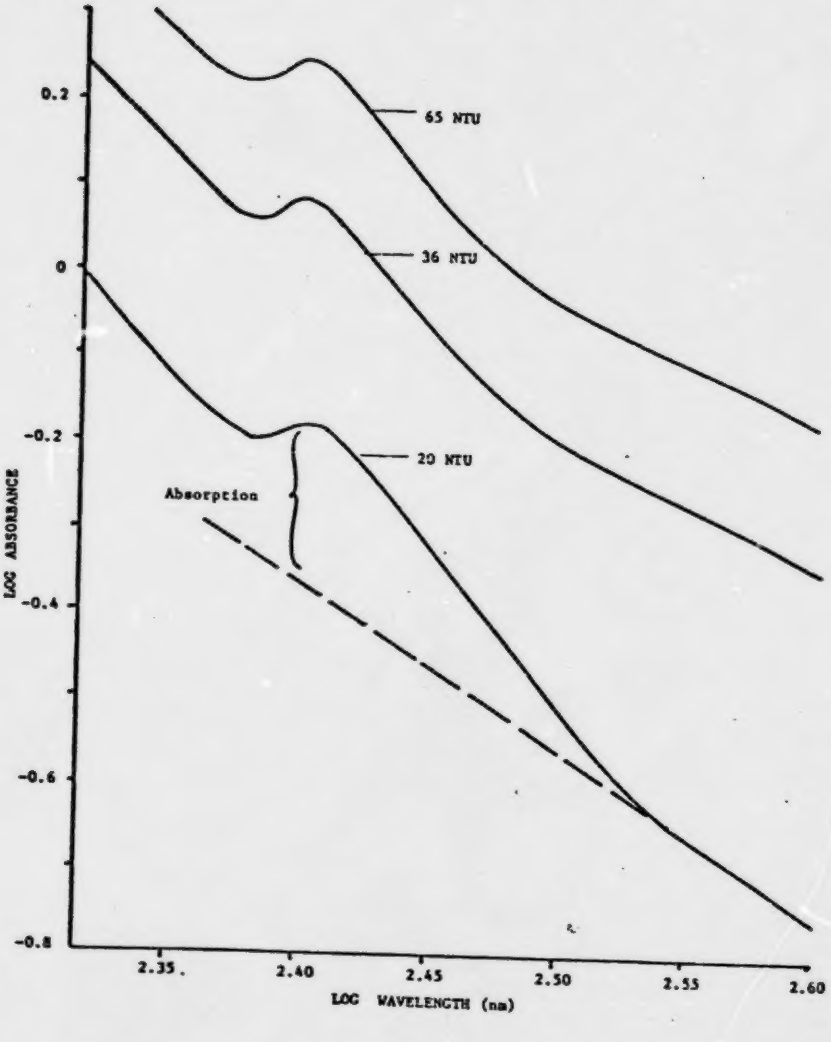

Fig. 6. Extrapolation method for separating true absorbance and scattering components. Autoclaved E. coli 20 NTU solution shown as example.

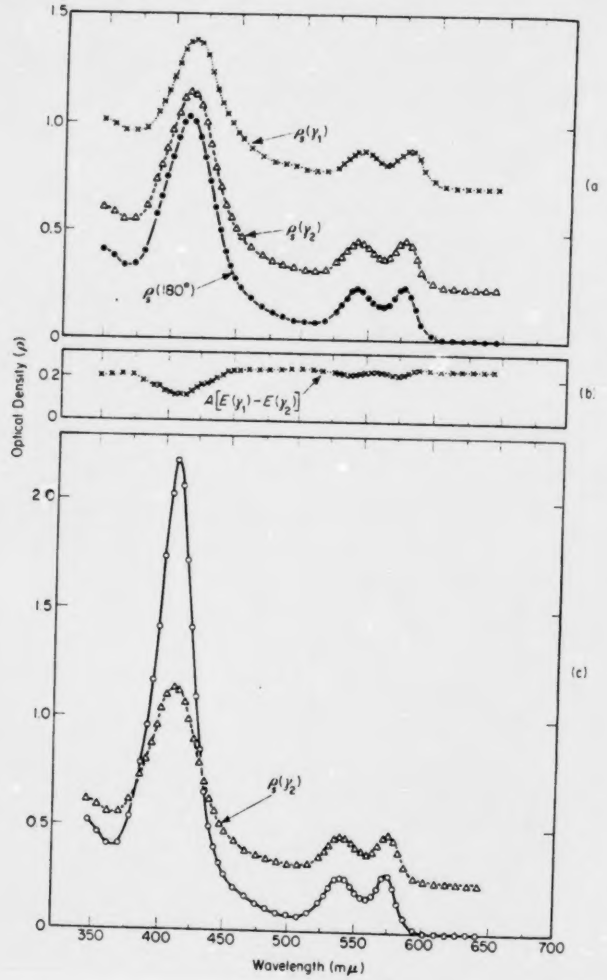

Fig. 7. The "specific correction method" for separating true absorbance and scattering components using opalescent plate cuvettes. (a) Absorption spectrum of a suspension of red blood cells, as measured in the normal way (top curve), as measured with opalescent plates (middle curve), and as calculated by making a specific correction for scattering bottom curve). (b) The scattering correction (see text) for the above suspension. (c) The absorption spectrum of the same suspension as measured with opalescent plates (triangles) and as corrected for both scattering and the seive effect (circles). (Latimer and Eubanks, 1962; reproduced from Jagger, 1967).

12) $$S = \frac{p_S(\gamma_2)}{p_S(\gamma_1) - p_S(\gamma_2)} \lambda_o$$

where $p_S(\gamma_1)$ and $p_S(\gamma_2)$ are the absorbances in the usual and opalescent plate cuvettes respectively at λ_o. The ratio of forward to total scatter is assumed to remain constant over the spectrum. Then the true absorbance p_S' is calculated at λ_2:

13) $$p_S' = p_S(\gamma_2) - S[p_S(\gamma_1) - p_S(\gamma_2)]$$

Latimer and Eubanks found the total scattering in a suspension of red blood cells to be relatively constant over the visible spectrum, a result typical for suspensions of large cells. The correction to total scatter can be applied only if a wavelength is found where there is no true absorption.

These scattering corrections may be used with other methods to estimate the true absorbance of the particles themselves (Jagger 1967).

Turbidity is an easily measured property and its relationship to UV absorbance in wastewater effluents has frequently been examined (e.g. Roeber and Hoot 1975). The turbidity measurement may reflect somewhat different properties when measured by different instruments but we will consider measurements of scattered light at 90° to the incident beam (e.g. nephelometer measurements). Light measured in this manner results mainly from 90° scattering but obviously absorption by the sample will influence the measurement by reducing the power of the incident and scattered rays. While turbidity reflects in general the amount of particulate matter in wastewater effluents the amount of scattering per unit weight or per particle depends on the sizes and shapes of the particles and the wavelengths of the light (Black and Hannah 1965). In considering the relationship of scattering of visible light at 90° to scattering of germicidal light,several general relationships are worthwhile to review. For particles whose diameters are somewhat larger than the wavelength of the incident light,the majority of the light is scattered in the forward direction (Black and Hannah 1965). Total scatter from very large particles is usually independent of the wavelength of the incident light. The maximum scattering for a given weight of suspended matter occurs when the particle size is approximately equal to the wavelength of the light. For a given number of particles the total amount of scattered light increases with increasing particle size (Oster 1948).

DISINFECTION OF WATER AND WASTEWATER

Disinfection of natural water

Ultraviolet light has been used successfully to treat municipal water supplies (Witherell, et al. 1972; Stiff 1971) but has been criticized because of its greater cost, maintenance problems and lack of residual protection in the distribution system. Its use has been advocated for several specialized uses such as disinfection of water on ships (Huff, et al. 1965) and disinfection of seawater for shellfish depuration (Kelly 1961).

Disinfection of wastewater effluents

While the more limited transmission characteristics of wastewaters may seem to decrease its susceptibility to UV disinfection, the lack of residual protection is not a problem as it is with potable water supplies. In general, as more investigations are carried out, UV treatment appears increasingly attractive as an alternative to chlorination of wastewater effluents.

Oliver and Cosgrove (1975) and Oliver and Cary (1976) performed laboratory and bench scale investigations on disinfection of several secondary effluents. They recommended an unusual design in which lamps were suspended over weirs of secondary clarifiers in a thin film. They also believed that bacteria inside aggregates of particulate matter were at least partially protected from the UV light. They supported this hypothesis by subjecting a sample to an ultrasonic treatment which dispersed the particles. The dispersed sample showed a much higher kill of bacteria.

A suspended-lamp, shallow-tray UV unit was used for experiments on activated sludge effluents by Roeber and Hoot (1975). An ultraviolet photometer was located at the bottom of the tray and was used to estimate UV absorbance and dosages. Supplemental static batch tests were performed in the tray to control the exposure time accurately for dose-survival curve data. UV absorbance correlated well with chemical oxygen demand (COD) but poorly with turbidity. Cultured F_2 bacteriophages were inoculated into the wastewater and irradiated. They showed linear dose-response curves and a sensitivity similar to that of the coliforms. Disinfection goals were generally met except when influent quality was poor (turbidity above 11 JTU).

Petrasek, et al. (1980) performed a pilot scale investigation of several types of wastewater effluents including a secondary activated sludge effluent, mixed-media and dual-media filtered effluent, tertiary clarified effluent, chemically clarified effluent, and a tertiary clarified plus dual media filtered effluent. Two types of UV units were used: a shallow tray exposure unit and a 9-lamp submerged lamp unit. The authors found the submerged lamp unit to be superior. One problem with the shallow tray unit was the accumulation of solids in the tray. They also found differences in the dose-response curves between the two units. These differences may have been due to the methods of estimating the UV doses. They attempted to correlate the UV % transmission with several water quality parameters (UV absorbance would have been more appropriate for linear correlation analysis). NH_4-N and organic-N correlated well with UV % transmission, presumably due to their correlation with other direct UV absorbers. COD showed a very weak correlation with UV % transmission. There was little or no correlation with turbidity, suspended solids, PO_4-P and NO_3+NO_2-N. The disinfection data also showed no correlation with turbidity or suspended solids, but the authors noted that the ranges of turbidity and suspended solids were not great. There was no correlation between UV "intensity" measured by a probe located in the reactor wall and the UV % transmission measured by a spectrophotometer.

EPA Form 2350-4 (4-80)
[PREVIOUSLY EIN. EPA FORM 247]
U.S. GOVERNMENT PRINTING OFFICE: 1980-660-839
TYPING GUIDE SHEET

The UV "intensity" at the wall did, however, correlate with log reductions of coliforms. They also plotted data as the extreme value with a given probability of finding 200 fecal coliforms/100 ml as a function of estimated dose. They estimated that at a flow of 1 MGD (3.8 million liters/day) an "equivalent" system would consume 8328 Watts input energy and would give excellent results.

They also attempted to demonstrate a relationship between UV disinfection reductions and average particle sizes among samples of activated sludge effluent with or without tertiary settling and multi-media filtration. Particle sizes were determined both microscopically and gravimetrically. They encountered some problems with the microscopic technique. The gravimetric technique involved filters of pore sizes 0.4μ to 5μ. They found a "hint" of a decreasing % inactivation with increasing weight of the larger particles. However, the results did not appear to be clear. They concluded that filtration did not noticeably affect the influent coliform counts but did exclude many of the larger particles and increased the inactivation of the bacteria.

Results of a full-scale UV disinfection project on an activated sludge effluent were reported by Scheible and Bassell (1981). A large array of 400 85W lamps (76 x 76 x 152 cm) was installed in a chlorine contact chamber. The normal exposure time in the array was about 2 seconds. Quartz sleeves were cleaned by a continuous mechanical system. Flow was perpendicular to the lamps. The axes of the lamps were in even rows 3.55 cm from one another; thus, it was a "thin film" design. By using a large array of lamps the design avoided much of the loss of light to the outer walls which may occur in smaller scale units; however, we believe the lamps may have interfered with one another. Dose response data were analyzed by methods previously reviewed. They reported a dosage of 60 mW-sec/cm^2 to be necessary to achieve a 200 MPN/100 ml fecal coliform effluent. Using multiple regression analyses they found no significant effects of water quality parameters or temperature on the dose response relationship. Design curves and economic analysis showed that amortized capital costs comprised about 50% of the annual cost. Of the remaining operation and maintenance costs, materials were 50-70% and power costs were only 5-10%. Costs for a 1 MGD (3.8 million liter/day) plant were 0.92 cents/1000 l. Overall the process was judged to be economical and competitive with alternative disinfection processes.

Singer and Nash (1979) tested a 3 l/sec commercial unit on a step aeration effluent. The unit employed a "thick film" design; the lamps were submerged and spaced about 7.5 cm apart. The power input was 360 W and flow rate was varied. An ultraviolet sensor located in the wall provided a relative indication of the UV intensity but no estimates of UV dose were attempted. Biochemical oxygen demand, suspended solids, turbidities and the UV meter readings were intercorrelated. The flow rate had little effect on disinfection results. Effluent fecal coliform densities (log) were highly correlated with the UV sensor readings and therefore with the other water quality parameters. However, results were not reported as log reductions. Costs of power were compared to costs for chlorine.

PHOTOREACTIVATION

In planning the UV dosage necessary to give a certain degree of disinfection, one must consider the photoreactivation of irradiated microorganisms. The basic mechanisms have been reviewed by Jagger (1967). Direct photoreactivation (PR), the most important type, is based on Michaelis Menten kinetics consisting of a dark enzymatic reaction followed by a reaction dependent on PR light. A PR enzyme must be bound to the UV induced dimer in order for the dimer to absorb photoreactivating light and thus repair the lesion. Since the reaction involves enzymes it is a temperature dependent reaction. The relationships between the dose response curves of the initial inactivation and the photoreactivated survival curves is often described by the dose-reduction factor (DRF), the dose for a given effect divided by the dose for the same effect in the presence of photoreactivating light. In many systems the DRF is constant, but not always. A DRF of about 0.3 is common (Jagger 1967).

Most species of bacteria are capable of undergoing photoreactivation but UV damaged phages must be adsorbed to a host bacterium in order to photoreactivate. One of the largest degrees of photoreactivation has been reported by Carson and Peterson (1975). They found 1 to 4 logs of photoreactivation in *Pseudomonas cepacia* after exposure to UV light and then fluorescent light.

In a study of PR of coliforms in UV treated wastewater effluent, Roeber and Hoot (1975) found PR of coliforms to be on the order of 1 log after 80 minutes in sunlight.

Petrasek *et al*. (1980) allowed UV irradiated effluent to flow into two parallel chlorine contact basins (without chlorine) with a detention time of about 1 hour. One side was darkened and one exposed to sunlight. Total coliforms increased 0.7 log in the lighted basin and 0.3 log in the dark basin. Fecal coliforms increased 1 log and 0.7 log in the light and dark basins, respectively. Statistically, however, the differences between the light and dark basins were not significant when overall means were compared.

Scheible and Bassel (1981) incubated UV treated effluent samples in light and dark bottles for 1 hour. They found about 1 log increases in total coliforms and 0.6 to 1 log increases in fecal coliforms in the light bottles. The dark bottles showed no regrowth. Dynamic tests were done on the effluent in the chlorine contact channel about 1 to 2 hours after irradiation. These showed similar results. Temperature had a significant effect on PR. Combining the results of the dosage and PR data, they found that a three-fold higher UV dosage would be required at 20°C if PR were considered.

SECTION 5

MATERIALS AND METHODS

PILOT PLANT EXPERIMENTS

The ultraviolet disinfection pilot plant was located in Durham, North Carolina, at the Sandy Creek wastewater treatment plant. Secondary filtered and unfiltered effluents from the contact stabilization plant were used as the feed to the UV units.

Pilot plant design

Effluent pumped out of the secondary clarifier flowed by gravity into one of three downflow multimedia filters. Effluent exiting the filters then flowed into a steel holding tank. For experiments requiring unfiltered effluent, the three filters were bypassed. Effluent was then pumped out the bottom of the holding tank and into one of two commercially available UV units. Plastic valves were located to direct and regulate the flow as desired. Valves were also located just before and after each unit for the collection of samples. Effluent leaving the units flowed into another steel holding tank, from where it was periodically pumped into a backwash tank.

The disinfection units

The Aquafine CSL-6 unit (Fig. 8) was a "thick film" submerged lamp unit. The cylindrical, stainless steel tank housed six 40 watt low pressure Hg vapor lamps mounted longitudinally inside 2.52 cm diameter quartz sleeves. The diameter of the lamps themselves were .794 cm. Two short pipes were mounted on the wall for inserting UV detectors. The effective volume of the unit was 11.0 liters. Each lamp had an effective length of 73.7 cm. Four sets of baffles were arranged inside the unit. The sectors of the baffles had a slight angle so that flow was given a somewhat helical component. Table 20 (results) also compares the two units. A special adapter was made so that a detector from a research radiometer (described later) could be inserted. However, the detector was located about 4.5 cm from the wall since a closer approach was impossible.

The Pure Water Systems (PWS) I-75 unit (Fig. 9) was a "thin film" submerged lamp unit. It employed a cylindrical, stainless steel tank with an unusual flow pattern. Fourteen 25 watt low pressure Hg vapor lamps with an effective length of 38.1 cm each were housed in 2.22 cm diameter quartz sleeves arranged around the upper 2/3 of the chamber. Water entered the unit through holes drilled along the bottom of a distribution tube extending

BEGIN
CENTER OF
TOP OF IMAGE

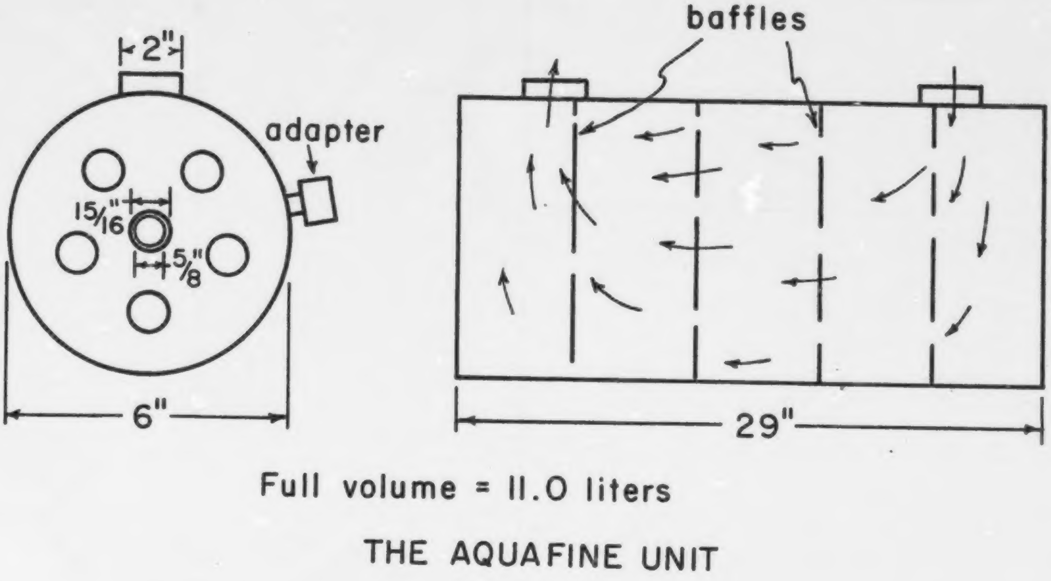
baffles
2"
adapter
15/16"
5/8"
6"
29"
Full volume = 11.0 liters
THE AQUAFINE UNIT

Fig. 8. The Aquafine unit. 1 in = 2.54 cm.

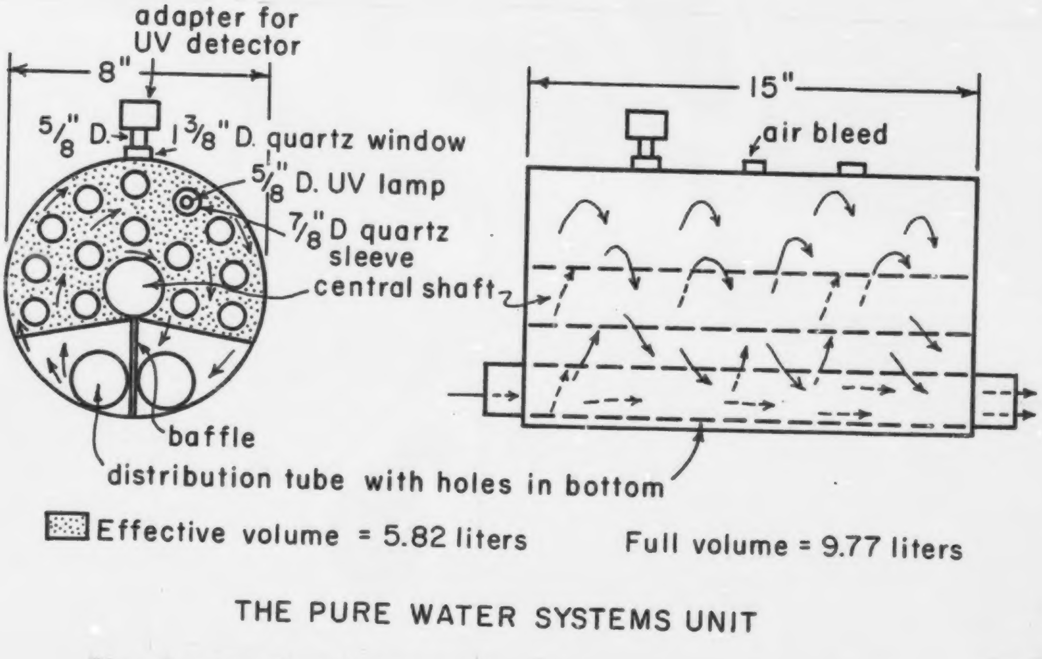
adapter for UV detector
8"
5/8" D.
1 3/8" D. quartz window
5/8" D. UV lamp
7/8" D quartz sleeve
central shaft
baffle
distribution tube with holes in bottom
15"
air bleed
Effective volume = 5.82 liters
Full volume = 9.77 liters
THE PURE WATER SYSTEMS UNIT

Fig. 9. The Pure Water Systems unit. 1 in = 2.54 cm.

the length of the unit. The holes decreased in diameter from the influent and to the opposite end. Fluid was forced up and over a central shaft before finally exiting the unit on the other side. Thus the water flowed generally across rather than along the lamps. While the volume of the entire fluid filled volume was 9.77 l, only 5.82 l of that was in the exposure chamber. A similar adapter was mounted on the wall to fit the radiometer detector, also 4.5 cm from the wall.

The total lamp wattage of the Aquafine and PWS units were 240 and 350 watts, respectively.

Pilot plant methods

Seventy-two experimental runs were conducted using a statistically randomized design with four independent variables, each of which could assume two conditions. These variables were: 1) flow rate through the units (2.21 l/sec or 4.79 l/sec), 2) lamp voltage (60 V or 125 V), 3) effluent quality (filtered or unfiltered) and UV unit (Aquafine or PWS). Each run involved both units at one flow rate only. The other variables were then selected randomly from a random number table with the restriction that nine replicates of each set of conditions had to be performed eventually.

Each week, two runs were performed on Monday mornings and two on Wednesday mornings. All samples were collected between 8:00 and 11:00 A.M. If both a filtered and an unfiltered run were required by the statistical design on a particular day, the filtered run was always performed first. This was necessary to insure that filtered effluent would not be available for use as backwash water. Effluent was first rinsed through both units for at least 30 minutes to flush the filters completely. During this time, the flow rate to be used for the first unit was set using a calibrated bucket and a stopwatch. Also, the UV lamps in that unit were warmed up to their optimum operating temperature of 35-40°C. The order in which the units were tested was determined by a coin toss. After the Variac was set at the proper voltage level, influent and effluent samples were collected from the first unit. Samples for physical and chemical analysis were collected in plastic jugs. Those for bacteriological examination were collected in sterile brown glass bottles. The temperature and dissolved oxygen of the samples were determined immediately upon collection, and then the samples were packed in ice for transportation back to the laboratory. Precautions were taken to avoid exposure of the samples to light. Samples were then collected from the other unit at the appropriate voltage and flow rate following the same procedure.

After the completion of each filtered run, the filter used was backwashed unless two filtered runs were required on a given day. In that case, backwashing took place only after the completion of both runs. The filters were backwashed first with compressed air for 2 to 3 minutes, then with filtered effluent pumped from the backwash tank for 5 to 10 minutes.

After the completion of both runs, the Aquafine unit was circulated with an acid cleaning solution for 15 minutes. The Pure Water Systems unit relied upon a wiper blade operating continuously to keep the quartz sleeves from accumulating slime.

Analysis of Samples

I. Physical and Chemical Analyses

In an effort to correlate parameters of water quality with efficiencies of disinfection, the following analyses were performed on all samples:

A. Influent Samples

1. Temperature - measured immediately upon collection of samples.
2. UV absorbance - measurements were made at 254 nm using a Beckman DB Spectrophotometer.
3. Alkalinity - Standard Methods (14th Ed, 1975).
4. Conductivity - determined using a Radiometer conductivity meter Model CDM 2e.
5. Total Suspended Solids - procedure according to Standard Methods (14th Ed, 1975).
6. Total Organic Carbon - samples were analyzed on a weekly basis using a Beckman Model 915A Combustion Infrared Carbon Analyzer.
7. Turbidity - HACH Model 2100 A Nephelometer.
8. pH - a Fisher Accumet pH meter.
9. Chemical Oxygen Demand - Dichromate reflux method according to Standard Methods (14th Ed, 1975).
10. Total Iron - determined by a Perkin Elmer Flame Atomic Absorption Unit.
11. Nitrogen Forms - determined according to methods outlined in Manual of Methods for Chemical Analysis of Water and Wastes (U.S. EPA, 1974).
    A. $NO_2^- + NO_3^-$ - N - the Automated Hydrazine Reduction Method using a Technicon Auto Analyzer
    B. NH_3 - N - the Automated Colorimetric Phenate Method
    C. Kjeldahl-N - the Automated Phenate Method using a block digester

B. Effluent Samples:

Seven water quality parameters were measured in the effluent samples. These included: (1) temperature, (2) dissolved oxygen, (3) nitrogen forms, (4) conductivity, (5) total organic carbon, (6) chemical oxygen demand, (7) pH and (8) alkalinity. The analytical methods were outlined for the influent samples. Dissolved oxygen was measured immediately upon collection of all effluent samples using a YSI model 52 dissolved oxygen meter.

II. Bacteriological Examination

For the enumeration of coliform organisms, the 5-tube 5 dilution fermentation procedure as outlined in Standard Methods (14th Ed., 1975, p. 913) was employed. Lauryl Tryptose was used as the presumptive medium. Both fecal and total coliforms were carried to the confirmed level. Results were reported as log reductions in bacterial counts, equal to the log influent minus effluent counts.

Virus Seeding Experiments

To test the effects of the various pilot plant treatments on an introduced virus, a culture of Type I LSc *Poliovirus* was added to the effluent in a holding tank. These solutions were subjected to the same treatments as samples in the coliform experiments except that only one run was performed. Influent and irradiated samples were frozen and later assayed by adsorption to mammalian cell cultures and plaque assay. Water temperature was 16°C during the experiment. UV absorbance was .207 and .143 for the unfiltered and filtered effluents respectively. All other water quality parameters were within one standard deviation of those in the coliform runs.

Photoreactivation

Effluent samples were taken from several disinfection runs with the Aquafine and PWS reactors to measure the effect of sunlight photoreactivation. Four types of samples were used: (1) influent (untreated) dark control, (2) influent (untreated) exposed to sunlight, (3) effluent (UV treated) dark control, (4) effluent (UV treated exposed to sunlight.

Samples were pipetted into petri dishes, covered, and placed in a water bath at 25°C (except for a 4°C temperature study). Sunlight exposure times of 15, 45 and 75 minutes were used. PR sunlight intensity was measured with a Schott filter adapted to a General Electric light meter. The meter measured intensity between 320 and 390 nm with an 85% maximum sensitivity at 350 nm. Total coliforms were enumerated by the membrane filtration technique using the lauryl sulfate broth enrichment step (Standard Methods, 1975). Samples were plated in triplicate.

Flow Distribution Studies

Dye studies were performed at three flow rates on both the Aquafine and the Pure Water Systems units. Commercially available red food color dye was used as a tracer. It had an absorbance peak at 515 nm, followed Beer's law and did not adsorb onto the quartz sleeves. The dye was injected into the flow stream immediately ahead of the units. Samples from the tap water exiting the chambers were then collected at the desired time intervals in test tubes arranged around the perimeter of a rotating sample holder. The sample with the highest absorbance was assigned an arbitrary relative absorbance of 1.0. All other values were calculated relative to this number and plotted vs. time from injection.

Actual average retention times were calculated at each flow rate using the data from the dye studies according to the equation:

$$14)\qquad \text{actual average retention time} = \frac{\Sigma\ t_i\ C_i\ \Delta t_i}{\Sigma\ C_i\ \Delta t_i}$$

where Δt_i = time interval between samples, and C_i = relative dye absorbance at time t_i from injection of dye.

Potassium ferrioxalate actinometry

The procedure of Hatchard and Parker (1952) for .006 M potassium ferrioxalate actinometry was used with the following exceptions. Tap water was used because of the large volumes required. No significant differences between tap and distilled water were observable in a preliminary lab scale test. Baxendale and Bridge (1955) found that it was unnecessary to prepare potassium ferrioxalate crystals and that it was sufficient to combine ferric sulfate (1.2 mg/l), potassium oxalate (3.32 mg/l) in 0.1 N H_2SO_4. Our lab scale tests indicated that it was unnecessary to purge dissolved O_2 with N_2 gas before irradiation.

For the pilot scale actinometry, the solution was contained in a large 1325 l polyethylene tank protected from all light. Plastic pipe and a rust-proofed pump fed the solution. The system was flushed with tap water prior to the runs and UV intensity readings were recorded to check output as a function of voltage (the actinometry solution itself absorbs all of the UV light). Each run involved collection of 8 samples from one unit at one flow rate. Duplicate samples were taken at the 47, 88, and 127 voltage settings. Two unirradiated samples were taken each time. All samples were taken in brown glass bottles.

Lamps were allowed to warm up for 1 to 3 minutes, the units rinsed for 45 sec with the solution and a blank was collected from the inflow sampling valve. Six irradiated samples were then collected in a predetermined random order, followed by a second blank. At least four retention times were allowed between samples.

Analysis for ferrous iron and calibration curves also followed Hatchard and Parker (1952). A Bausch and Lomb Spectronic 20 was used. The calibration curve yielded a molar absorptivity of 12,198 cm^{-1} with r = .998.

Growth of E. coli cultures

All cultures used for the inoculations were grown under identical conditions. One loop of a strain of E. coli B was transferred from a nutrient agar slant to approximately 500 ml of lactose broth (Baltimore Biological Laboratories, Inc.) in a 2000 ml flask. The flask was shaken gently and

EPA Form 2360-4 (4-80)
(PREVIOUSLY EIN. EPA FORM 287)
U.S. GOVERNMENT PRINTING OFFICE 1980-660-609
TYPING GUIDE SHEET

then stored undisturbed at room temperature overnight. The next day, approximately 12 hours after the inoculation, the culture was placed on a wrist action shaker to accelerate the growth. The turbidity of the broth was monitored during this period on a Hatch 2424 Analytical Nephelometer. Cultures were used 2 hours into the stationary phase.

Irradiation of E. coli in tap water in the UV reactors

The large polyethylene tank was first filled with tap water. Ammonium chloride (20 mg/l NH_4 - N), sodium thiosulfate (3.45 mg/l) and potassium phosphate monobasic (10 mg/l PO_4 - P) were then added, followed by just enough 1.0 N sodium hydroxide to bring the final pH to 7.1 to 7.2. The thiosulfate was added to neutralize any chlorine residual present in the tap water.

In addition to the chemicals mentioned above, approximately 750 ml of diatomaceous earth was added to the tank to act as a UV absorber. At the time this was thought to be necessary after an earlier experiment with no absorber added had revealed that maximum kills could be obtained at the minimum possible dosage level. With the addition of the diatomacous earth, it had been hoped the amount of UV able to penetrate the solution would be reduced so that a more meaningful dose-response curve could be obtained.

A total of four runs was performed on each unit. As in the actinometry studies, each run consisted of sampling from one unit at one flow rate only while the voltage setting was varied. In general, the method of sampling was identical to that described for the actinometry studies with the following exceptions: (1) All sample bottles were pre-sterilized, (2) intensity readings were recorded at each voltage level simultaneously with the drawing of the samples, (3) only one blank was drawn per run, and (4) samples were immediately placed on ice following their collection. In addition, for two of the Aquafine and one of the PWS runs, only 127 and 65 voltage levels were tested. Two runs, one on each unit, were always performed per tankful of inoculated tap water. This was done in order to eliminate the error involved in comparing two units irradiating waters of somewhat variable chemical composition and initial cell density. The order in which the two units were tested was randomly decided, and the blanks were always the first and last samples collected.

The 5-tube multiple tube fermentation technique as described in Standard Methods (1975) was chosen for enumeration of the microorganisms. Because a pure culture of E. coli was used in the experiments, only the presumptive lactose test was performed. All counts were made after 48 hours of incubation at 35°C in a dry incubator. The samples were protected from direct sunlight at all times to eliminate any possibility that photoreactivation might affect the results.

The counts were reported as the most probable number (MPN) per 100 ml. Log reductions of E. coli were calculated as follows:

$$\text{15)} \quad \log \left(\frac{\text{untreated MPN/100 ml}}{\text{treated MPN/100 ml}} \right)$$

BEGIN LAST LINE OF TEXT
BOTTOM OF IMAGE AREA; OUTSIDE DIMENSION FOR TABLES AND ILLUSTRATIONS
3/8"

where the numerator was the average of the two blank counts obtained from each tankful of culture, and the denominator was the average count of each pair of duplicates.

EXPERIMENTAL WORK

Measurements of UV output at 254 nm

All radiometric measurements of planar energy flux density at 254 nm (or "intensity") in this study were made with an International Light 500 radiometer with a model SEE-240 detector, employing a narrow bank interference filter (NBS-254), which was cosine corrected. The radiometer was initially calibrated by the company according to National Bureau of Standards (NBS) specifications. The calibration was checked several times during the study by Dr. D. G. Sharp (Univ. of N. C.). A bismuth-silver thermopile was calibrated using an NBS standard carbon filament lamp. A standard low pressure Hg vapor lamp was calibrated against the thermopile and then used to calibrate the detector. The original calibration setting held throughout the study.

To measure the output of a lamp the following method of integrating the intensity measurements over a sphere centered on the centroid of the lamp (Fig. 10) was used. The lamp was mounted in sockets fixed to a block of wood. A nail was placed below the centroid of the lamp and a string attached above a protractor likewise centered. The detector was rotated around the 90° arc described by the string at a radius of 190 cm. The long radius was essential so that light coming from each end of the lamp was nearly normal to the surface of the detector and the planar energy flux density approaches the energy flux density. The detector face was oriented toward the lamp centroid. Output is calculated as follows (Barrows 1951):

> Dose rate (I) was measured at angles θ between 0° and 180°. The outer surface area of a "slice" of the sphere of radius r with arc length dθ is 2π adθ, (Fig. 10), where a = r sin θ. The energy leaving the surface of the "slice" is I 2π adθ. The energy leaving the surface of the sphere is:
>
> $$2\pi r^2 \int_0^{\pi} I \sin \theta d\theta$$
>
> The I sin θ values were plotted as a function of θ (radians) and the area under the curve from 0 to π was measured gravimetrically.

Once the distribution of intensity around one particular lamp has been determined at θ = 90° and r = 190 cm), a measurement at that point is all that is necessary to correct the output for variations in output at different voltages, temperatures, etc.

Measurements of the output at various voltages for lamps in the commercial units were made by first using the entire procedure in a mounted apparatus. Then the *in situ* output was approximated by attaching the unit's wiring

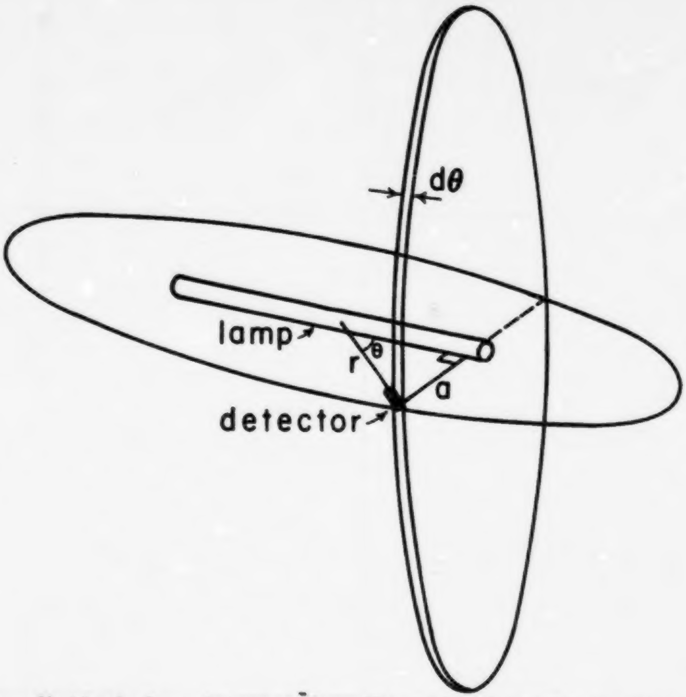

Fig. 10. Method for determining UV output of tubular lamp. Intensity values are taken with a radiometer detector around radius r around the centroid of the lamp. Energy leaving spherical "slices" of width dθ are integrated over a sphere surrounding the lamp.

to the lamps mounted just outside the unit and proceeding as in step 4 above.

Collimated beam irradiation apparatus

To develop accurate dose response data, and to use in experiments where true UV doses must be known, we assembled an apparatus in which a small stirred sample could be irradiated in a nearly collimated beam. The radiometer could then be used to measure the I_0 and calculations of the average dose rate would be relatively straightforward. We also wanted to use an apparatus readily assembled by anyone with basic UV disinfection equipment.

A lamp supplied with the Aquafine unit was mounted in sockets attached to a piece of wood and wired to a ballast and a Variac (Fig. 11). The lamp was suspended over a long tube painted flat black. At the bottom of the tube the maximum deviation of rays from normal was about 6°. Solutions were contained in a small dish made so that 10 ml gave a depth of 1 cm. The bottom of the dish was quartz to allow crude measures of % transmission. The dish was placed on a magnetic stirrer and solutions stirred with a "micro" stir bar of negligible volume. Measurements of I_0 at the surface of the liquid were made by removing the dish and stirrer and placing the detector at the corresponding position. Intensities varied less than 3% during times corresponding to irradiation times.

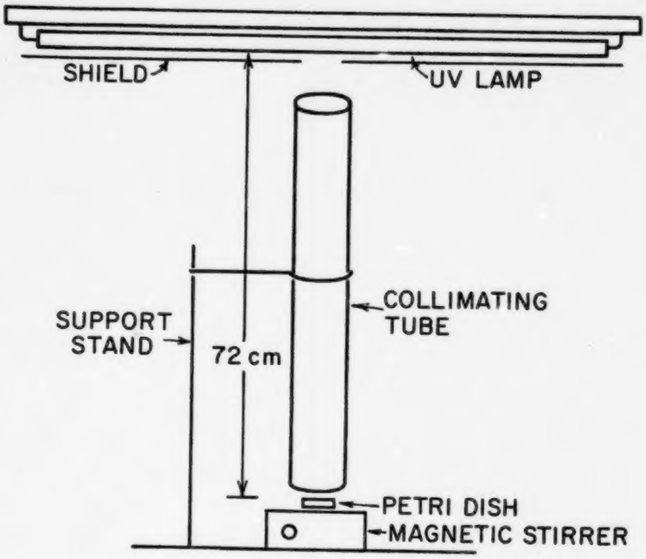

Fig. 11. Collimated beam apparatus.

Calculations of the average dose rate in the stirred solutions were made using the radiometer I_0 measurement and equation 3 (Lit. Rev.). The calculation requires use of the absorbance. If scattering was suspected in the specific solution, efforts were made to separately evaluate absorbance and scattering.

Bacillus subtilis spore preparation

In order to measure the relatively high UV dosages necessary to disinfect wastewater effluent containing resistant organisms, we used a stock of relatively resistant Bacillus subtilis spores to prepare a standard dose-survival calibration curve. This stock was prepared by T. S. McGrath for use as a standard in a study of HOCl disinfection kinetics (unpublished thesis, 1979). The spore stock was prepared by the following method (adapted from McGrath). The culture (ATCC 6633) was originally from Lily Research Labs of Eli Lily and Co. It was cultured from North Carolina Memorial Hospital stocks, maintained on Penassay Agar (Difco) slants, and refrigerated. Mass production of free spores was done using Schaeffer's Medium (paper presented at CNSR Symposium, France, 1965).

Formula for Schaeffer's Medium (per liter):

BEGIN LAST LINE OF TEXT
3/8"
PAGE NUMBER
BOTTOM OF IMAGE AREA: OUTSIDE DIMENSION FOR TABLES AND ILLUSTRATIONS
EPA Form 2350-4 (4-80)
(PREVIOUSLY CIN. EPA FORM 237)
U.S. GOVERNMENT PRINTING OFFICE 1980-660-
TYPING GUIDE SHEET

Part 1

Nutrient Broth (Difco)

$MgSO_4 \cdot 7H_2O$

KCl

$FeSO_4$

Autoclave Part 1 after neutralizing to pH 7 with NaOH

Part 2

$Ca(NO_3)_2$

$MnCl_2$

Autoclave and do not neutralize.

Mix Part 1 and 2 so that the final concentrations in the solution are those given above.

Procedure:

Part 1. Dissolve the following in 1 l of distilled H_2O:

280 mg $MgSO_4 \cdot 7H_2O$

1.11 g KCl

1 ml of a solution made by dissolving 31 mg $FeSO_4 \cdot 7H_2O$ in 100 ml of H_2O

Part 2. Dissolve the following in 200 ml of H_2O:

470 mg $Ca(NO_3)_2 \cdot 4H_2O$

390 mg $MnCl_2 \cdot 4H_2O$

(If using salts of different hydrations, apply the appropriate gravimetric factor)

Neutralize part 1 to pH 7 using NaOH. Do not adjust the pH of part 2 as it will cause precipitation during autoclaving. Autoclave both parts while separate.

These two parts may be made in quantity for later use. If for immediate use, add 8.9 g of nutrient broth to part 1 before autoclaving. If for later use, add nutrient broth to part 1 at 8.9 g/l and reautoclave before adding part 2 aseptically. Mix 9 portions of part 1 to 1 portion of part 2 to yield 10 parts of Schaeffer's Medium.

The prepared Schaeffer's Medium was inoculated from the agar slants and incubated on a shaker table at 37°C. Samples were checked at 48 and 72 hours for spore production with a microscope. When most cells had sporulated the suspensions were heated to 80°C for 10 minutes to kill the remaining vegetative cells. The spore suspensions were then sonicated for 2 minutes at 70 watts in an ice bath to insure separation of the spores from the cell debris.

The spore suspensions were washed by centrifugation at 1500 rpm for one hour . The resulting supernatant was poured off and the pellet resuspended in distilled water. It was necessary to lower the centrifuge speed slowly over several minutes to prevent a vortex from forming. This procedure was repeated until microscopic examination showed individual cells free of cell matter. After the last centrifugation the spores were again sonicated to insure non-aggregated spores and were stored in distilled water at 4°C. The concentration of spores in the stock was about 2×10^8 viable spores/ml. Stocks remained viable for several months. During the UV experiments, stocks were usually shaken daily to maintain suspension and no progressive change in UV sensitivity was observed over a three-month period.

Calibration of Bacillus subtilus as a bioassay for UV dose

Aliquots of the B. subtilus spore stock were diluted to a concentration of 5×10^4 spores/ml (5×10^5 spore/ml stock were used for inactivations over 3.5 log) at which absorbance is negligible, and therefore, calculations of average dose rate are more straightforward. All dilution water used in this study was magnesium sulfate-phosphate buffer (Standard Methods). The lamp of the collimated beam apparatus was equilibrated and I_o was measured at the level of the top of the solution. Ten ml (1 cm depth) solution was added to the stirred petri dish and exposed for an exact time. After irradiation samples were handled aseptically and stored in the dark no longer than 45 minutes before plating. Dilutions were planned to give about 50 counts per plate. All samples were plated in triplicate using Thermoacidurans Agar (Difco) pour plates.

Irradiations were done to give data at 0.5 log intervals up to 5 logs inactivation. In all, 5 sets of curves were produced during the study.

Calculation of the doses was made by assuming that 4% of the measured I_o was reflected from the water surface (Jagger 1967). The average dose rate (eq. 3) x exposure time was used as the dose. The concentration of spores was such that the UV absorbance of the solution was very small and hence any error in calculation of absorbance was almost negligible. The solution used showed a spectrophotometric UV transmission (1 cm) of 96%. A correction for scattering was made by the extrapolation method and the "true" % transmission was 98%.

Since all values in a run incorporated the initial spore concentration (N_o), ten plate counts were made for each unexposed solution. The N_s value was the mean of three plate counts on each exposed sample.

Fulvic acid as an absorber

Experiments to test models of dose rate in an absorbing solution with a UV bioassay procedure required a non-toxic, non-scattering UV absorber. Many compounds were tested but fulvic acid was chosen because: 1) it is a very strong UV absorber at low concentrations, 2) it is likely to be a major absorber in actual wastewater effluents. The fulvic acid was isolated from a blackwater lake as part of another project. Most fulvic acids are of lower molecular weight than other humic acids and are less likely to scatter light. Bioassays using spores showed no toxicity at the exposure times used. Irradiations at 1, 2, 3 and 4 cm depths gave bioassay results as predicted from the spectrophotometric absorbance.

Cylindrical irradiation apparatus

In order to confirm the point source summation method experimentally as a means of calculating the dose rate distribution around a line segment source, a series of cylindrical irradiation chambers were built (Fig. 12). From the predicted dose rate profile around the source, an average dose rate within the entire volume enclosed by a cylinder of radius r could be predicted. Thus a correspondence between the experimentally measured average dose rate within the cylinder and the theoretical prediction was taken as confirmation of the model.

The apparatus had to meet several requirements: 1) it was a batch irradiation so that exposure time was accurately known, 2) the lamps had to be warmed up and equilibrated when exposure began so that output did not vary, 3) the solution had to be well mixed with minimum interference.

Several plexiglass cylinders of radii 1.86, 2.54, 3.81, 5.40 and 6.35 cm were fitted with a bottom. A quartz sleeve from the Aquafine unit ran through a hole in the bottom along the axis. A lamp could be inserted and centered on the axis. Wiring was arranged so that a paper tube, painted flat black, could rapidly be raised and lowered between the lamp and the inner surface of the quartz sleeve. The exposed lamp length was 60 cm. Solutions were stirred rapidly with a ringlike device. Tests with dyes and particles showed mixing to be thorough both radially and axially.

The experimental procedure consisted of warming up the lamp to equilibrium at the beginning of a series of runs for 2 minutes at 100% voltage (on the Variac) and then reducing to 35% voltage and equilibrating for 5 minutes. Buffered dilution water (Standard Methods) was added as the black tube was raised to cover the lamp. Fulvic acid was added to the water if needed to give the desired absorbance of 0, .08, .16, .24 or .32. An aliquot of *Bacillus subtilis* spore stock was added and mixed to give a final concentration of 5×10^4 spores/ml (not enough to significantly affect absorbance). After exactly 90 seconds from the time the black tube was raised it was lowered to begin exposure. The solution was stirred continuously. Exposures varied from 6 to 45 sec and were chosen to give about a 3 log survival. Exposure was ended by turning off the lamp. Samples were taken before and after exposure.

It was important that the lamp output be known during the irradiation. An apparatus identical to the first was located beside it but had no plexiglass cylinder around it. Thus the intensity at 90° and 190 cm could be monitored and the output calculated under identical experimental protocol. Temperature probes inserted in the air space showed that the presence of the water filled plexiglass cylinder did not bias these measurements. Raising the black tube for only 90 sec did not significantly affect the output by raising temperature. During the experiments the output of the lamp was checked every third trial by carefully transferring the lamp between setups. Day to day variation was greatest and ranged from 44.0 mW/cm length to 49.4 mW/cm length.

Two trials each were done at absorbances of 0, .16, and .32 on all 5

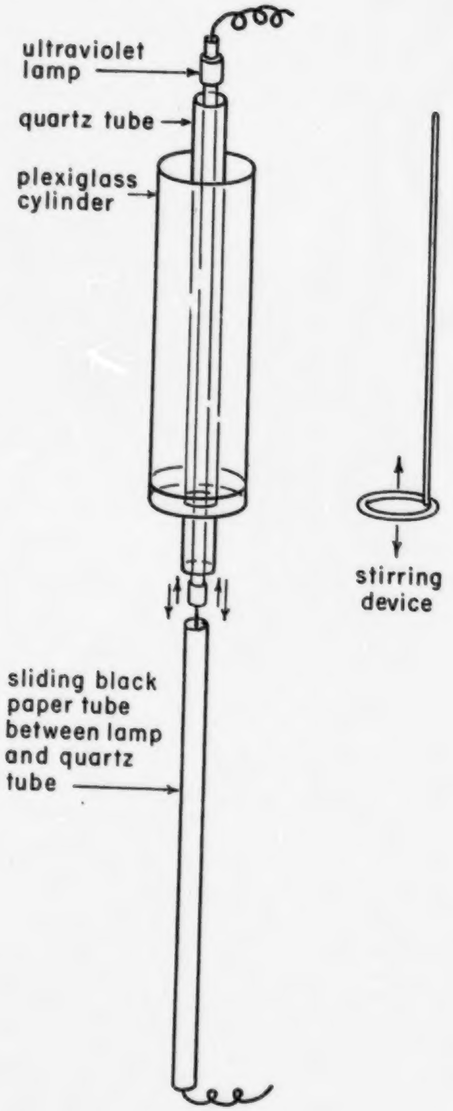
ultraviolet lamp
quartz tube
plexiglass cylinder
stirring device
sliding black paper tube between lamp and quartz tube

Fig. 12. Cylindrical batch irradiation apparatus. A paper tube slides up between the UV lamp and the quartz sleeve and may be lowered quickly for a precise exposure. The solution is placed in a plexiglass cylinder open at the top and sealed at the bottom and is stirred well during exposure

tube sizes. To provide a more complete set of absorbance data, trials at absorbances of .08 and .24 were done in the 2.54 and 5.40 cm radius cylinders. Two trials were done consecutively on one cylinder, but otherwise randomized with the restriction that no two replicates were done on the same day to avoid systematic changes in lamp output.

Bacillus spore titers were assayed as described previously.

Flowthrough irradiation experiments

The lower radii of the preceding apparatus were limited by the stirring device. In order to test the distribution of dose rate very near the quartz sleeve a glass tube was centered around a quartz sleeve containing a lamp. Tubes for influent and effluent were attached at the ends and rubber "O" rings sealed the annular space at the ends. Output was checked as previously.

Two sorts of experiments were performed: 1) continuous flowthrough of a solution already mixed with spores and absorber. There, exposure time was calculated as volume/flow rate. This design did not consider the effects of flow dispersion. 2) Injection experiments: A solution was allowed to flow continuously through the tube. However, the spores were injected into the influent port while the effluent stream was diverted simultaneously into a rotating sample tray. The rotating tray was assembled from a Technicon Autoanalyzer II mounted on an axle of a variable speed stirring apparatus carefully calibrated with a stopwatch. Thus, retention time of each flow fraction was known. Retention times were corrected for passage through a short exit tube by using the flow rate and exit tube volume to estimate exit tube retention time. Injection time was less than 0.1 seconds.

Irradiated concentrations were assayed from samples when the light was on. The light was immediately turned off and an identical injection was made. These samples served as the unirradiated concentrations. Two replicates were performed for each treatment in these experiments. Dye injections were also performed to confirm dilution factors for the injections.

SECTION 6

RESULTS AND DISCUSSION

PILOT PLANT RESULTS AND DISCUSSION

Summary of Pilot Plant Results

Results of the pilot plant experiments showed in general:

1) significantly better disinfection with dual media filtration;

2) that filtration had relatively little effect on UV absorbance of the effluent, although it removed much of the suspended solids and some of the turbidity;

3) that the Aquafine unit achieved much better disinfection than the Pure Water Systems unit; the latter suffered from severe short circuiting of flow as determined by dye studies;

4) that different treatments of applied voltage and flow rate had relatively small and occasionally inconsistent effects;

5) that the multiple regression of randomly varying water quality parameters on log survival of coliforms showed some correlations with dissolved oxygen, turbidity, UV absorbances, and pH, depending on other treatments. However, auto-correlations among many of the water quality parameters made interpretation of the stepwise regressions subject to qualification;

6) that spectrophotometric UV absorbance was predicted best by total or fecal coliform counts, or, if these were not considered, by COD, turbidity, and suspended solids.

Effects of filtration on disinfection and UV absorbance

Means of the log total and fecal coliform MPN's in the effluent after UV irradiation (Table 2) show that a disinfection goal of 200 fecal MPN/100 ml was achieved with the Aquafine unit in the filtered and unfiltered effluent. Standard deviations are shown for each mean given in Table 2. With the PWS unit, the titers usually exceeded the goal, often by an order of magnitude or two. The inactivation as means of the (- log) survivals of both total and fecal coliforms (Table 3) are broken down by filtration status, unit, applied

Table 2. Mean log total and fecal coliform MPN/100 ml in UV effluent for each treatment broken down by filtration status, disinfection unit, flow rate and applied voltage. Standard deviations (of logs) are shown in parentheses.

		Aquafine		Pure Water Systems	
Flow Rate (1/s)	Voltage	Unfiltered	Filtered	Unfiltered	Filtered
		Total coliforms			
4.92	60	2.50 (.50)	1.85 (.89)	3.87 (.33)	4.11 (.77)
	128	2.17 (.48)	1.66 (.43)	3.42 (.43)	3.33 (.84)
2.27	60	2.21 (.66)	1.51 (.80)	3.69 (.85)	3.60 (.75)
	128	2.48 (1.1)	2.10 (.93)	3.65 (.72)	2.62 (.94)
		Fecal coliforms			
4.92	60	1.98 (.56)	1.17 (.88)	3.43 (.38)	3.33 (.62)
	128	1.71 (.68)	.95 (.74)	2.85 (.44)	2.79 (.70)
2.27	60	1.59 (.99)	.85 (.61)	3.13 (.65)	3.11 (.66)
	128	1.80 (1.0)	1.25 (.97)	3.06 (.38)	1.99 (.92)

voltage and flow rate. In most cases, the disinfection of the filtered effluent was better than that of the unfiltered effluent. Exceptions were in the PWS high flow rate treatments, in which highest survival rates of any of the treatments occurred. Individual t-tests show most of the filtration differences to be significant ($p < .05$).

Stepwise multiple regressions were also performed. Separate regressions were performed for all the data where (1) all variables were allowed to enter freely and (2) where treatments were forced to enter first (Table 4, first four columns). Filtration status is shown to be significant for fecal coliforms when all variables are allowed to enter; however, it was not significant for total coliforms while turbidity was. When treatments were forced in, the turbidity was no longer significant, perhaps indicative of the association between turbidity and filtration (Table 5). The differences between filtered and unfiltered means were frequently greater than 0.5 log, particularly at the lower ranges of survival.

The greater coliform reduction in filtered compared with unfiltered effluent was not caused by changes in UV absorbance. The dual media filtration method used in this study resulted in little reduction in the spectrophoto-

BEGIN LAST LINE OF TEXT
BOTTOM OF IMAGE AREA, OUTSIDE DIMENSION FOR TABLES AND ILLUSTRATIONS
3/8"

PAGE NUMBER
EPA-287 (Cin.)
(4-76)

Table 3. Inactivation shown as mean -log survival of total and fecal coliforms in unfiltered and filtered secondary effluent, broken down by filtration status, disinfection unit, applied voltage, and flow rate. Standard deviations (of logs) shown in parentheses.

		Aquafine		Pure Water Systems	
		Unfiltered	Filtered	Unfiltered	Filtered
Flow Rate(l/s)	Voltage	Total coliforms (-log survival)			
4.92	60	3.29 (.13)	4.08 (.18)	2.10 (.17)	1.95 (.08)
	128	3.69 (.16)	4.27 (.20)	2.47 (.12)	2.48 (.12)
2.27	60	3.91 (.14)	4.37 (.25)	2.25 (.19)	2.42 (.17)
	128	3.61 (.28)	3.94 (.14)	2.80 (.28)	3.02 (.32)
		Fecal coliforms (-log survival)			
4.92	60	3.08 (.20)	3.88 (.19)	1.76 (.13)	1.78 (.10)
	128	3.41 (.23)	4.17 (.18)	2.41 (.15)	2.42 (.16)
2.27	60	3.91 (.23)	4.29 (.17)	2.13 (.14)	2.44 (.15)
	128	3.47 (.28)	3.92 (.24)	2.86 (.27)	2.97 (.22)

metric UV absorbance of the effluent (Table 6). While suspended solids, the large particles, were greatly reduced by filtration, they contributed less to the turbidity reduction and to the TOC reduction and very little to UV absorbance. Thus, most UV absorbance was associated with either the very small particulates or the soluble components. Further lab studies were performed to confirm this finding.

Effects of water quality parameters on coliform survival

Except for the treatments--unit, filtration status, applied voltage and flow rate--other water quality parameters were allowed to vary randomly throughout the runs. Analysis of their possible effects on both total and fecal coliform survival was performed using stepwise multiple regression of the treatments and the randomly varying water quality parameters on both total and fecal coliform log survival (Table 3). In order to separate the effects of the treatments and water quality parameters, separate analyses were performed for (1) all data, (2) all data with the treatments forced to enter the regression, and (3) data broken down by unit and filtration status. Care must be exercised in interpreting a stepwise multiple regression when

BEGIN LAST LINE OF TEXT
BOTTOM OF IMAGE AREA; OUTSIDE DIMENSION FOR TABLES AND ILLUSTRATIONS
3/8"

EPA-287 (Cin.)
(4-76)

Table 4. The importance of independent variables in explaining variation in log survival of total and fecal coliforms; results of stepwise multiple regression. Numbers indicate order of importance in explaining variation. Separate analyses were performed for all data, all data with the treatments forced to enter the regression and data broken down by unit and filtration status. X's are shown where data not applicable.

Independent Variables	All variables		Treatments forced in		PWS unfiltered		PWS filtered		Aquafine unfiltered		Aquafine filtered	
	Total	Fecal	Total	Fecal	Total	Fecal	Total	Fecal	Total	Fecal	Total	Fecal
Unit	1	1	X	X	X	X	X	X	X	X	X	X
Filtration	-	3	X	X	X	X	X	X	X	X	X	X
Voltage	4	4	X	X	1	-	2	1	-	-	-	-
Retention time	3	2	-	-	2	2	3	2	-	-	-	-
UV Intensity	-	-	-	-	-	1	-	-	-	-	-	-
Lamp Temp.	5	-	2	-	3	-	-	-	1	1	-	-
Dissolved O_2	-	5	-	1	-	3	-	-	-	-	-	-
Turbidity	2	-	1	-	-	-	1	-	-	-	-	-
UV Transmittance	-	-	-	-	-	-	-	-	-	2	-	-
pH	-	-	-	-	-	-	-	-	-	-	1	2
Sample size	136	136	136	136	36	36	34	34	34	34	32	32
R^2	.65	.64	.65	.64	.38	.52	.34	.40	.07	.20	.25	.29

Table 5. Correlations among water quality variables for the filtered and the unfiltered effluent. An entry indicates a significant (95%) correlation.

	Filtered									
Variable	1	2	3	4	5	6	7	8	9	10
1. UV absorbance	-									
2. Turbidity	.52	-								
3. Suspended solids	.51	.30	-							
4. TOC	.25			-						
5. Conductivity	.37		.31		-					
6. COD	.72	.42		.44		-				
7. Dissolved O_2							-			
8. Total iron		.34						-		
9. Water temp.									-	
10. pH	.58		.38		.52	.31				-

	Unfiltered									
	1	2	3	4	5	6	7	8	9	10
1. UV absorbance	-									
2. Turbidity	.60	-								
3. Suspended solids	.62	.66	-							
4. TOC	.42		.31	-						
5. Conductivity	.44	.39	.39		-					
6. COD	.68	.60	.69	.47		-				
7. Dissolved O_2		.41			.32		-			
8. Total iron								-		
9. Water temp.							.28		-	
10. pH	.63	.53	.49							-

EPA-287 (Cin.)
(4-76)

Table 6. Effects of filtration on mean water quality parameters and log survival of fecal coliforms in pilot plant study. Standard deviations shown in parentheses.

Parameter	Unfiltered	Filtered	Percent Difference
UV absorbance	0.179(.031)	0.161(.029)	10
UV transmittance (%)	66(4)	69(4)	5
Suspended solids (mg/l)	13.7(7.7)	3.8(4.1)	72
Turbidity (NTU)	4.9(1.8)	2.1(1.4)	57
Total organic carbon (mg/l)	10.1(2.9)	7.9(2.1)	22
COD (mg/l)	31.6(6.9)	23.4(7.9)	26
Total iron (mg/l)	0.59(.33)	0.53(.42)	10
Influent fecal coliforms[1]	5.29(.41)	5.15(.61)	--
Log survival, fecal coliform[2]	-3.08(.20)	-3.88(.19)	--

---

[1] Log (cells/ml).

[2] Data for Aquafine unit, low voltage, high flow shown as an example.

many of the variables are intercorrelated. The regression may choose one variable over a more directly related variable because the two are correlated with one another, but because of chance or analytical error, the first shows a slightly higher correlation with the dependent variable. Separation of the effects of the different water quality parameters was complicated by significant intercorrelations among them during the runs. Some of the variation in water quality during the runs was due to dilution. Severin (1978) also noted this problem in analysis of his pilot plant experiments. Only variables which significantly ($p < 0.05$) explain variation are shown in Table 4. Other variables which were not significant were: suspended solids, alkalinity, total organic carbon, NH_3-N, NO_2- +NO_3-N, total Kjeldahl-N and total iron. The numbers indicate the relative importance of the factors in the regression. If all variables are considered together, the unit, retention time (≈ flow rate), filtration status and voltage all are significant in that order when fecal coliform survival is considered. In addition, lamp temperature appears significant and may be related to voltage treatments. Dissolved oxygen also appears in the multiple correlation with all variables considered but when broken down by unit and filtration status appears only in the PWS, unfiltered regression on fecal coliforms. Dissolved oxygen is correlated significantly

BEGIN LAST LINE OF TEXT
BOTTOM OF IMAGE AREA, OUTSIDE DIMENSION FOR TABLES AND ILLUSTRATIONS
3/8"

EPA-287 (Cin.)
(4-76)

(but with low r) with turbidity and conductivity in the unfiltered treatments.

When the regressions were broken down by unit and filtration status, differences emerged in the response to the other treatments (applied voltage and retention time) and the randomly varying parameters. The PWS unit showed a more definite response to the dose related variables, applied voltage and retention time. The survival means (Table 3) showed the reverse of the expected results in the applied voltage treatments in the Aquafine unit at the slower flow rate. Otherwise, the other means showed small but expected dose-response related differences (checks of the UV intensity and original data bore out these unexpected responses to applied voltage). These results were probably one reason why the Aquafine unit showed no significant voltage or retention time effects. Lamp temperature was significant in the Aquafine, unfiltered treatment regression and was simultaneously correlated with applied voltage and flow rate. Among the other variables, UV intensity (at the reactor wall) appeared only once and probably replaced applied voltage as a treatment related variable. Other variables which appeared were dissolved oxygen, turbidity, UV transmittance, and pH. Perhaps the most notable was the absence of a consistent correlation with UV transmittance which is related to average intensity. In fact, none of the water quality variables appeared consistently. It may be noted that pH correlated somewhat with several other variables including UV absorbance, turbidity, suspended solids, conductivity and dissolved oxygen. The multiple r^2 was high only for the regressions in which all data were entered and for one of the PWS unfiltered treatments.

To summarize the results of the stepwise regressions with randomly varying water quality parameters:

1) the treatments made a difference as to what variables were significant.

2) no single water quality parameter consistently correlated with log coliform survival.

The most likely cause for the lack of significance of UV transmittance in the multiple regressions was the lack of a large variation in the UV transmittance during the experiments. The coefficient of variation for UV transmittance was only 6% for the unfiltered water and 6% for the filtered water. The UV intensity measured at the reactor wall showed an average coefficient of variation of only 19% for the Aquafine and only 9% for the PWS units. This variation may be regarded as maximum since for a given UV absorbance, the % UV transmitted declines as the path length increases when expressed as a % of maximum (absorbance = 0). Thus the variation in UV at the farthest point from the reactor wall as a % of the mean was probably much greater than that of the average intensity. The random variation in average UV intensity due to random water quality variations during the experiments may not have been great enough to be separated from other confounding variables.

Prediction of spectrophotometric UV absorbance from water quality parameters

Stepwise multiple regression of the major water quality parameters on

BEGIN LAST LINE OF TEXT
BOTTOM OF IMAGE AREA OUTSIDE DIMENSION FOR TABLES AND ILLUSTRATIONS
9-1/8"
3/8"
PAGE NUMBER
EPA-287 (Cin.)
(4-76)

spectrophotometric UV absorbance (Table 7) showed the fecal or total coliform densities to best predict the absorbance. The regressions were broken down by filtration status. The difference between the filtered and unfiltered r^2 was slight. The total and fecal coliform parameters were probably interchangeable with one another in the two regressions. Suspended solids and either turbidity or COD also entered the regressions. However, when the coliform densities were excluded from consideration, COD became the major factor predicting the variation in UV absorbance . Turbidity, suspended solids, and conductivity appeared as lesser factors.

Table 7. Stepwise multiple regression of the effects of selected randomly varying water quality parameters on the UV absorbance (spectrophotometric) for unfiltered and filtered treatments.

Model:
UV absorbance = turbidity, suspended solids, COD, TOC, conductivity, fecal and total coliforms before irradiation

Unfiltered		Filtered	
Variable added to regression	Multiple R^2	Variable added to regression	Multiple R^2
Fecal coliforms	.60	Total coliforms	.55
Suspended solids	.69	Suspended solids	.64
Turbidity	.71	COD	.66

Model:
same as above but excluding both fecal and total coliforms in influent

Unfiltered		Filtered	
Variable added to regression	Multiple R^2	Variable added to regression	Multiple R^2
COD	.45	COD	.41
Turbidity	.53	Suspended solids	.54
		Conductivity	.56

The prediction of a substantial part of the variation in absorbance by coliform densities does not necessarily mean that the bacterial cells themselves caused most of the absorbance. Filtration (0.45 μ) of samples indicated that most of the UV absorbance was caused by the soluble component (results shown later). The soluble absorbers may have been closely associated with the bacterial titers, however. The partial replacement of coliform titers by COD in the second model may be an indication of the fact that the COD reflects both the soluble and particulate organics. Another explanation may be that the particulate absorbance component varied more than the larger soluble absorbance component.

One factor which made prediction of UV absorbance from the common water quality parameters more difficult was that the UV absorbance was the sum of a soluble and a particulate component which could vary independently. Figure 13 shows an effort to predict the spectrophotometric absorbance of the particulate fraction from the turbidity. Data were selected where dual media filtered and unfiltered samples were taken from the same effluent batch. The Δ spectrophotometric absorbance (unfiltered - filtered) was plotted against the Δ turbidity (NTU)(unfiltered - filtered). These values were assumed to be the absorbance and turbidity of the particles removed by the dual-media filter. The data fit a regression line $y = .010\ x + .004$ with $r = .74$. Thus the dual media filterable particulates showed about .009 spectrophotometric units per NTU, but there was much variation. The dual media filtration tended to remove the larger particles (Table 6) and did not completely reduce the turbidity. Thus, the results do not represent the entire particulate fraction.

Poliovirus inoculation results

A culture of poliovirus was mixed with a batch of secondary effluent to compare its survival with that of the fecal coliforms in the pilot plant unit treatments (Table 8). The means shown represent only two replicate runs on one batch of inoculated effluent as opposed to 8 or 9 runs per treatment in the coliform experiments. Kills of the poliovirus were generally greater than those of the fecal coliforms. Furthermore, the virus inactivation patterns conformed more to those expected from the applied voltages and flow rates. There was no difference between the filtration treatments, but it must be remembered that the viruses were added as a spike and were not protected by particulate matter.

Photoreactivation results

The log survival of several UV irradiated samples exposed to 75 minutes of sunlight is plotted against the log survival of the dark control sample in Figure 14. The dark control was the same UV treated sample held in the dark for 75 minutes. Four samples were from PWS runs and four were from Aquafine runs. The straight line indicates where there would be no effect of photoreactivation. The vertical distance from the line to the points represents the photoreactivation. Photoreactivation increased survival an average of .97 log units and ranged from .14 to 1.81 log unit increases.

BEGIN LAST LINE OF TEXT
BOTTOM OF IMAGE AREA; OUTSIDE DIMENSION FOR TABLES AND ILLUSTRATIONS
3/8"

EPA-287 (Cin.)
(4-76)

Table 8. Survival of poliovirus (plaque forming units) inoculated into secondary effluent

		Poliovirus (-log survival)[1]			
		Aquafine		Pure Water Systems	
Flow rate (gpm)	Voltage	Unfiltered	Filtered	Unfiltered	Filtered
35	60	3.10	3.18	2.26	2.14
	120	>4.74	4.74	2.79	2.61
75	60	2.29	2.18	1.96	1.61
	120	4.74	>4.74	2.29	2.06

---

[1] initial titer was 4.44 pfu/ml for all treatments

6-1/2"

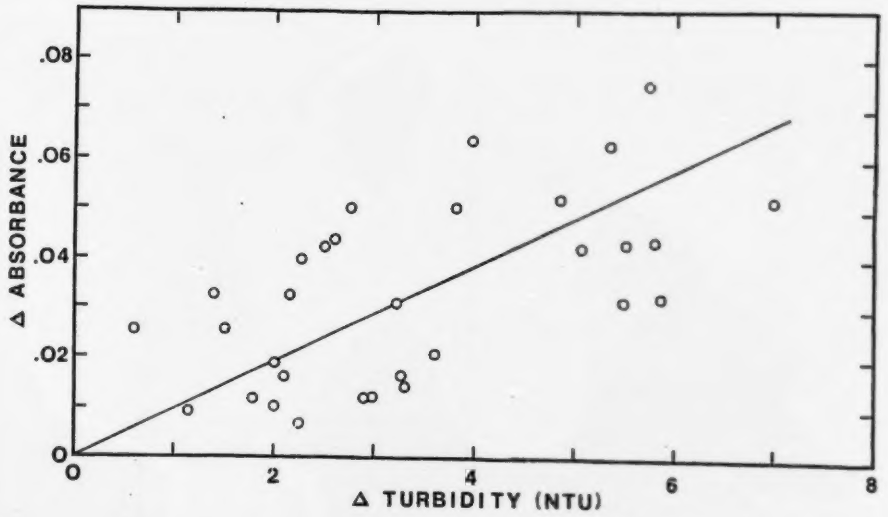

Fig. 13. Δ turbidity (unfiltered-filtered) vs. Δ absorbance for only paired samples in pilot study of dual media filtration.

BEGIN LAST LINE OF TEXT
BOTTOM OF IMAGE AREA; OUTSIDE DIMENSION FOR TABLES AND ILLUSTRATIONS
3/8"

EPA-287 (Cin.)
(4-76)

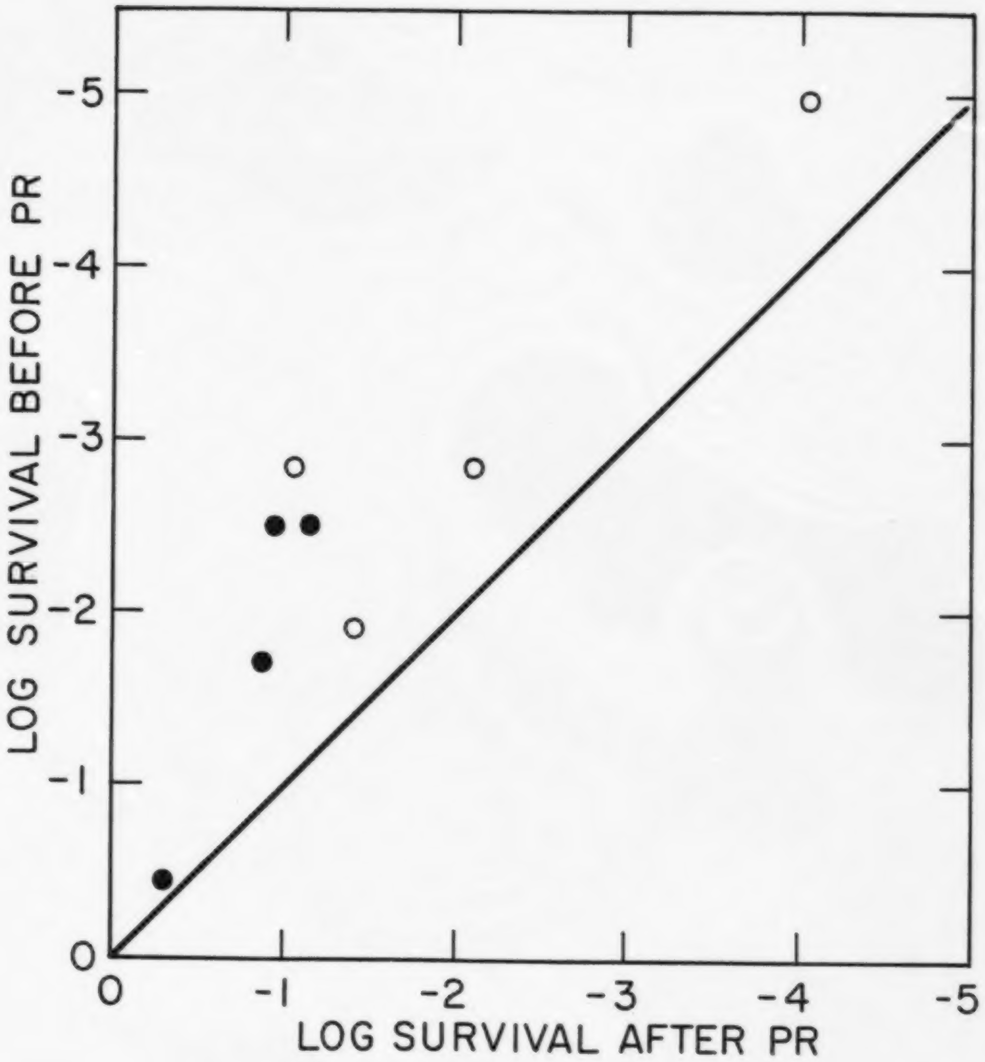

Fig. 14. Photoreactivation; log survival of UV irradiated effluent total coliform exposed to 75 minutes of sunlight shown vs. log survival of the dark controls. Solid symbols were from the PWS unit samples and open symbols from the aquafine unit samples.

The data showed no clear pattern of differences as a function of log survival of the dark controls. The latter samples were also treated for 45 minutes of photoreactivating light and the log reductions of the photoreactivated samples were not significantly different.

To study the effect of temperature, tests of photoreactivation at 25°C and 4°C was made on three samples. Two showed much greater photoreactivation at 25° but a third sample showed less. Thus, a t-test showed no significant effect due to temperature.

ESTIMATION OF DOSE IN PILOT PLANT EXPERIMENTS

Summary

In order to compare units and compare log survivals in terms of a dose response curve, it was necessary to estimate dose and separately estimate the retention time and the average dose rate.

1) Dye studies revealed considerable flow dispersion in the Aquafine reactor. Thus, considerable volumes of fluid were exposed for less than the theoretical retention (RT) time (volume/flow rate), but the average RT (centroid of dispersion curve) was close to the theoretical RT. In contrast, the PWS unit exhibited a severely skewed dispersion curve. The average RT was much less than the theoretical RT. Thus, theoretical RT was of little value in comparing doses.

2) Intensity readings taken at the wall of the reactor were of little use in estimating doses.

3) Attempts were made to measure the output of the units by *in situ* ferrioxalate actinometry. Using flow rate in the calculations of actinometry dose produces some problems related to non-ideal flow. The UV output calculated by actinometry is higher than that accounted for by either rated UV output or the spherical integration method.

4) *E. coli* B proved too sensitive to provide an *in situ* relative assay of dose and showed no dose response. Differences between survival in the two units illustrated the effects of non-ideal flow.

Dye studies of retention time

Dye injection distribution curves for the Aquafine and Pure Water Systems Units (Figures 15 and 16 respectively) both showed considerable dispersion. The curves for the Aquafine unit are relatively symmetrical and the theoretical retention times (volume/flow rate) are not too different from the average actual retention times (centroid of distribution curves). However, at an average retention time of 3.75 sec, at least 10% of the dye had exited by

BEGIN FIRST LINE OF TEXT HERE
CENTER OF PAGE
TOP OF IMAGE AREA
DROPPED HEAD, BEGIN SECTIONS HERE
BEGIN LAST LINE OF TEXT
BOTTOM OF IMAGE AREA, OUTSIDE DIMENSION FOR TABLES AND ILLUSTRATIONS
3/8"
PAGE NUMBER
EPA-287 (Cin.)
(4-76)

TYPING GUIDE SHEET
BEGIN FIRST LINE OF TEXT HERE
DROPPED HEAD: BEGIN SECTIONS HERE
CENTER OF PAGE
TOP OF IMAGE AREA
BEGIN LAST LINE OF TEXT
BOTTOM OF IMAGE AREA; OUTSIDE DIMENSION FOR TABLES AND ILLUSTRATIONS
3/8"

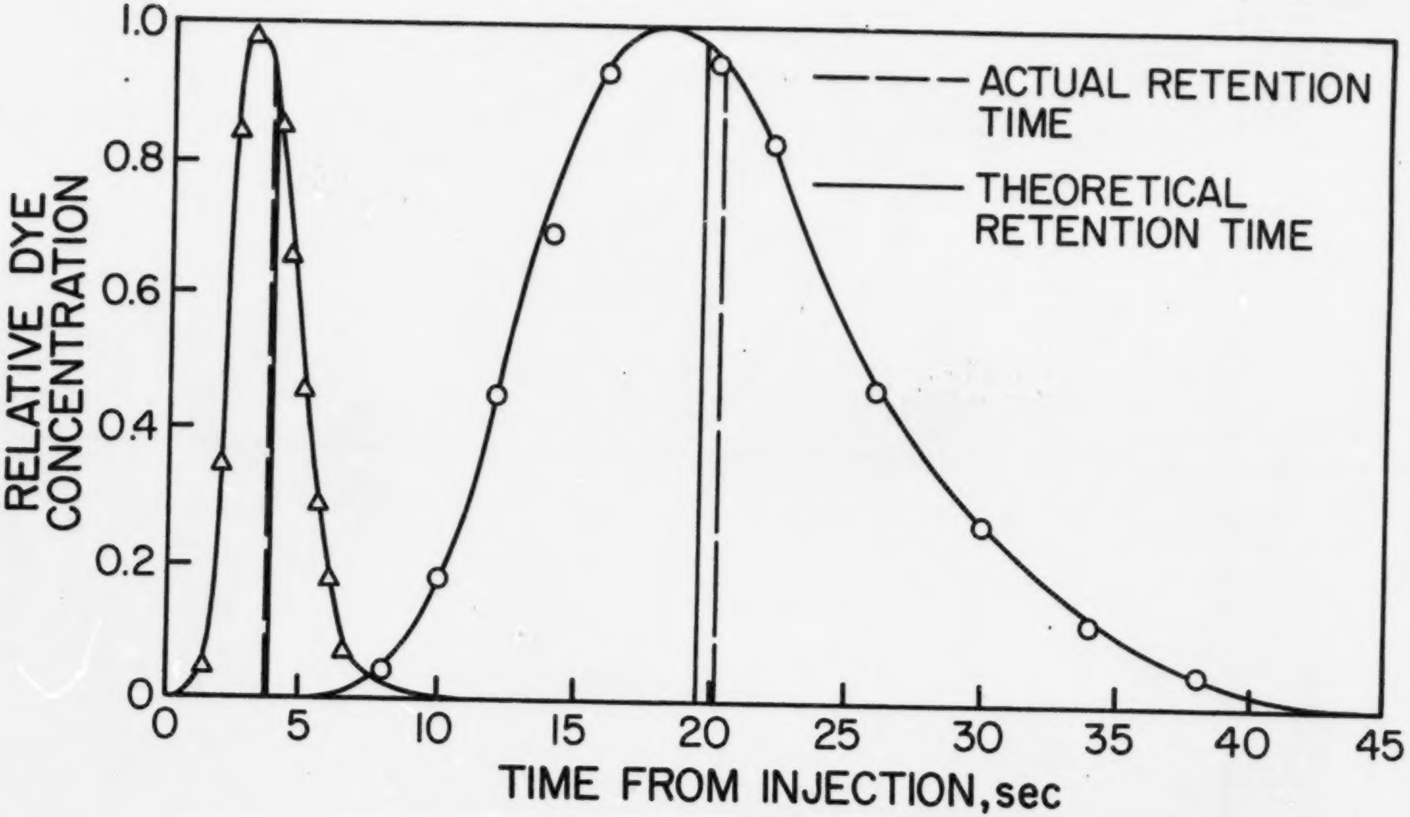

Fig. 15. Aquafine unit dye studies at flow rates of 2.87 and 0.56 l/sec.

EPA-287 (Cin.)
(4-76)

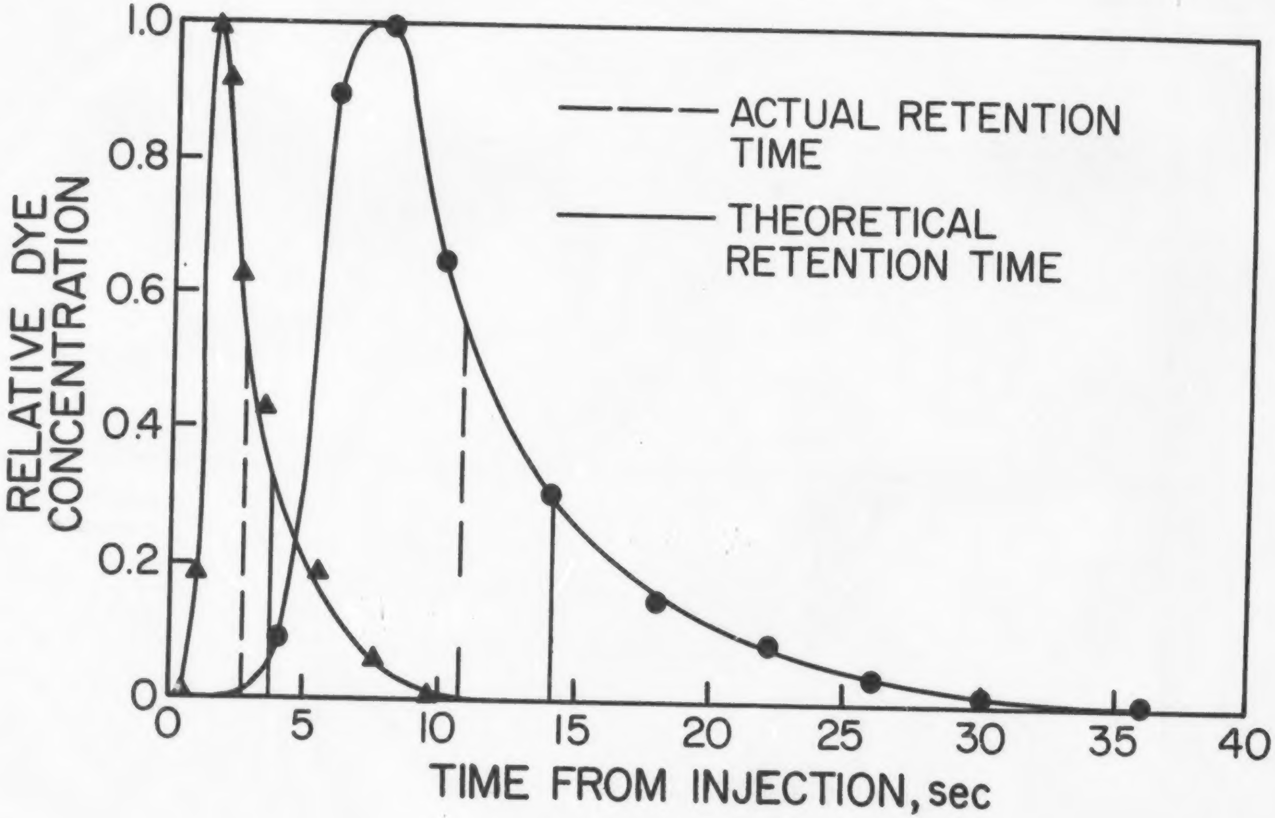

Fig. 16. PWS unit dye studies at flow rates of 2.04 and 0.56 l/sec.

TYPING GUIDE SHEET
BEGIN FIRST LINE OF TEXT HERE
CENTER OF PAGE
TOP OF IMAGE AREA
DROPPED HEAD: BEGIN SECTIONS HERE
BEGIN LAST LINE OF TEXT
BOTTOM OF IMAGE AREA, OUTSIDE DIMENSION FOR TABLES AND ILLUSTRATIONS
3/8"
PAGE NUMBER
EPA-287 (Cin.)
(4-76)

2.25 sec.

The flow distribution in the Pure Water Systems unit was highly skewed. The average retention times were considerably shorter than the theoretical retention times. For example, at a theoretical retention time of 4.9 sec, the average retention time was only 2.8 sec, but at least 10% of the dye had exited by about 1.4 sec. Thus, this unit exhibited severe short circuiting of flow, probably because some of the water traveled to the ends of the distribution tube and exited by the nearest exit holes in the exit distribution tube. The retention times shown include the time spent in the distribution tubes. The dye front did not enter the actual disinfection chamber at once. The volume of the actual disinfection chamber was 5.82 ℓ while the total volume was 9.77 ℓ. To calculate exact exposure times for separate fractions of the flow distribution, it must be assumed that the time spent in the UV chamber is proportional to that spent in the whole unit and that these are inversely proportional to the volumes of the UV chamber and the entire unit.

In situ estimations of UV output and dose

Actinometry doses for both reactors are shown as a function of (1) applied voltages (but shown as the corresponding UV intensity at the reactor wall in flowing tap water) at several flow rates and (2) as a function of theoretical retention time at several applied voltages (as UV intensity) (Figures 17 and 18). Actinometry doses are expressed as energy per unit volume of fluid which more directly reflects the method of measurement than the expression of dose as intensity times time. These actinometry doses should be proportional to total UV output rather than the average intensity within the reactors since the solution absorbs all the light emitted. All points shown are the average of two replicate runs.

The actinometry curves should ideally be linear as a function of UV intensity at the reactor wall (in a non-absorbing medium) and as a function of retention time. However, for the Aquafine unit, erratic results were obtained at the low voltage settings. After several runs were performed, it was discovered that three of the lamps shut off at some voltage below 60 which was apparently dependent on the lamp temperature. At the 56 V input level used in two of the runs, three of the lamps were known to be out. Thus unusually low actinometry doses were obtained at this setting since intensity data were taken from several tap water runs. However, when 47 V were used, a similar effect should have been observed, yet all six lamps were operating at that time. Lamp temperatures were lower during those runs and the voltage at which the lamps cut off was found to decrease to 45 to 50 V at these colder temperatures.

The PWS lines of actinometry dose vs. UV intensity were consistently nonlinear. The actinometry procedure measures some non-germicidal light that is emitted by the lamps, and the ratio of light at 254 nm to other wavelengths may change as a function of applied voltage. Also, differences between lamps in output as a function of applied voltage may result in bias in the readings at the reactor wall since the UV intensity probes respond mainly to the near-

BEGIN LAST LINE OF TEXT
BOTTOM OF IMAGE AREA, OUTSIDE DIMENSION FOR TABLES AND ILLUSTRATIONS
3/8"

PAGE NUMBER
EPA-287 (Cin.)
(4-76)

TYPING GUIDE SHEET

BEGIN FIRST LINE OF TEXT HERE

DROPPED HEAD; BEGIN SECTIONS HERE

CENTER OF PAGE

TOP OF IMAGE AREA

BEGIN LAST LINE OF TEXT

BOTTOM OF IMAGE AREA, OUTSIDE DIMENSION FOR TABLES AND ILLUSTRATIONS

3/8"

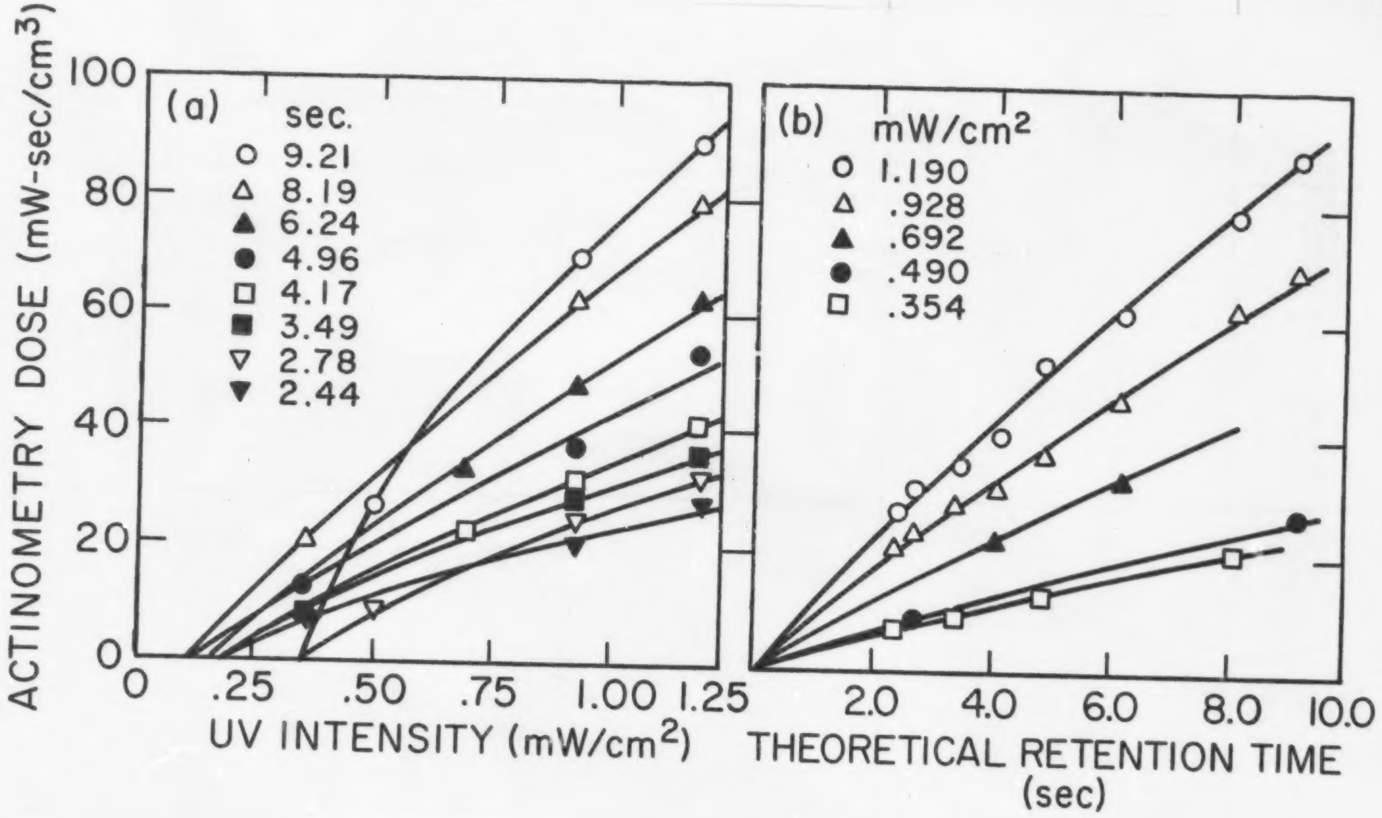

Fig. 17. Aquafine unit actinometry dosages vs. a) UV intensity at reactor wall and b) theoretical retention time.

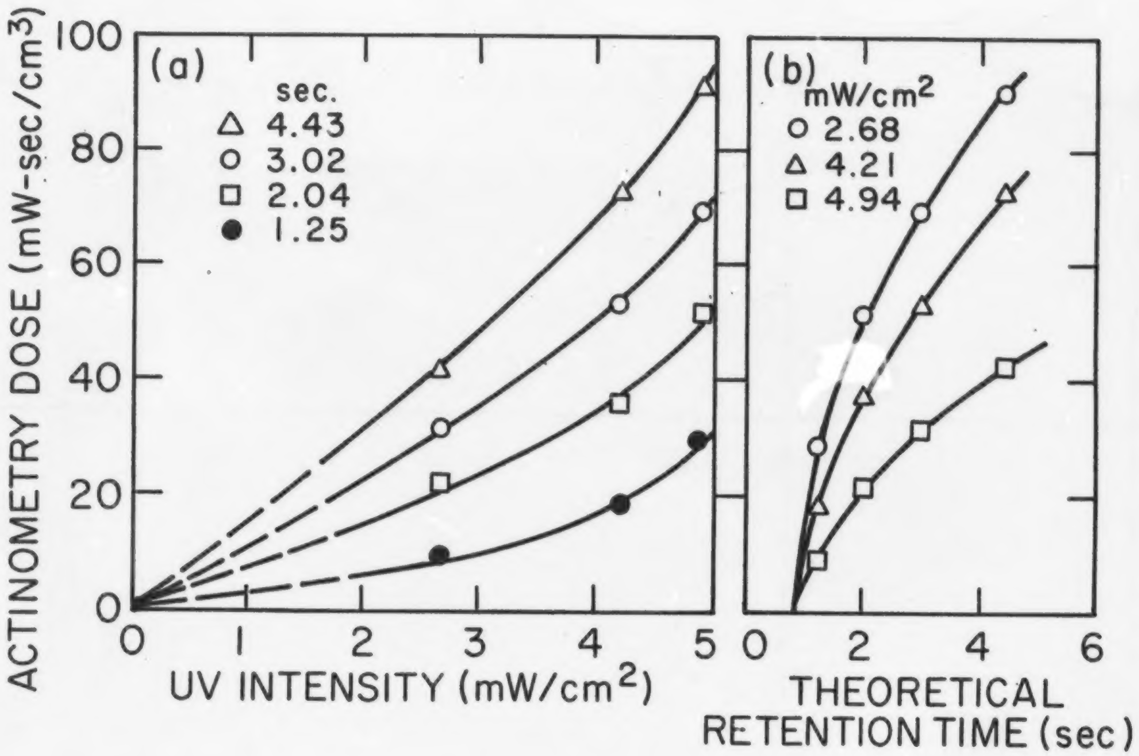

Fig. 18. Pure water systems unit actinometry dosages vs. a) UV intensity at reactor wall and b) theoretical retention time.

BEGIN LAST LINE OF TEXT
BOTTOM OF IMAGE AREA; OUTSIDE DIMENSION FOR TABLES AND ILLUSTRATIONS
3/8"

EPA-287 (Cin.)
(4-76)

est lamps. While curves of actinometry dose vs. theoretical retention time are reasonably linear for the Aquafine unit, those for the PWS unit again reflect the non-ideal flow patterns. For the PWS unit only the volume of the UV exposure chamber itself was used to calculate theoretical exposure times. The fact that the lines are curved and do not intersect zero may be due to the fact that ratio of the average retention time to the theoretical retention time was not constant as a function of flow rate and that the relative retention times in the distribution tube and the exposure chamber were not inversely proportional to their volumes.

Comparison of the PWS and Aquafine reactors are limited by biases in the methods of dose estimation. The intensity at the reactor wall in the PWS reactor is 4.02 times that of the Aquafine reactor but the different placement of the probes in the reactor clearly biases the comparison. The presumed measurement of UV dose per retention time by actinometry in the PSW unit was 2.23 times that of the Aquafine unit at full voltages and comparable flow rates. The rated total input wattage for the PWS was 350 W and 240 W for the Aquafine. The total output wattage at 254 nm measured by the spherical integration method (performed on one lamp) was 77.8 W for the PWS and 62.3 W for the Aquafine units. However, calculations of output from the actinometry dose divided by flow rate (at full V) yield total outputs of 133 W for the PWS and 113 W for the Aquafine units. Though the ratios are similar, the actinometry measurement appears to yield a high value for output, perhaps partially because some light not at 254 nm is included in the actinometry measurement. However, the rated efficiencies would not appear to account for that much non-254 light (Voltarc information circular).

We made an initial attempt to measure relative doses in the two UV units using tap water solutions inoculated with pure cultures of the *E. coli* B strain. No dose response was found in experiments where both lamp voltage and retention time were varied (Figures 19 and 20). To verify this statistically, a two-way analysis of variance was performed on all of the data excluding those results obtained at the 88 voltage level. At the 95% confidence level, we found no effect of theoretical retention time or voltage on log survival. The UV intensities recorded at the wall of the reactors as each sample was drawn varied about 25% throughout the experiments at a given voltage. Perhaps the output of the lamps varied somewhat during the experiments. However, these variations were not as great as those due to changes in voltage and thus random variations did not cause the lack of dose response.

Results are shown two ways: (1) log survival plotted vs. conventional dose, calculated as the radiometer "intensity" reading at the wall of the reactor times the theoretical retention time, and (2) log survival plotted vs. the ferrioxalate actinometry "dose" expressed as mW - sec/cm^3. Neither method of expression of relative dose attempted to express the true dose by taking into account the distribution of retention times or the average dose rate. Use of the radiometer "intensity" at the wall represents at best a minimum measure of dose rate and may be biased by placement, proximity to the nearest lamps, and systematic differences in the planar and three dimensional energy flux density as the absorbance varies.

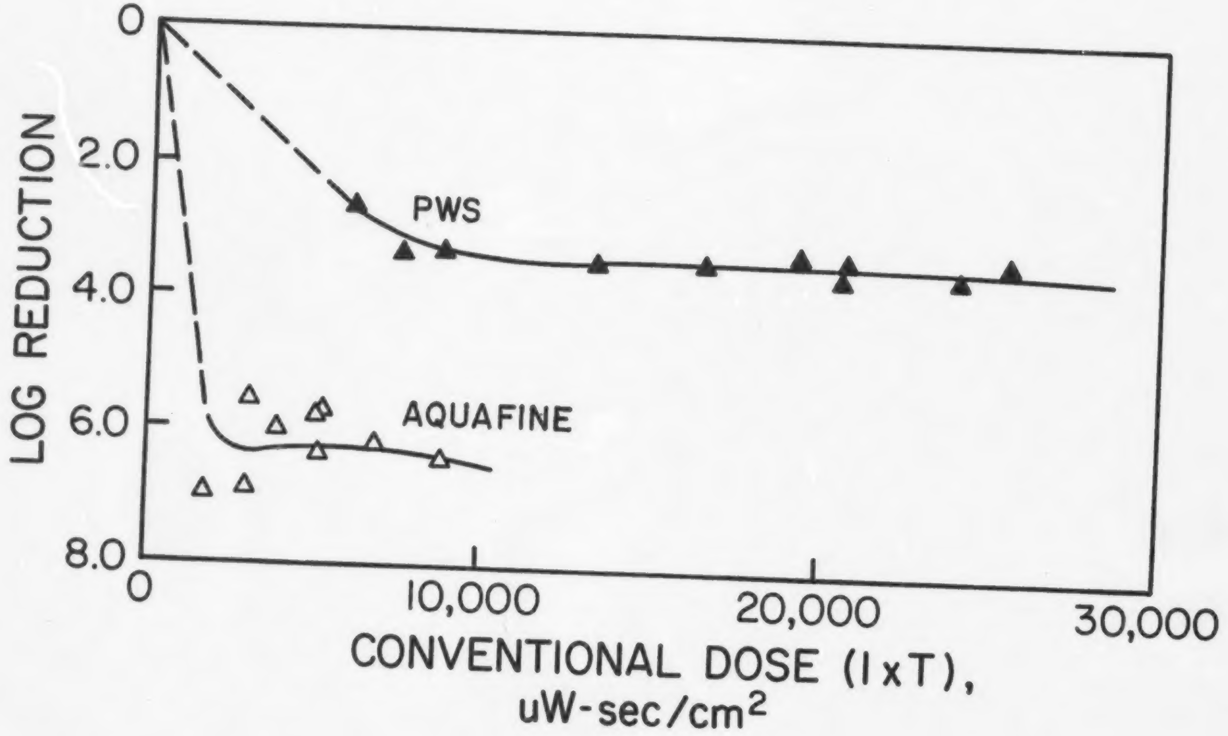

Fig. 19. Log reductions of E. coli vs. conventional dose.

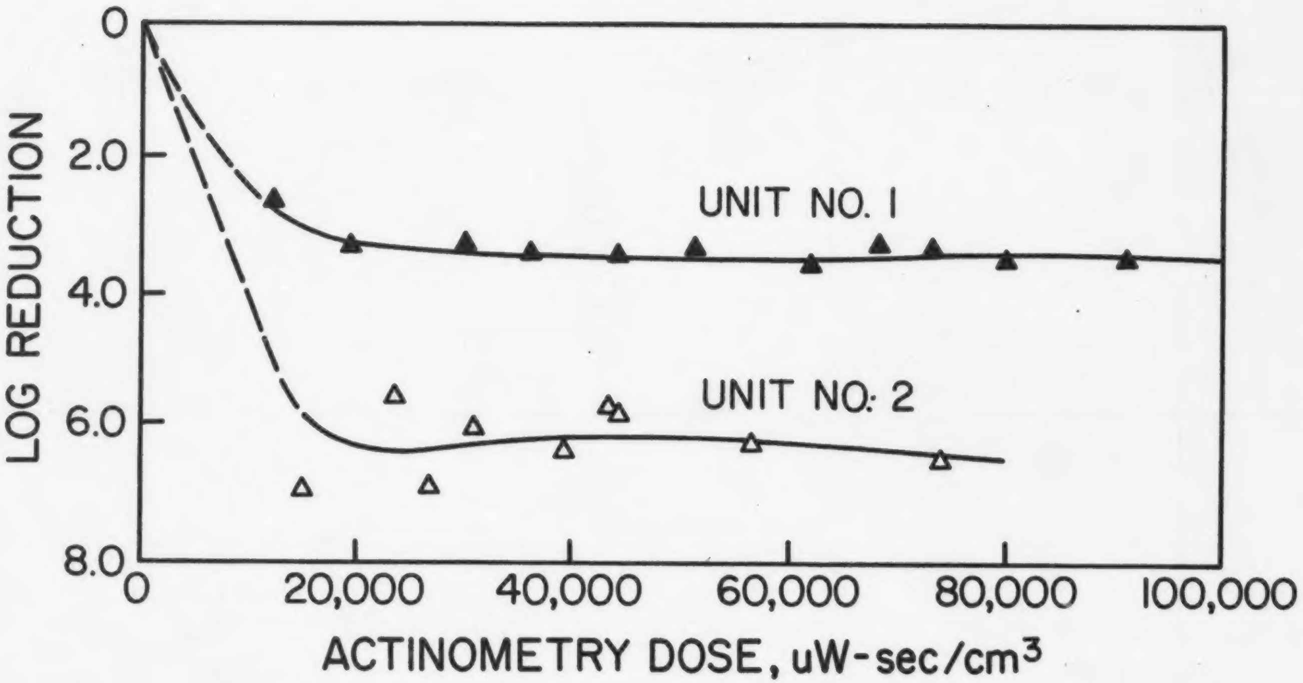

Fig. 20. Log reductions of E. coli vs. actinometry dose.

BEGIN LAST LINE OF TEXT
BOTTOM OF IMAGE AREA; OUTSIDE DIMENSION FOR TABLES AND ILLUSTRATIONS
3/8"
PAGE NUMBER
EPA-287 (Cin.)
(4-76)

We later found that the diatomaceous earth added to reduce the dose rate produced little true UV absorbance compared to its scattering of UV. The retention times and lower dose rates needed to show a dose response could not be achieved with such a sensitive strain of E. coli, using the commercial units. The low survival of bacteria in the Aquafine reactor meant that most effluents contained less than 100 MPN/100 ml, and the survivors were less than 1 in 10^6, which may easily include aggregated bacteria. Thus the strain was too sensitive to achieve reasonable measurements on the Aquafine reactor. While the PWS reactor showed much higher survival, the highly skewed flow distribution and possible lack of a linear relationship of theoretical retention time and retention time of the first significant flow fraction must be considered. Comparison of the results of actinometry and E. coli inoculation data show that the short circuiting in the PWS reactor produces a greater difference between the two reactors when the bacteria are used because the bacterial count decreases more or less exponentially with dose, while the Fe^{2+} produced by actinometry varies linearly with dose.

LABORATORY EXPERIMENTAL RESULTS AND DISCUSSION

Separating effects of absorbance and scattering

Summary

9-1/8"

To calculate and test methods of estimating average dose rates in wastewater effluent it was first necessary to separate the effects of true absorbance and scattering.

1) Most of the spectrophotometric absorbance of the secondary and tertiary effluents examined was due to dissolved components. Of the spectrophotometric absorbance due to particulates, most was due to particles between .45 and 70 μm.

2) Strains of E. coli used proved too sensitive to UV to enable construction of useful dose response curves for high doses. However, later tests with a stock of B. subtilis spores showed that the spores were sufficiently resistant to make possible the study of a wide range of dose levels. The spores also showed better reproducibility and were easier to handle when used as a calibrated biological assay for UV dose.

3) The extrapolation method worked well in the colorless artificial turbidity solutions and showed the spectrophotometric absorbance greatly overestimated the true absorption in these solutions. However, since the wastewater effluent showed true absorption in the visible wavelengths, the extrapolation method could not be used.

4) By using .45 μm filtered effluent to dilute unfiltered effluent, the particulate absorbing and scattering component was varied independently of the soluble absorbance. The bioassay technique was then used to estimate the true absorbance and scattering as a function of turbidity.

BEGIN LAST LINE OF TEXT
BOTTOM OF IMAGE AREA; OUTSIDE DIMENSION FOR TABLES AND ILLUSTRATIONS
3/8"

PAGE NUMBER
EPA-287 (Cin.)
(4-76)

Scattering appeared to comprise about 25% of the spectrophotometric absorbance due to the particulate component. This was only slightly more than the forward scattering measured by the opalescent plate method.

5) Using these methods to estimate true absorbance in effluent samples, the effects of protection of bacteria by particles was found to be significant by examining survival curves of effluent with various particle sizes filtered out.

Results

Spectrophotometric UV absorbance of various fractions of a Sandy Creek secondary effluent sample (Table 9) showed that most of the spectrophotometric absorbance was associated with the soluble fraction. The ultrafiltrate excluded particles over the 10^4 Dalton nominal molecular weight. Thus, it was unlikely to contain particles of the size to cause significant scattering. Indeed, its absorbance was similar to the .8 and .22μ filtrate absorbances. The value of the .45μ filtrate was anomalously lower than that sample for unknown reasons. Nevertheless, most of the particulate spectrophotometric absorbance was due to particles between 0.8 and 5μ, the size of bacteria and possibly of small aggregates of bacterial detritus. The soluble component was not ether extractable but about half was XAD-2 resin extractable.

9-1/8"

Table 9. Spectrophotometric absorbance of various fractions of Sandy Creek secondary effluent at 254 nm.

Treatment	Absorbance
unfiltered	.215
5 filtered	.197
0.8 filtered	.173
0.45 filtered	.142
0.22 filtered	.168
ultrafiltrate (10^4 Dalton NMW)	.168
0.45 μ filtered and ether extracted	.142
0.45 μ filtered and XAD-2 extracted	.075

BEGIN LAST LINE OF TEXT
BOTTOM OF IMAGE AREA; OUTSIDE DIMENSION FOR TABLES AND ILLUSTRATIONS
3/8"

PAGE NUMBER
EPA-287 (Cin.)
(4-78)

Initially an *E. coli* B strain was used for the bioassay procedure, but it proved quite sensitive to UV compared to natural unfiltered effluent *E. coli* (see later results). The calibration curve of log survival vs. dose (Figure 21) in the collimated beam appears fairly linear as far as -3.5 logs survival. Other experiments, however, showed a leveling out of the curve at -5 or -6 log survivals. Each point shown on Figure 21 is the result of 1 trial with 2 plate counts.

The dose-survival calibration curve for *Bacillus subtilis* spores (Figure 22) showed that they are about ten times more resistant than the *E. coli* B strain. They showed less scatter and better reproducibility. Five runs were performed during the study with exposures at about every 0.5 log survival to -4.5 logs. The curve has a "shoulder" but appears to be linear from at least -0.7 to about -4 log survival, as exemplified by the high correlation (r^2= 0.96). the curve appears to begin flattening out at -4.5 log survival and to show increased scatter. This survival curve may be compared with others shown in Figure 2. The spores appear more resistant than most cited coliform curves except that of Scheible and Bassel (1979); however, the method of dose estimation must be considered.

The use of the extrapolation method and the role of scattering and absorbance in artificial turbidity solutions using *E. coli* B to assay dose appears in Figures 23 and 24. Figure 23 shows log survival in solutions of several turbidities and three depths (0.5, 1 and 4 cm) where dose is calculated using the spectrophotometric absorbance, Equation 2. The I_0 was measured with the radiometer in the collimated beam apparatus. The greater the turbidity and depth, the greater the deviation from the line described by the calibration curve. However, when the extrapolation method was used to separate the scattering and true absorbances, and the true absorbance was used in Equation 2 to calculate dose, the scatter was greatly reduced (Figure 24) and the regression line was similar to the calibration curve regression (Figure 21). Note that the lower the percentage of transmission of the solution, e.g. higher absorbance or greater path length, the greater the effect of an erroneous absorbance on the calculated dose.

The spectrophotometric absorbance of the artificial turbidity solutions was separated into filterable (0.45μ) and nonfilterable scattering and absorbance (Table 10). The true absorbance averaged 33% of the spectrophotometric absorbance of the unfiltered solutions but 75% of the filtered solutions. Apparently the lysis of the cells during autoclaving to produce the artificial turbidity may have released some subcellular particles smaller than 0.45μ which scattered light, assuming the method was accurate. However, most true absorbance passed the filter. A secondary effluent of high turbidity was subjected to the same fractionation but the extrapolation method was found to be inapplicable because it absorbed throughout the spectrum. Ultrafiltered samples of several secondary and tertiary effluents showed absorption at wavelengths up to 600 nm. Since it was assumed the ultrafilter eliminated any particles large enough to cause significant scatter, the absorbance was true absorbance. Since one must extrapolate from a region of the spectrum where there is only scatter and no true absorbance, the extrapolation method could not be applied.

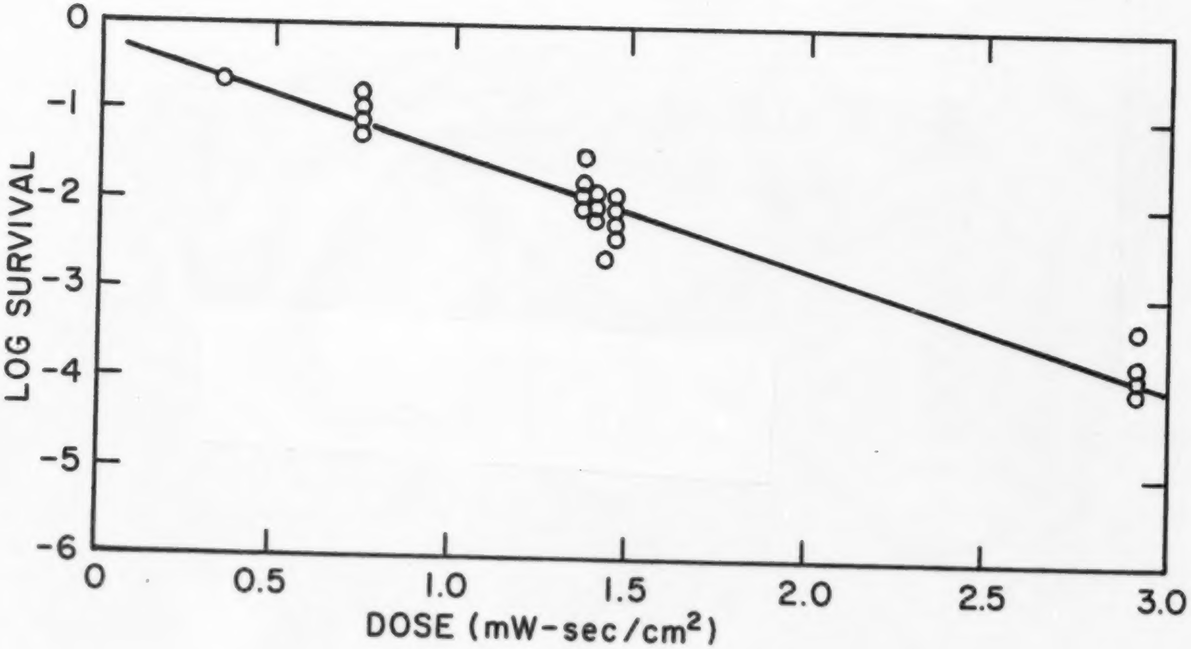

Fig. 21. *E. coli* B calibration curve, log survival vs. dose in collimated beam. Regression line: $y=-1.2x-0.2$, $r^2=.90$.

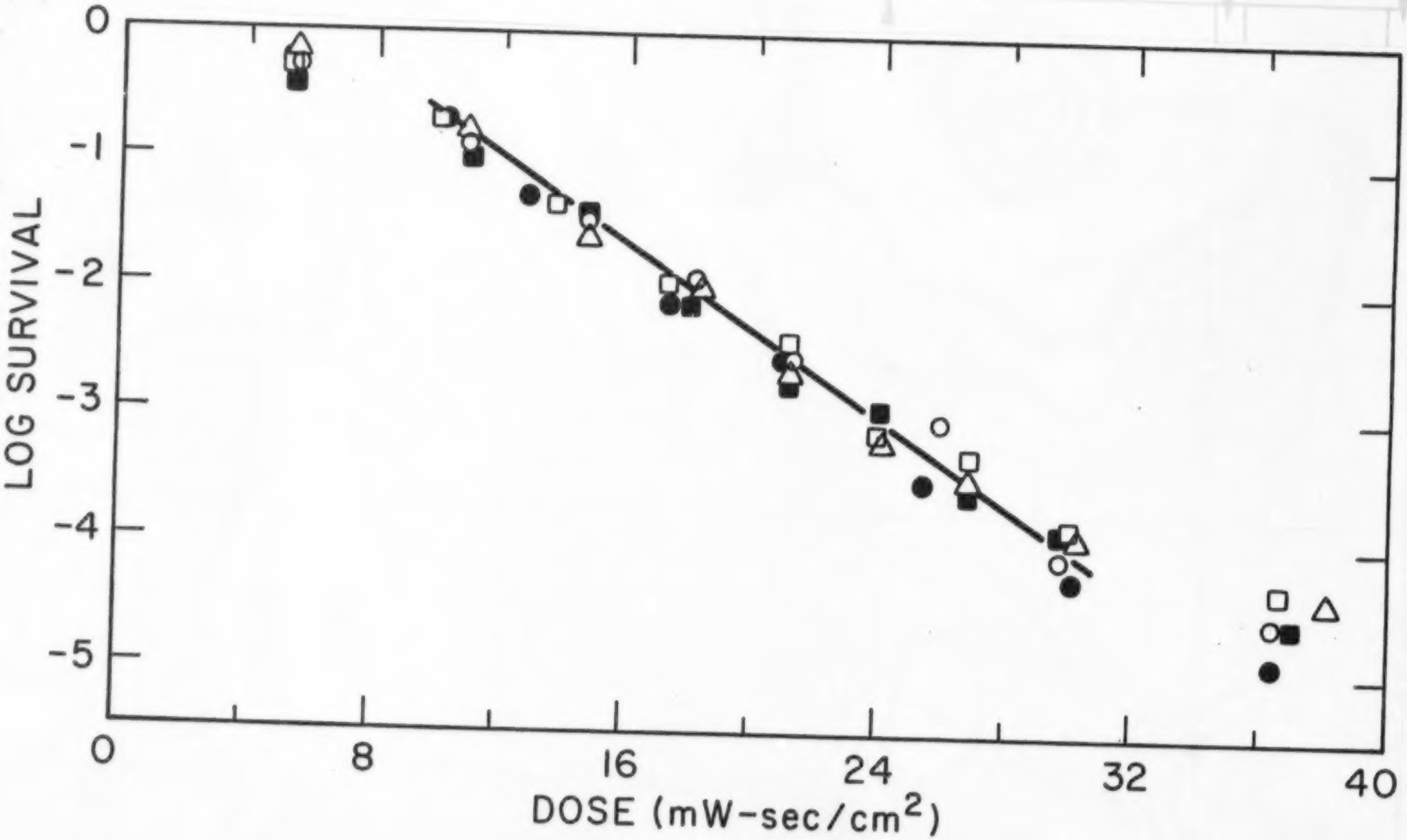

Fig. 22. Log survival of *Bacillus subtilis* spores vs. UV dose in a collimated beam of known dose rate. Different symbols represent 5 different runs. Data from doses of 10-30.5 mW/cm^2 appeared linear and fit the regression line $y = -.167 + 1.01$ ($r^2 = .96$).

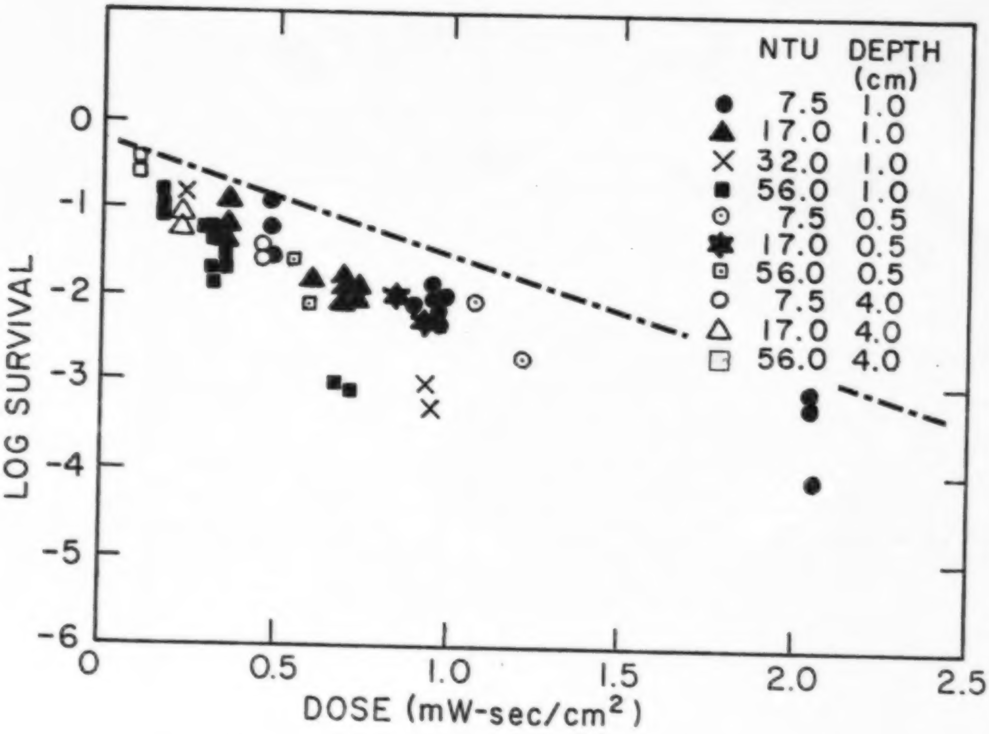

Fig. 23. E. coli B log survival in solutions of various turbidities (NTU) and depths in a collimated beam. Dose is calculated using the spectrophotometric absorbance. Broken line represents calibration curve (Fig. 21).

Spectra of both unfiltered and filtered fractions of a Chapel Hill tertiary effluent sample (14 NTU) are shown using regular and opalescent plate cells (Figure 25). The back face of 2 scratched quartz cells were ground so as to be opalescent. Oil saturated paper may be attached to the quartz face for the same effect (Shibata et al., 1954). The opalescent plate corrects only for forward scatter within our cell and may have varied from 30° to almost 90° depending on the position in the cell. The Latimer-Eubanks correction for total scatter again depended on finding an area of the spectrum with no true absorbance. Although nearly all of the spectrophotometric absorbance at 600 nm was due to the particulate fraction, we could not be assured that all of the particulate spectrophotometric absorbance was due to scatter. In fact, the slightly grey appearance of the centrifuged particles made it appear likely that there was some true absorbance at 600 nm. The filtered sample spectra indicate that there was little or no scattering in the $.45\mu$ filtrate and its similarity to the absorbances of the ultrafiltrate indicates it was soluble absorbance.

BEGIN LAST LINE OF TEXT
BOTTOM OF IMAGE AREA OUTSIDE DIMENSION FOR TABLES AND ILLUSTRATIONS
3/8"
PAGE NUMBER
EPA-287 (Cin.) (4-76)

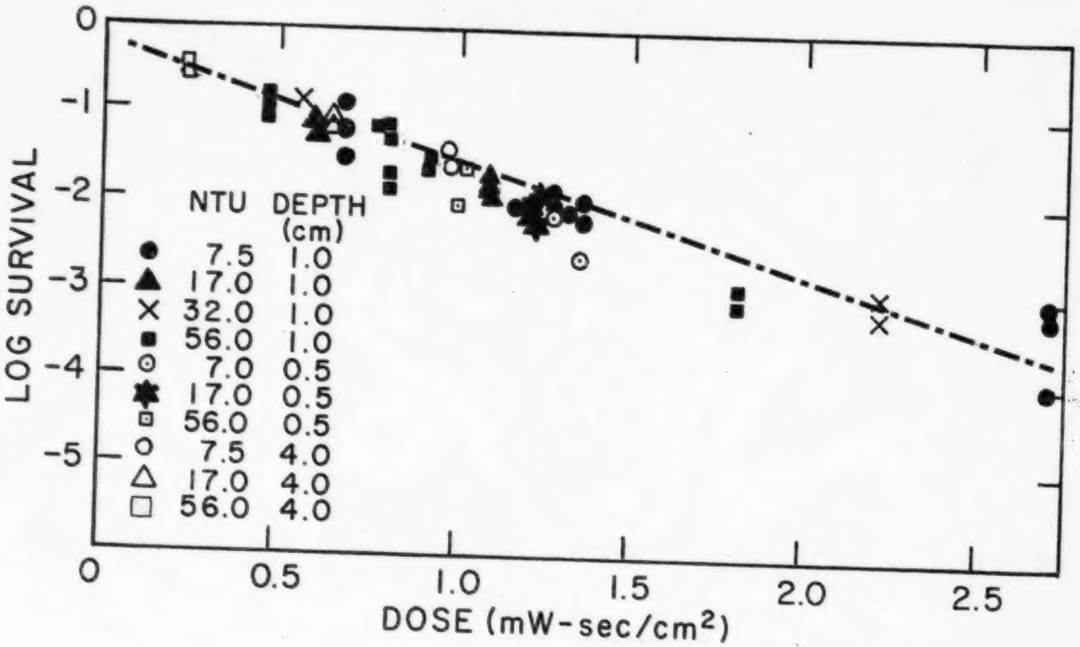

Fig. 24. E. coli B log survival in solutions of various turbidities (NTU) and depths in a collimated beam. Dose calculated using extrapolation method to estimate true absorbance. Broken line represents calibration curve (Fig. 21).

The spore bioassay method was used to estimate the true absorbance and total scattering as a function of turbidity (Table 11, Figure 26). The same 14 NTU effluent was .45μ filtered and used to dilute the unfiltered sample for intermediate turbidities. The bioassay was done in the collimated beam at 2, 3, and 4 cm depths. The assayed absorbance was calculated by using log survival to estimate the dose and dividing by the exposure time to obtain the average dose rate (I_{ave}). Values of I_{ave}/I_0 were plotted against absorbance for each path length using Equation 3, and assayed absorbance was read from these plots.

The difference between the data and the solid straight line where spectrophotometric absorbance equals assayed absorbance is considered to be the total scatter component of the spectrophotometric absorbance. About 75% of the particulate spectrophotometric absorbance was true absorbance if data at turbidity 14 NTU were considered.

Table 12 compares several methods of measuring the absorbance of the same 14 NTU effluent sample. The % T with UV meter was obtained by placing the radiometer probe under the quartz dish in a collimated beam using distilled water as a reference. It was a crude method and may be expected to be some-

BEGIN LAST LINE OF TEXT
BOTTOM OF IMAGE AREA: OUTSIDE DIMENSION FOR TABLES AND ILLUSTRATIONS
3/8"
PAGE NUMBER
EPA 287 (Cin.) (1-76)

Table 10. Effect of .45 μ filtration on UV absorbance of synthetic turbidity standards.

Unfiltered				Filtered			
Turbidity (NTU)	Absorbance[a]	Scattering Coefficient[b]	Estimated True Absorbance[c]	Turbidity (NTU)	Absorbance[a]	Scattering Coefficient[b]	Estimated True Absorbance[c]
9.6	0.270	0.178	0.092	0.47	0.142	0.060	0.081
20.0	0.660	0.437	0.223	0.48	0.250	0.050	0.200
36.0	1.20	0.851	0.349	0.57	0.381	0.103	0.278
65.0	1.76	1.17	0.590	1.20	0.615	0.063	0.552

---

[a] absorbance of synthetic turbidity solutions at 254 nm measured on Cary 219 spectrophotometer.

[b] absorbance due to scattering as obtained from extrapolation of the straight line of log A vs. log λ at 254 nm

[c] total absorbance (at 254 nm) - Scattering Coefficient (at 254 nm)

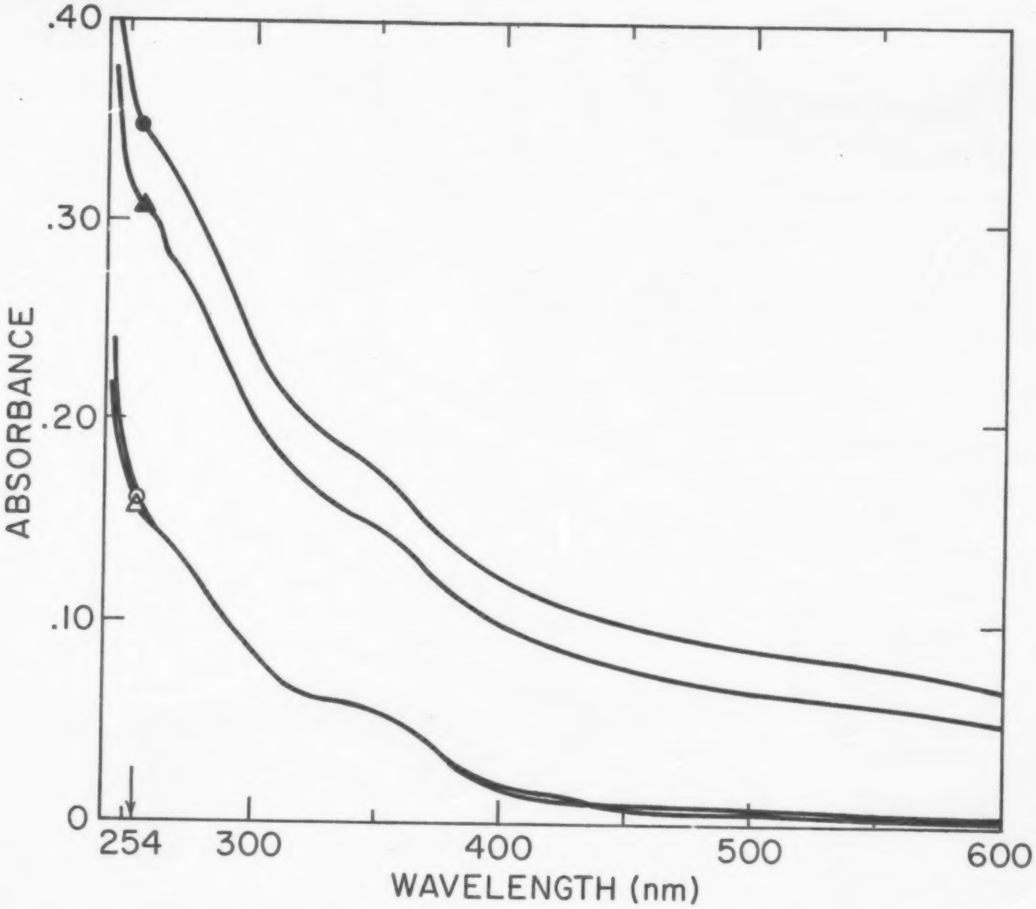

Fig. 25. Absorption spectra of unfiltered (solid symbols) and .45 μ filtered (open symbols) Chapel Hill tertiary effluent measured in a Cary spectrophotometer. Spectra were measured in regular cells (circles) and in "opalescent plate" cells (triangles) which correct for forward scattering. Note that the regular and opalescent plate filtered spectra are nearly identical. Unfiltered turbidity was 14 NTU.

Table 11. Separation of the soluble and particulate absorbance fractions and bioassayed absorbances by varying the particulate component and keeping a constant soluble fraction

Turbidity (NTU)	Spectrophotometric absorbance	Depth (cm)	Assayed dose rate [1] (mW/cm^2)	Assayed absorbance
0.67	.159	2	.0595	.167
		3	.0543	.155
		4	.0471	.166
7	.251	2	.0515	.240
		3	.0457	.220
		4	.0388	.226
11.5	.304	2	.0509	.245
		3	.0412	.271
		4	.0335	.273
14	.347	2	.0455	.308
		3	.0326	.301
		4	.0309	.304

[1] Average of two replicates.

TYPING GUIDE SHEET
BEGIN FIRST LINE OF TEXT HERE
DROPPED HEAD BEGIN SECTIONS HERE
CENTER OF PAGE
TOP OF IMAGE AREA
BEGIN LAST LINE OF TEXT
BOTTOM OF IMAGE AREA, OUTSIDE DIMENSION FOR TABLES AND ILLUSTRATIONS
9-1/8"
1/8"
PAGE NUMBER
EPA-287 (Cin.) (9-76)

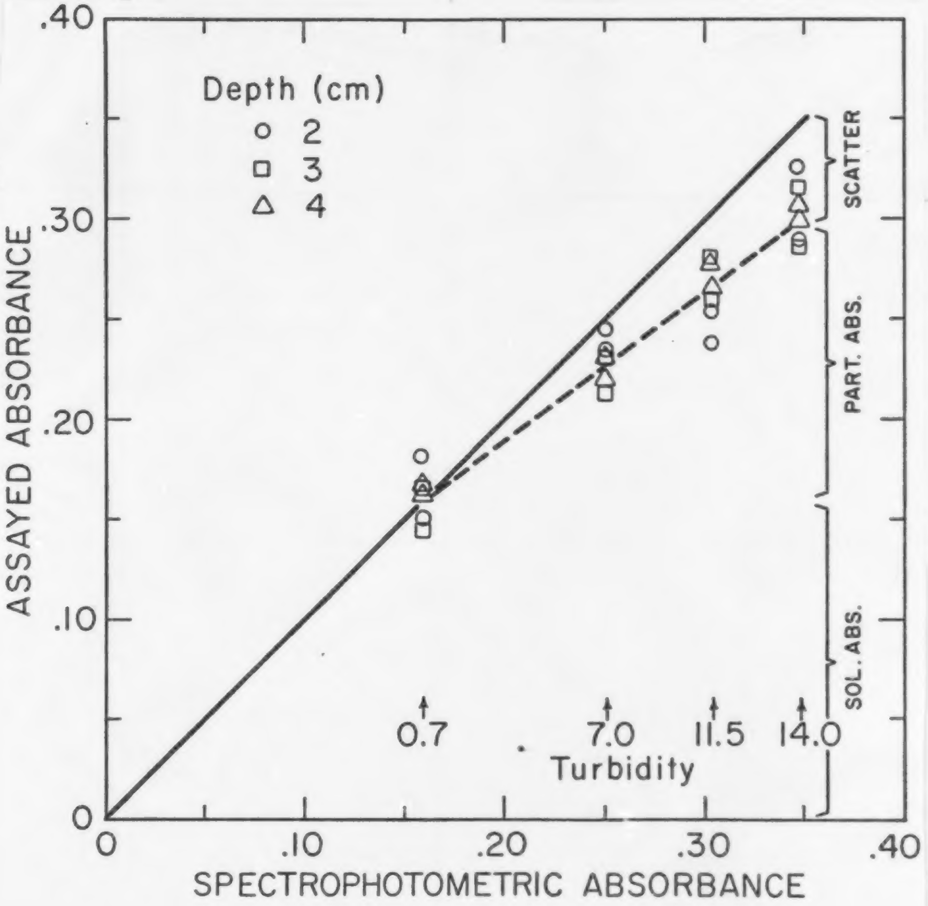

Fig. 26. Spectrophotometric absorbance vs. absorbance measured by the bioassay method for a Chapel Hill tertiary effluent sample. The soluble UV absorbance was kept constant and the particulate concentration varied by diluting the unfiltered (14 NTU) sample with filtered (.067 NTU) sample. The straight line represents an exact correspondence between the two methods. The dotted line is a regression through the data points.

BEGIN LAST LINE OF TEXT
BOTTOM OF IMAGE AREA, OUTSIDE DIMENSION FOR TABLES AND ILLUSTRATIONS
3/8"

PAGE NUMBER
EPA-287 (Cin.)
(4-76)

Table 12. Comparison of methods of measuring the true absorbance of a turbid 3° effluent (14 NTU) and the same sample .45 μ filtered (0.67 NTU).

	% T with UV meter	Spectrophotometer (Cary 14)	Opalescent plate method	Bioassay[1]
Absorbance Unfiltered	.269	.347	.307	.304
Absorbance Filtered	.179	.159	.157	.163

[1] Average of 6 values in 2, 3, and 4 cm depths.

what inaccurate. It appears to slightly overestimate the filtered absorbance and underestimate the unfiltered absorbance. The other methods agree closely on the filtered absorbance, as expected. The estimate of true absorbance by the bioassay was only slightly less than the estimate of true absorbance and non-forward scatter by the opalescent plate method. Thus if the two methods were correct, most of the scatter by particles was forward scatter. However, there was too much variability in the bioassay data to precisely estimate the ratio of forward to total scatter.

In this sample of relatively high particulate content (14 NTU), the assayed absorbance was about 88% of the spectrophotometric absorbance. This discrepancy would be less in samples of lower particulate content and would depend on the soluble absorbance component.

In an effort to test whether the particulate spectrophotometric absorbance component could be predicted by the turbidity, the 14 NTU sample was compared with two Sandy Creek secondary effluent samples taken on different dates by filtration and the opalescent plate method. The particulate spectrophotometric absorbance/NTU was .0133, .0192, and .0127 for the 3 samples respectively. The forward scattering components were 21, 16, and 19% of the spectrophotometric particulate absorbances respectively.

Protection of coliforms by particles influences the shape of the dose-survival curves (Figure 27). The exclusion of particles by filtration above 70 μ and above 8 μ resulted in a trend of decreasing effect of the small numbers of protected coliforms at high doses. The 8 μ filtered samples exposed to 12.7 and 17.4 mW-sec/cm^2 had no detectable survivors with the sample volume used and thus the log survival was less than about -4.9. The 8 μ filtered survival curve did not level out within one log survival unit of the 70 μ filtered curve. The lines coincide until only a small minority of bacteria less than 1 or 0.1% remain, but at higher doses the presence of particles begins to control the resulting survival.

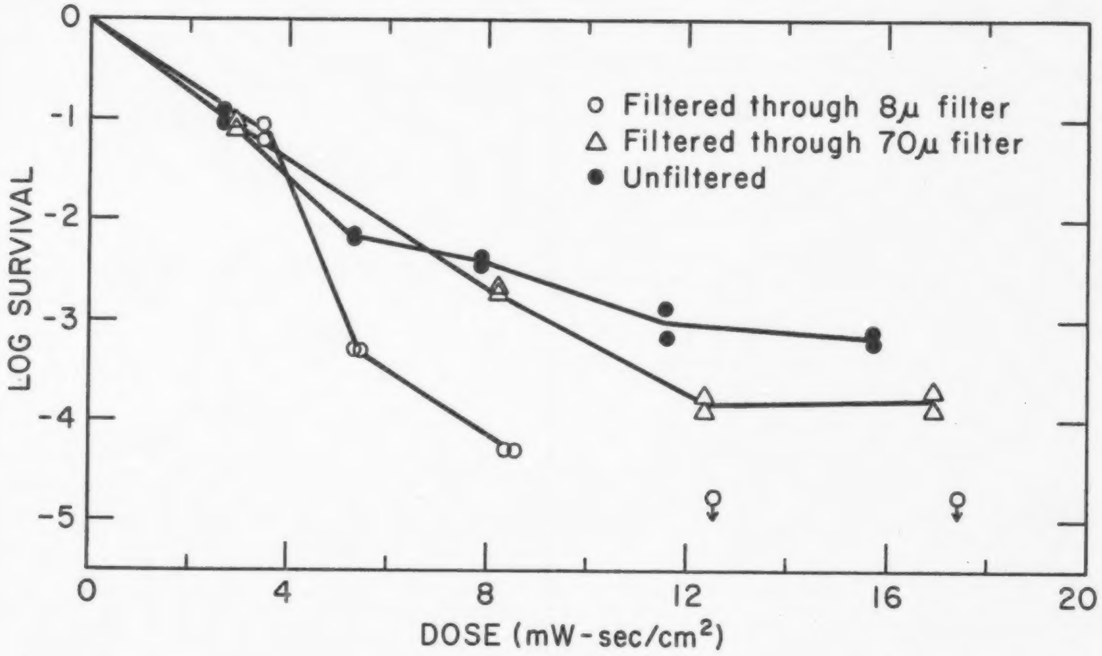

Fig. 27. Effect of filtration on survival of total coliforms in Sandy Creek effluent. Each point represents one separate exposure. Points with arrows indicate limits of detectibility for exposures in which no survivors were found.

BEGIN LAST LINE OF TEXT
3/8"
BOTTOM OF IMAGE AREA; OUTSIDE DIMENSION FOR TABLES AND ILLUSTRATIONS

EPA-287 (Cin.)
(4-76)

The calculation of dose in this experiment depended on correct measurement of the average dose rate in the presence of turbidity. The opalescent plate method was used to estimate the true absorbance. A small correction was made for non-forward scatter based on the ratio of total scatter to forward scatter in the experiments shown in Figure 26 and Table 13. Since the turbidity of the sample was only 3.8 NTU the correction for scattering was small (6.2% in 3.8 NTU) and thus error from that source was minor. The average dose rate was calculated by (Equation 2) using the estimated true absorbance.

The dose-survival curve for the unfiltered sample was plotted in Figure 2 and may be compared to other curves from the literature. The discrepancies are due at least in part to improper estimates of dose in some studies.

CALCULATION AND MEASUREMENT OF DOSE RATE AROUND A CYLINDRICAL SOURCE

Summary

The point source summation method to calculate the dose rate around a line source was tested by using the bioassay method in well-mixed cylinders surrounding the lamp. The data generally fit the predicted average dose rate in various size cylinders and at different absorbances. For small tube sizes a flowthrough technique was used by injecting spores and collecting different fractions as a function of time from injection so that the actual exposure time of each fraction was known as well as the log survival. Calculation of average dose rate using a continuous flow of assay spores and using the flow rate to estimate average retention time yielded a grossly low estimate of average dose rate. The injection technique is presented as a model for use in full scale flowing UV reactors. The assayed absorbance of a turbid effluent sample was used to predict the average dose rate. Bioassay results in the cylinder were only slightly below predicted values.

Results

Comparison of collimated beam experiments at low dose rate and cylinder experiments at high dose rates requires that the Bunsen-Roscoe law holds; that is, that the reciprocity of time and intensity in calculating dose and its effects holds. It was impossible to obtain a collimated beam of comparable dose rate to that near a tubular lamp,and thus directly test a dose rate effect over the entire range. It was possible to vary the time and dose rate reciprocally with the collimated beam apparatus at dose rates below about .09 mW/cm^2. Since breakdowns in the Bunsen-Roscoe law occur at very low dose rates (see Literature Review), one would expect that reciprocity of dose rate and time at the lowest dose rates would imply reciprocity at higher ranges. When exposure time and dose rate were varied reciprocally at .090 and .045 mW/cm^2 almost identical log survivals were observed (Table 13). Results were

Table 13. Test of adherence to Bunsen-Roscoe Law (reciprocity of time and intensity) in calculating dose in the time frame of the petri dish and cylinder experiments. Exposure time was varied reciprocally with a measure of intensity to yield the same expected doses and log reductions in the diagonal columns. Each log reduction shown was the mean of two replicate exposures.

	Petri dish:log survival			Cylinder:log survival	
Exposure(sec)	I_o(mW/cm^2)		Exposure(sec)	Output/cm(mW/cm)	
	.090	.045		49	73
311	-2.96	--	9.4	-2.95	--
622	--	-2.99	6.3	--	-2.82

similar when output (proportional to average dose rate) and exposure time were varied reciprocally in the cylinders at high dose rates.

The point-source summation calculations for a 60 cm lamp yielded curves of dose rate vs. radial distance shown in Figure 28. The measured output of the lamp was 48.6 mW/cm length. Note that the greatest % difference between dose rates in solutions of different absorbances occurs at greater radial distances. It would be impossible to use a constant factor to relate average dose rate to dose rate at a certain distance unless the absorbances were constant. Thus the placement of a radiometer detector will bias even relative comparisons of average dose rate at different absorbances.

These calculations, weighted by the volume of fluid in each radial increment, yielded the curves of average dose rate within a cylinder of outer radius r shown in Figure 29. The spore bioassayed dose rate within the cylinders showed a general agreement with the point-source summation model. Data from three sorts of experiments were collected:

1) for cylinder stirred batch experiments, of radius 1.86 cm and above;

2) injection of spores into flowthrough tubes and collection of fractions vs. time from injection;

3) flowthrough tubes of radii 1.32 and 1.59 cm in which a spore-inoculated solution flowed through and mean retention time was calculated from flow rate and volume.

EPA Form 2350-4 (4-80)
(PREVIOUSLY EIN. EPA FORM 281)
TYPING GUIDE SHEET

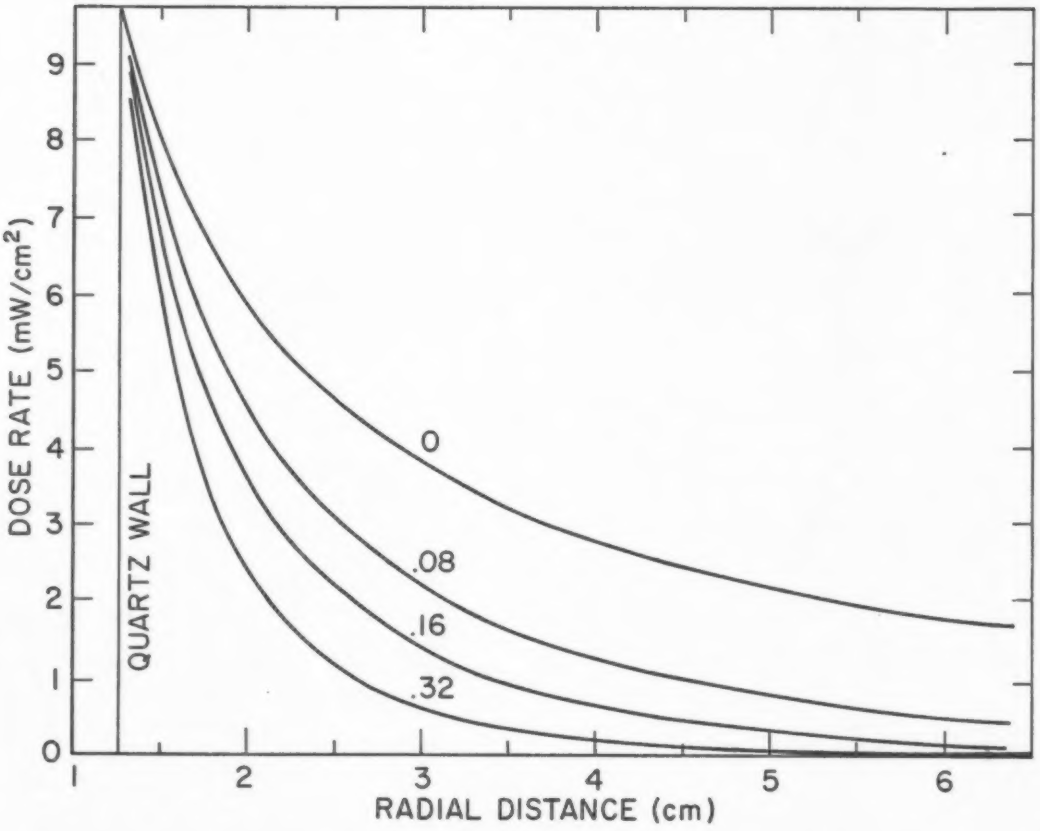

Fig. 28. Dose rate at reactor mid-length vs. radial distance from the lamp axis. Curves are shown for four indicated absorbance values calculated by the point source summation method for a lamp of 48.6 mW output/cm lamp length and lamp length 60 cm.

BOTTOM OF IMAGE AREA OUTSIDE DIMENSION FOR TABLES AND ILLUSTRATIONS

BEGIN LAST LINE OF TEXT

3/8"

PAGE NUMBER

EPA-287 (Cin.)
(4-76)

BEGIN FIRST LINE OF TEXT HERE
TYPING GUIDE SHEET
CENTER OF PAGE
TOP OF IMAGE AREA
DROPPED HEAD; BEGIN SECTI HERE

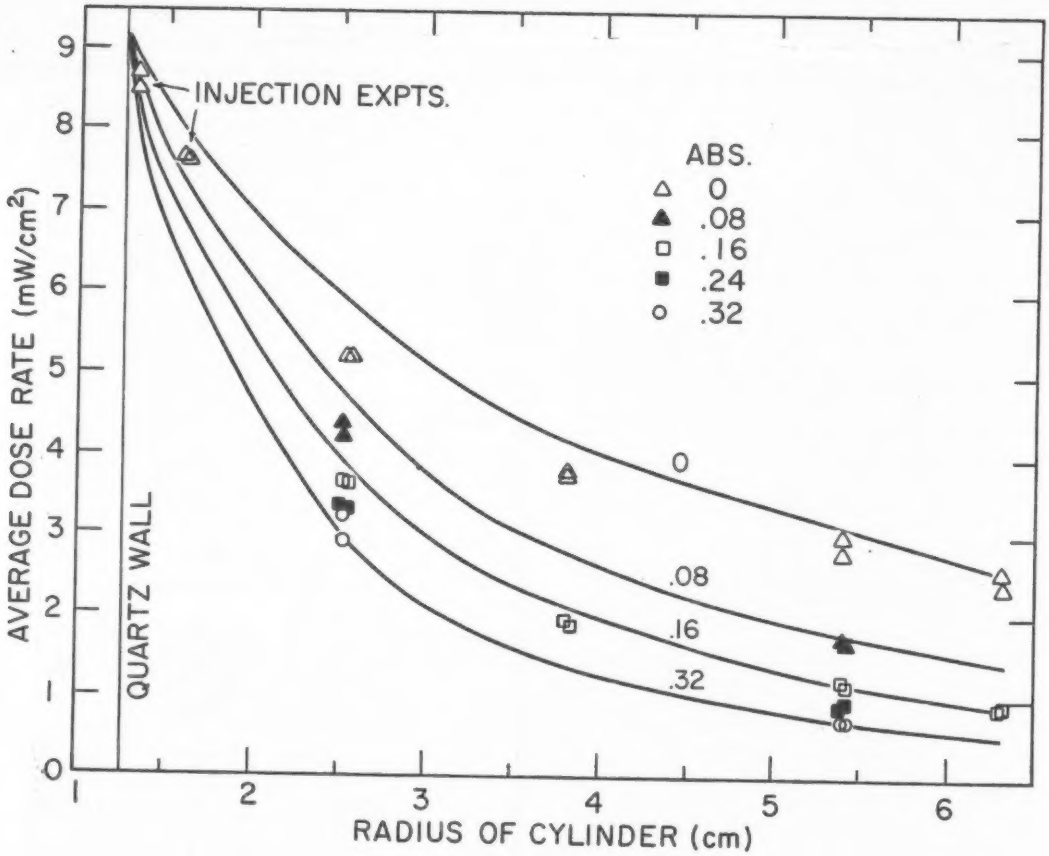

Fig. 29. Average dose rate within a cylinder of radius R. Calculated curves using model and experimental bioassay data for several different absorbances and cylinder sizes. The data points are normalized to correspond to an output/cm lamp length of 48.6 mW to compensate for small variations in output. Data points for 1.32 and 1.59 cm radius were obtained from flowthrough tubes rather than batch.

BEGIN LAST LINE OF TEXT
BOTTOM OF IMAGE AREA. OUTSIDE DIMENSION FOR TABLES AND ILLUSTRATIONS
3/8"

EPA-287 (Cin.)
(4-76)

The stirred batch experiments fit the calculated curves well in the larger cylinders but tended to be somewhat lower in the smaller cylinders at the lower absorbances, but the deviation was small. Shadowing by the stirring devices was not included in the calculated curves and was probably negligible in the larger cylinders. However, by necessity, the stirrer rings covered a larger proportion of the radius in the smaller tubes and the pattern of deviations are what may be expected from the shadowing. The type 3 experiments, where exposure time was assumed to be the average retention time, were done to illustrate the error in that assumption.

Bioassay experiments were performed in a flowthrough tube for two reasons:(1) to verify the PSS calculation at distances close to the quartz wall, which was impossible with the batch apparatus and (2) to demonstrate a method for bioassay of dose rate in a flowthrough system. Real UV reactors are flowthrough systems and have a distribution of retention times. To use the bioassay of dose rate in a flowthrough system we needed a way to determine a definite exposure time. To do this we used the spores in a manner analogous to a tracer injection study. Spores were injected into the flow stream at the entrance to the tube and fractions were collected as a function of time from injection. The experiment was performed with the UV light off and repeated with the UV light on. The density of unirradiated spores (N_O) vs. time from injection is shown in Figure 30A. The distribution of unirradiated spores reflects the retention time distribution and was somewhat skewed. The density of surviving irradiated spores (N_S) are shown in Figure 30B. Since the spores were injected as a spike at time zero, we had a definite exposure time for each fraction collected at the tube exit. The survival (N_S/N_O) can be calculated for each flow fraction separately by comparing spore densities in the corresponding fractions at a given time from injection. Assayed dose rate is calculated as follows:

(a) $N_{O(t)}$ = spore density, unirradiated in fraction collected at time t
$N_{S(t)}$ = surviving spore density, irradiated, in fraction collected at time t
Survival$_{(t)}$ = $N_{S(t)}/N_{O(t)}$

(b) Dose$_{(t)}$ assayed from survival $_{(t)}$: using calibration curve

(c) Dose rate = Dose$_{(t)}$/time from injection

The assayed dose for each flow fraction is also plotted in Figure 30B. The slope of the regression line of assayed dose vs. time from injection also corresponds to the average of the assayed dose rates in the separate fractions.

The bioassayed average dose rates with the flowthrough tubes corresponded well with the calculations of the PSS model (Figure 29, "injection expts.). The fit of the bioassay measurement to the PSS calculation in these thin film tubes demonstrate that the PSS calculation is relevant very close to the lamp as well as in the larger cylinders.

The distribution of unirradiated and irradiated viable spores in Figure 30 also show that most of the surviving spores were those which emerged from

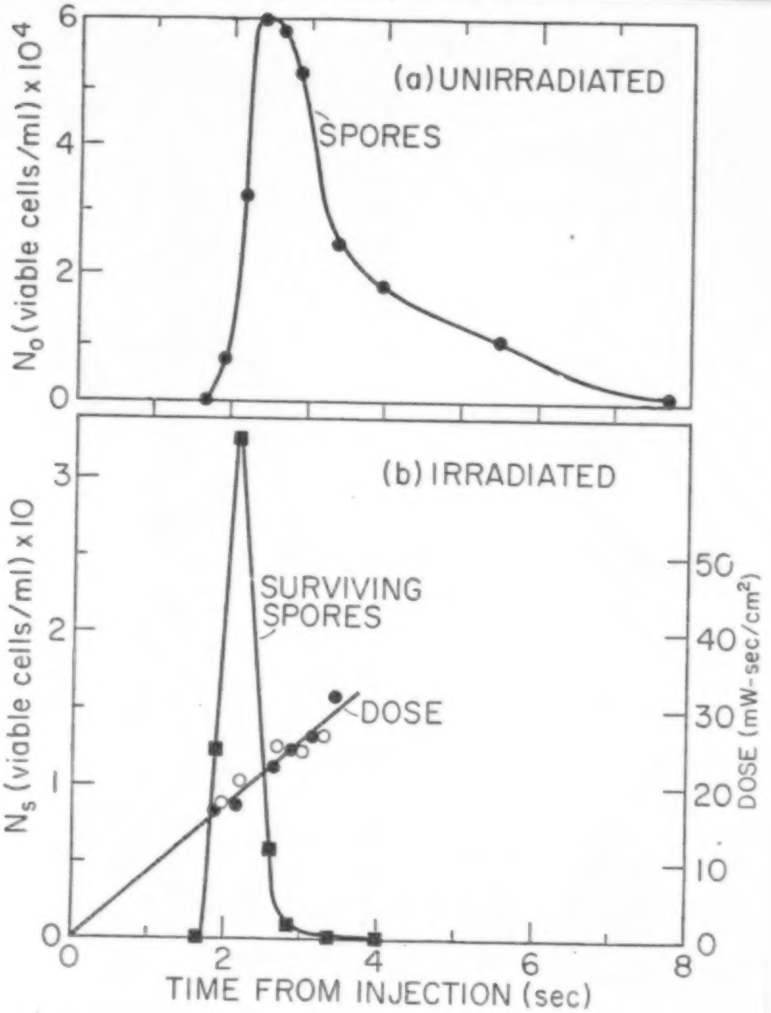

Fig. 30. Assay of average dose rate in 1.32 cm radius flowthrough tube by injection of spores and collection of separate fractions over time after injection. Fig. 30 A shows the concentration of spores vs. retention time (time after injection) with no irradiation. Fig. 30 B shows the spore concentrations as a function of retention time when irradiated at the same flow rate. Also shown is the assayed dose calculated from the N_O, the N_S of each fraction collected, and the calibration curve. For clarity the viable spore distribution curves are shown for only one experiment but the assayed dose vs. retention time shows data from two experiments. The assayed dose rate for each point is (the assayed dose)/(retention time), and the average corresponds to the slope of the regression line through all the points forced through the origin.

BEGIN LAST LINE OF TEXT
BOTTOM OF IMAGE AREA; OUTSIDE DIMENSION FOR TABLES AND ILLUSTRATIONS
3/8"

PAGE NUMBER
EPA-287 (Cin.)
(4-76)

the tube before the average retention time of all spores. In fact, comparing Figures 30A and B the peak number of surviving spores occurred at a time corresponding to the passage of about the first 10% of the unirradiated spores. This fact reflects the logarithmic nature of the dose-survival curve. It illustrates the drastic effect that flow dispersion can have on the disinfection efficiency.

In a continuous flow of spores, the sample is subject to a wide distribution of exposure times. If we attempted to use the average survival and the theoretical retention time to determine average dose rate we got an average dose rate far below that calculated by the PSS model. For the 1.32 cm radius tube, with a continuous flow of spores, we got an assayed intensity of 4.8 mW/cm^2 compared to 8.6 mW/cm^2 calculated by the PSS model. The error in using a continuous flow of spores resulted from the high number of spores which survive in the fractions passing before the mean retention time.

The prediction of the point-source summation model was tested in the 14 NTU turbidity effluent in the 3.82 cm radius tube by the bioassay method (Table 14). The assayed dose rates were somewhat below the predicted values (less than 14% low in both filtered and unfiltered samples.) The shadowing of the stirrer may have contributed to the low value as it did in Figure 29. The absorbance used to calculate the predicted value was the bioassayed absorbance from Table 12. Thus the presence of particles and scattering did not appear to seriously affect the applicability of the model to turbid effluent solutions in the cylindrical geometry.

EFFECTS OF FLUID DEPTH AND LAMP SPACING ON EFFICIENT USE OF UV LIGHT.

Summary

The effectiveness of various fluid depths in a collimated beam and in the cylindrical geometry is illustrated. It is shown that thin film depths waste light when there is little or no reflection. The tradeoff between lower average dose rate and greater volume treated, favors the greater fluid depths under such circumstances. The (dose rate)(volume) product is a measure of the treatment capacity of a unit and can be used to compare various geometries. The dose rate-volume per unit input energy is a measure that can be used to compare the efficiency of various designs. Little UV is transmitted by neighboring lamps and thus close spacing of lamps decreases efficiency if flow characteristics are not a factor. This effect was illustrated using a simulation of the Bergen County system. Various lamp spacing and the cost of lamps and equipment vs. size of shell were considered. The Aquafine and Pure Water Systems units' average dose rates were simulated and although the Aquafine unit had a lower average dose rate, its larger volume made it more efficient on a dose rate-volume basis.

Table 14. Effects of scattering and absorbance in a cylindrical reactor (3.82 cm radius) using the bioassay of average dose rate in a filtered and unfiltered (14 NTU) effluent sample.

	Filtered		Unfiltered	
Bioassay abs.[1]	.163		.304	
Predicted average dose rate (mW/cm^2)*	2.11		1.53	
Assayed average dose rate (mW/cm^2)**	1.92	1.72	1.27	1.55

[1] In collimated beam apparatus (Figure 11)

*From (Fig. 29)

**Two trials shown for each sample

Results

Having shown the validity of dose calculations in the collimated beam and the validity of the point-source summation calculations in the cylindrical system, we can show the relationship between fluid depth or lamp spacing and effectiveness with derived calculations.

An illustration of this relationship in the simplest system, the collimated beam, is shown in Table 15. Data from Figure 24 are shown as both fluid depth and turbidity (with absorbance) are varied. The log survival and the dose calculated as in Figure 24 are shown. All samples were exposed for 60 seconds; thus the average dose rate clearly decreases as depth increases and turbidity increases. Although the average dose rate decreases in the greater fluid depths, more fluid is being treated in that 60-second exposure. This tradeoff may be quantified by a product we shall call the dose rate-volume product and is a measure of the effectiveness of the dose when given volumes or flow rates of water are being treated.

16) dose rate-volume product = (average dose rate)x(volume of fluid treated)
= (dose)x(volume treated/second)

In units: (mW/cm^2)x(ml treated) = $(mW\text{-}sec/cm^2)$x(ml treated/sec)

Table 15. Effectiveness of various fluid depths in a collimated UV beam. The E. coli B strain was used as a bioassay in various artificial turbidity solutions. All samples were exposed for 60 sec. Dose was calculated by using the extrapolation technique for absorbance. The dose rate-volume product takes into account that more volume is being treated in a unit time in the greater fluid depths.

Fluid depth (cm) Turbidity (NTU):	-Log survival			Dose (mW-s/cm^2)			Dose rate vol. product (mW/cm^2)(ml treated)		
	0.5[2]	1.0[1]	4[2]	0.5	1.0	4.0	0.5	1.0	4
1.2	2.45	2.17	1.65	1.38	1.36	1.36	.115	.235	.908
7.5	2.44	2.08	1.50	1.31	1.29	.981	.105	.214	.654
17	2.17	1.88	1.08	1.20	1.12	.657	.100	.187	.438
56	1.90	1.47	0.55	1.00	.84	.250	.084	.140	.167

[1] Average of three values.

[2] Average of two values.

[3] or (average dose rate)(volume treated).

As depth increases, dose decreases, but the volume treated increases more rapidly than the decrease in dose. Thus, greater fluid depths are more effective at treating volume of fluid and the difference is greater at lower absorbances where dose decreases the least.

The same relationships extend to the single lamp cylindrical geometry, assuming reflection from the walls is minimal. Figure 31 and Table 16 show calculations derived from Figure 29 which were supported by bioassay data. Clearly the dose rate-volume product is greater the larger the radial fluid depth, and the differences are greatest at lower absorbances. The increase in effectiveness becomes minimal at a radial fluid depth of about 4.5 cm in a fluid of absorbance .16, which is close to the average absorbance of the effluent samples.

Another way of illustrating this relationship is to calculate the (seconds exposure)/(liter treated) necessary to achieve a certain log survival,

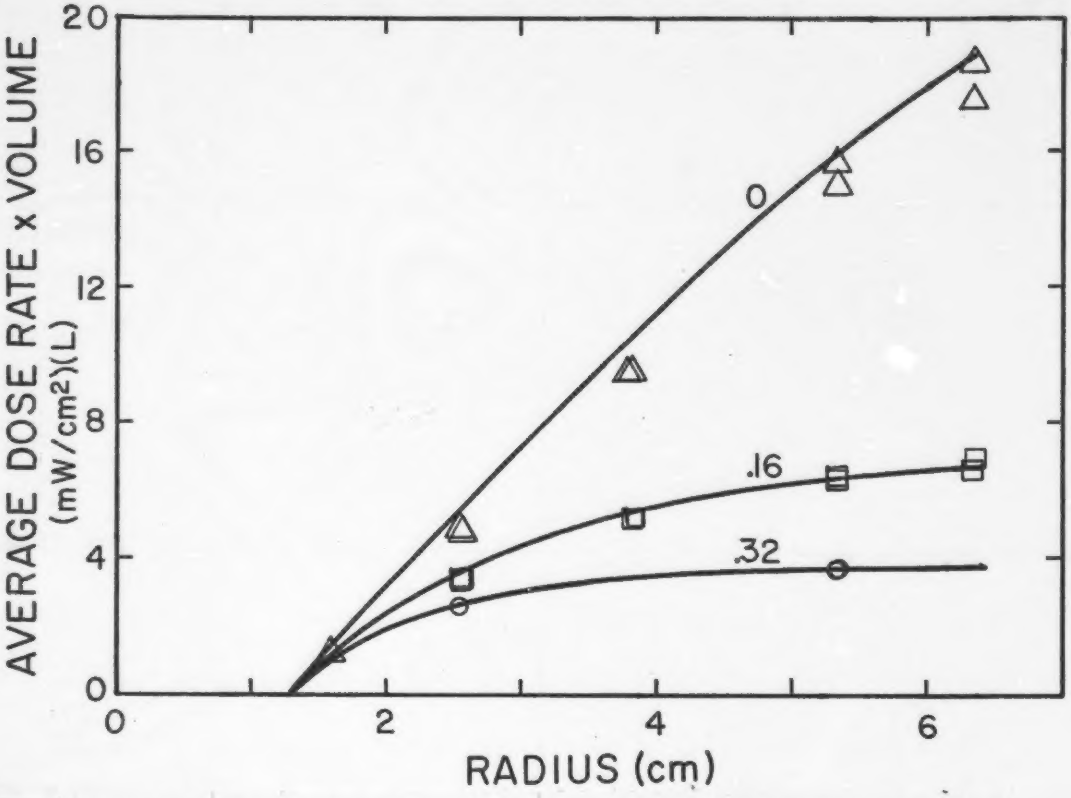

Fig. 31. Effectiveness of various fluid depths in cylinders of radius r around UV lamps. Calculated values of the product of average dose rate in a cylinder of radius r times the volume of that cylinder are shown vs. the outer radius of the cylinder for fluids of absorbances 0, .16 and .32. Calculated from data shown in Fig. 29.

using Bacillus spores, as a function of radial fluid depth (Figure 32 and Table 17). If an analogy is made to a flowthrough system where a certain log survival is required, the graph shows that the greater fluid depths can handle greater flow rates or higher absorbances.

Interference by neighboring lamps

To evaluate the effect of lamp spacing on efficiency and the possible interference by neighboring lamps, we made an approximate measurement of the proportion of light from one lamp transmitted by a neighboring lamp (Figure 33). Two lamps were set up 3.55 cm on center from one another and black paper shields arranged so that the only light from lamp A reaching the Il-500 radiometer detector must travel through lamp B. All but a 1 cm length of each lamp in line with the normal to the probe was also shielded so that light from lamp A reaching the detector crossed lamp B at approximately right angles. The approximate percent transmission of light from A by B was calcu-

Table 16. Effectiveness of various fluid depths in cylinders surrounding UV lamps. In parentheses beside each average dose rate is the average dose rate-volume product, a measure of the effectiveness of the system at treating given volumes of fluid.

r (cm)	vol (l)	absorbance 0	absorbance .160	absorbance .320
		Average dose rate (avg. dose rate x vol.)		
1.82	.320	7.42 (2.37)	5.78 (1.85)	5.10 (1.63)
2.56	.931	5.80 (5.40)	3.85 (3.58)	2.86 (2.66)
3.82	2.45	4.21 (10.31)	2.14 (5.24)	1.37 (3.36)
5.32	5.03	3.17 (16.0)	1.24 (6.24)	.718 (3.61)
6.32	7.23	2.59 (18.7)	.925 (6.69)	.512 (3.70)

lated as:

17) $$\frac{I_B - I_A}{I_{AB}}$$

where I_A is intensity with lamp A on and lamp B off,

I_B is intensity with lamp A blocked (between A and B) and lamp B on,

I_{AB} is intensity with both lamps on.

Thus this % transmission uses an unlit tube as the reference,while it may actually reflect and refract some of the light incident on the tube. For the unlit B tube, a burned-out tube was cleansed inside and substituted to avoid absorption by condensed mercury.

Very little 254 nm UV, if any, was transmitted from the lighted lamp B. The percent transmission ranged from 6 to 11%. The variation was caused by drift of the meter and the very high value of I_B relative to I_A. Some of the transmitted light may have been refracted through the upper and lower quartz wall of lamp B or passed through a very short cord of the lamp circumference.

Multiple lamp systems have the advantage that UV light from the central lamps may penetrate greater fluid depths before encountering the containing walls. However, neighboring lamps have been shown to interfere with (shade) one another. The large lamp array design of Pure Water Systems, used in the Bergen County Study, provides a good example of a system where the light loss to the containing walls is minimized by the size of the array. However, it also provides an example to simulate the effects of different lamp spacing on

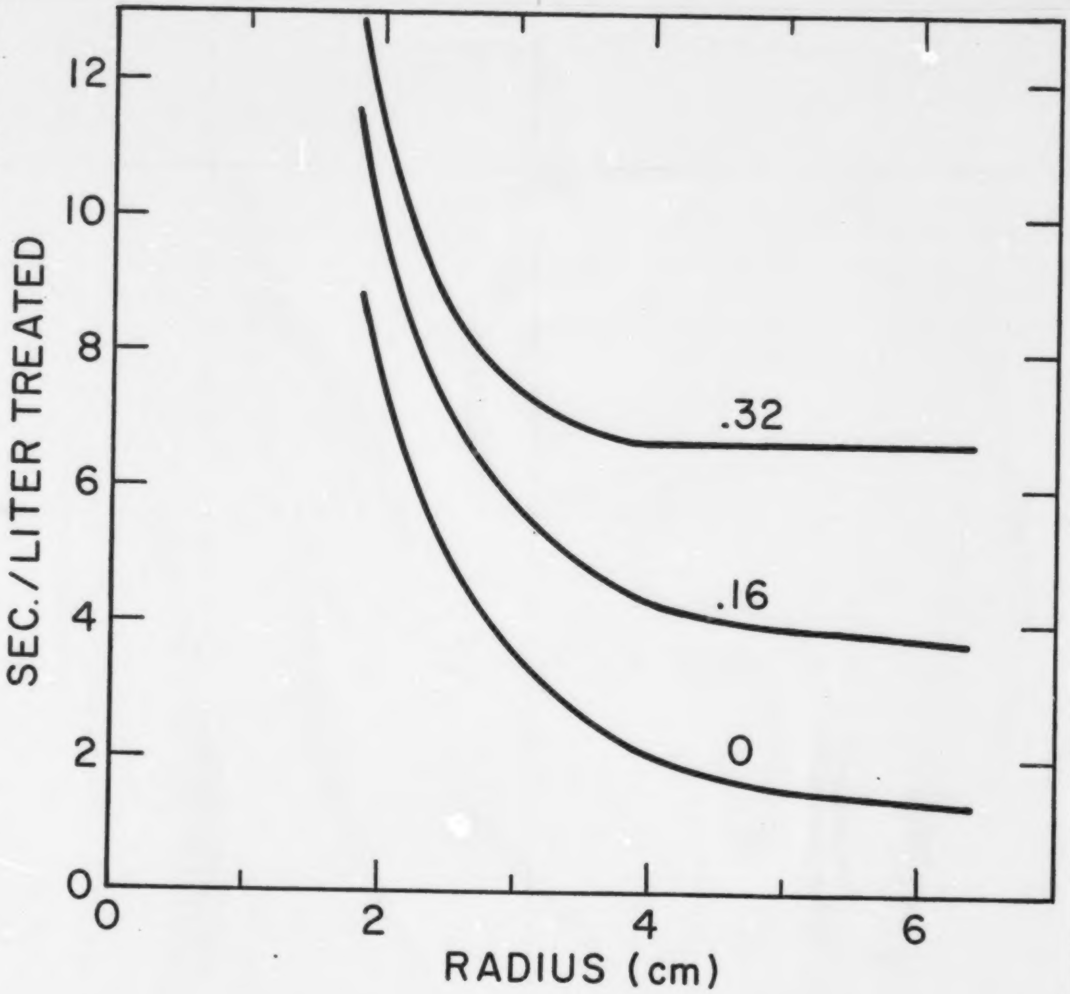

Fig. 32. Average seconds exposure per liter of fluid treated in cylinders of radius r needed to produce a log survival of -3 using Bacillus spores (ave. dose of 23.8 mW-sec/cm^2) for fluids of absorbances 0, .16 and .32. Calculated from data shown in Fig.29.

BEGIN LAST LINE OF TEXT
3/8"
BOTTOM OF IMAGE AREA; OUTSIDE DIMENSION FOR TABLES AND ILLUSTRATIONS

PAGE NUMBER
EPA Form 2350-4 (4-80)
(PREVIOUSLY GIN. EPA FORM 28)
U.S. GOVERNMENT PRINTING OFFICE 1980-060-638
TYPING GUIDE SHEET

Table 17. Average seconds exposure needed per liter to treat fluid in cylinders of various radii. Calculated from data in Fig. 29. The seconds needed to treat the entire batch to -3 log survival are shown, and in parentheses, the average seconds exposure required per liter volume.

r	vol	absorbance		
(cm)	(l)	0	.16	.32
1.82	.320	3.21 (10.0)	4.12 (12.9)	4.67 (14.6)
2.56	.931	4.10 (4.41)	6.18 (6.64)	8.32 (8.94)
3.82	2.45	5.65 (2.31)	11.1 (4.54)	17.4 (7.10)
5.32	5.03	7.51 (1.49)	19.2 (3.82)	33.1 (6.58)
6.32	7.23	9.19 (1.27)	25.7 (3.56)	46.5 (6.43)

the efficiency of the array. A computer program used the point source summation to calculate the dose rate due to each lamp within 3 rows at a point p in the cross section of the area occupied by fluid. The absorbance was assumed to be .15. If another lamp lay between the center of the source lamp and the point, the contribution from that lamp was omitted. The dose rate at point p was considered the sum of the dose rates due to the contributing lamps. Dose rate was calculated for each point (on a 1 mm grid) in a representative cross section,and the dose rates averaged. Several cross sections along the length of the lamp axes were averaged. Several alternative lamp spacings were simulated, and the increase in void volume due to expanding the matrix was calculated. The flow rate which gave an average of 200 MPN/100 ml in Scheible and Bassel's data was chosen as the baseline case. The retention times for that given flow rate were calculated for the different void volumes resulting from an expanded lamp matrix. The retention time times the simulated average dose rate gave the simulated dose for each lamp spacing at a constant flow rate.

The simulated doses (Table 18) show that interference by neighboring lamps may have a detrimental effect on the effectiveness. The simulated doses are greater at greater lamp spacings but the increase is less than 5% after the distance between lamps is doubled. The thin film (2.5 cm spacing) showed a dramatic reduction in dose.

These simulations make several assumptions:

1) that the lamps transmit no UV from a neighboring lamp

2) that there is no reflection from the walls

BEGIN LAST LINE OF TEXT
BOTTOM OF IMAGE AREA, OUTSIDE DIMENSION FOR TABLES AND ILLUSTRATIONS
3/8"

Table 18. Effect of expanding lamp spacing and total volume of lamp array on the simulated dose at a constant flow rate using Pure Water Systems' design (from Scheible and Bassel (1981)).

Spacing factor	Distance between lamps (cm)	Total volume[1] (m^3)	Volume factor	Void volume (m^3)	Retention time(s)	Average I (mW/cm^2)	Dose ($mW\text{-}sec/cm^2$)[2]
0.707	2.51	0.363	0.5	0.127	0.324	95.2	30.8
1	3.55	0.726	1	0.49	1.25	51.5	64.4
1.14	4.05	1.45	2	1.21	3.09	25.8	79.7
2	7.10	2.90	4	2.67	6.81	12.9	85.1
3	10.65	6.53	9	6.30	16.17	5.64	87.8
4	14.20	11.62	16	11.38	29.0	3.15	92.4

[1] Volume of quartz sleeves was .236 m^3 (1.15 cm radius)

[2] At flow rate of .392 (m^3/sec)

BEGIN FIRST LINE OF TEXT HERE
DROPPED HEAD; BEGIN SECTIONS HERE
CENTER OF PAGE
TOP OF IMAGE AREA
BEGIN LAST LINE OF TEXT
3/8"
BOTTOM OF IMAGE AREA; OUTSIDE DIMENSION FOR TABLES AND ILLUSTRATIONS
PAGE NUMBER
EPA Form 2350-4 (4-80)
(PREVIOUSLY CIR. EPA FORM 287)
© U.S. GOVERNMENT PRINTING OFFICE 1980-665-639
TYPING GUIDE SHEET

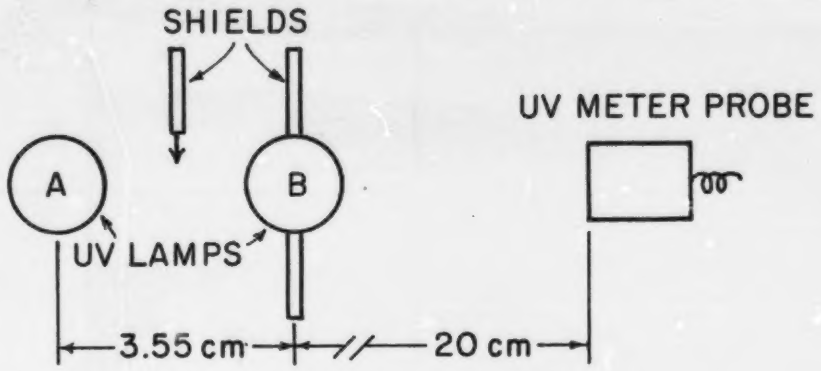

Fig. 33. Setup for approximate UV% transmission of lamp A through lamp B.

3) that refraction by the quartz sleeves does not alter the path lengths in the solution, and

4) that the flow distributions and radial mixing properties are unaltered by the lamp spacing changes.

Since the larger lamp spacing and volume results in higher doses at a given flow rate, the calculations indicate that fewer lamps may be employed (and volume reduced proportionally) at larger lamp spacings to achieve a given dose to the effluent. For example, since the doses at 1 and 2 times the base case lamp spacing were 64.4 and 85.1 (Table 18), to achieve the same dose, 64.4, it was assumed that the number of lamps could be reduced to 64.4/85.1 or 75.7% of the lamps present in the base case to achieve the same dose that gave a 200 MPN/100 ml effluent in the base case. The relative economic costs then become a tradeoff between the reduced cost of lamps and associated equipment (quartz sleeves, ballasts, etc.) and the increased cost of a containing shell of greater volume. The relative costs of the different lamp spacing designs for lamps and shell are compared to the base case where lamps are spaced 3.55 cm apart (Table 19). Rather than assume specific costs, three situations are shown where the cost of lamps and associated equipment is 80, 90 or 95% of the total equipment cost in the base case. The relative costs are calculated as follows:

18) (a) = (the cost of lamps relative to base case total cost) = (proportion of total cost spent on lamps)x(dose with base case/dose with spacing s)

Table 19. Relative costs of designs using different lamp spacing (and total volume of unit) based on the Bergen County design. Costs are shown as a proportion of the total equipment cost of the base case (=1.0) where lamps were spaced 3.55 cm apart. Three situations are shown where the lamps and associated equipment (sheaths, ballasts, etc.) are 80, 90 or 95% of the total equipment cost in the base case. The number of lamps used are based on calculations shown in Table 19. Relative costs of power are shown in parentheses.

	80% Lamps			90% Lamps			95% Lamps		
Lamp spacing	Lamps	shell	total	Lamps	shell	total	Lamps	shell	total
Base case	.80	.20	1.00	.90	.10	1.00	.95	.05	1.00
(power)			(1.00)			(1.00)			(1.00)
double	.64	.30	.94	.66	.15	.81	.75	.08	.83
			(.79)			(.79)			(.79)
triple	.57	.39	.96	.64	.19	.83	.68	.10	.78
			(.71)			(.71)			(.71)
quadruple	.56	.46	1.02	.63	.23	.86	.67	.11	.78
			(.70)			(.70)			(.70)

19) (b) = (cost of shell relative to base case total cost) = (proportion to total cost spent on tank)x[(spacing factor $s)^{0.6}$]

20) (c) = (total cost of unit a spacing s relative to total cost of base case) = (a + b)

The power cost is also shown and is calculated as the equal number of lamps relative to the number of lamps in the base case. However, power is a relatively minor cost compared to construction and equipment (Scheible and Bassel, 1981). The optimum lamp spacing depends on the cost of lamps, etc. vs. the shell but the benefits are, at most, marginal beyond double lamp spacing.

BEGIN LAST LINE OF TEXT
1/8"
BOTTOM OF IMAGE AREA; OUTSIDE DIMENSION FOR TABLES AND ILLUSTRATIONS

SECTION 7

SUMMARY DISCUSSION

DOSE RATE MEASUREMENT

Bioassay method

The bioassay method of determing germicical dose using *Bacillus subtilis* spores calibrated in a collimated UV beam provided an *in situ* method with reasonable precision. It could be used (1) in complex geometries where UV radiometer probes were inapplicable, (2) in effluents with both absorbance and scattering effects, and (3) in flowthrough systems with accurate knowledge of the exposure time. In addition, the spores can be prepared in large batches, transported, and stored for at least several months. A good deal of effort was expended working with an *E. coli* B and a radiation resistant B/r strain, but the spores proved much more precise and reproducible, and were not subject to the rapid changes in resistance as growth conditions change. However, it was essential to perform the experiment before any spores began to germinate when placed in a nutritive fluid.

Several authors have suggested using bacteria to determine relative doses (Jagger, *et al*. 1975; Morris 1972; Yip and Konasewich 1972). However, by calibrating the spores in a collimated beam the bioassay result can be expressed in actual units which relate the three dimensional dose rate to radiometer measurements. In addition, we illustrated that to use the bioassay in a flowthrough system for dose rate measurements, it is essential to separate fractions with different exposure times because of non-ideal flow.

The *B. subtilis* spores were useful for a dosage range up to about 30 mW-sec/cm^2. For measurement of doses above that level, it may be possible to use other more UV resistant fungal spores such as those of *Aspergillus* spp. Choice of plating medium may affect the ability to recover and hence the apparent resistance. For example, the *Bacillus* spores appeared more resistant when plated on nutrient agar than on *Thermoacidurans* agar.

Low absorbance actinometry

Substantial effort was also directed at developing a ferrioxalate actinometry technique for an actinometry solution with absorbances comparable to effluent. A modified procedure using bathophenanthroline to detect very low concentrations of ferrous ion was used with the collimated beam apparatus.

However, the quantum yield was greatly reduced at the low concentrations of ferrioxalate and results were erratic. The ferrioxalate also responds to non-germicidal light from the lamps. The ferrioxalate method could not be used *in situ* with actual effluent as could the spores. One potential advantage of a ferrioxalate method would have been the linear relationship of ferrous ion produced to dose, so that *average* retention time would suffice to calculate average dose rate in a flowthrough system. However, the superiority of the spore bioassay made the low absorbance actinometry unnecessary.

SEPARATING EFFECTS OF ABSORBANCE AND SCATTERING OF UV LIGHT

Any direct method of calculating average dose rate in effluent disinfection requires use of an absorption coefficient for the fluid. Since spectrophotometric absorbance measurement includes both true absorbance and scattering components, the measurement should be corrected for scattering. In an effluent of "typical" soluble and particulate absorber content, the scattering component of the spectrophotometric absorbance is a significant but not the major component.

Our approach to estimating the true absorbance of the effluent samples was to separate the spectrophotometric absorbance into three components: (1) soluble absorbance, (2) particulate true absorbance and (3) particulate scattering. The ultrafiltration and opalescent plate results showed no appreciable particulates or scattering in the .45 μ filtrate.

Bioassay experiments in turbid solutions of autoclaved washed *E. coli* cells where scattered light comprised most of the spectrophotometric absorbance showed that the scattered light remains an effective germicidal agent. Experiments in the collimated beam showed that the scattered light could be considered along with the unscattered, unabsorbed light in calculations of average dose rate; i.e., the scattering component may be subtracted from the spectrophotometric absorbance. Apparently, modification of path lengths and multiple scattering effects did not seriously affect the calculations. The spore bioassay supported this method of calculation for turbid effluent in the cylindrical geometry.

Our average UV absorbance for the unfiltered samples, .179, seems fairly representative of UV absorbances found in other studies. Selected averages from several studies of secondary or tertiary effluents were: Scheible and Bassel, .170 (.096-.24, 95% CI); Petrasek *et al*. (runs U1-U6), .218; Severin (activated sludge effluent), .085; Roeber and Hoot, .209.

Since most data in the literature and the data from the pilot plant were not separated into soluble and particulate absorbance, we tried to find a relationship between turbidity and particulate spectrophotometric absorbance. The turbidity removed by the dual media filter exhibited a crude correlation with the spectrophotometric absorbance removed, but there was a great deal of variability due in part to erratic performance of the filters. The dual media filter tended to remove the larger particles which may not have been representative of the whole particulate fraction. In fact, measurements of the fractions passed through different filter sizes showed that the larger particles had a lower ratio of particulate UV absorbance to turbidity. Four samples of .45 μ filtered effluent showed an average ratio of particulate spectrophotometric absorbance/NTU of .013 ± .003. The value of this prediction would be to estimate a scattering correction from data on spectrophotometric absorbance and turbidity. In the bioassay of the scattering component in the Chapel Hill tertiary effluent, the scattering was about 25% of the spectrophotometric particulate absorbance component. Although these figures are based on a limited number of effluent samples, a generalization to the pilot plant studies might be informative. Using these approximate corrections, the scattering component would be about 9% of the spectrophotometric absorbance mean for the unfiltered effluent. Our turbidities and UV absorbances were in the general range of several other studies and this scattering correction may be in the general range for other studies. However, more research needs to be done on prediction of the various absorbance components from water quality data for a wide range of sewage effluents.

The spectrophotometric absorbances of the pilot plant samples were, to a large extent, predictable from water quality data. Since the absorbance is caused by both particulate and soluble components, the prediction would probably have been improved by separate water quality data on .45 μ filtered samples. We believe that the ability of coliform titers to predict UV absorbance does not directly reflect the absorbance of the bacteria themselves. Absorbances of cultured E. coli indicate that the numbers of bacteria in the effluent were insufficient to account for most of the absorbance, most of which was soluble. However, the UV absorbers may be largely a product of the bacterial activity. When the coliforms were not considered, COD proved the best predictor but had a lower correlation. This observation corresponds with other studies covered in the literature review. Turbidity and suspended solids also added somewhat to the regression, probably by their relationship to the particulate component.

The lack of direct data in the literature on the identity of the major UV absorbers in wastewater effluents hinders the ability to predict absorbance and the effects of various treatment schemes. Findings on the humic acid content of effluents (Literature Review), our fractionation of UV absorbances, and absorbance spectra suggest that humics, especially fulvic acids, may be the major UV absorbers in effluents. If so, extra biological treatment would be unlikely to reduce these resistant compounds. They also suggest that color may be a good predictor of soluble UV absorbance. The role of free nucleic acids and byproducts as UV absorbers should also be investigated.

CALCULATION AND SIMULATION OF DOSE

Point source summation technique

Our bioassay experiments demonstrated that the point source summation

(PSS) calculations gave a good fit to the bioassay measurements in the cylindrical geometry. The method basically assumes that the cylindrical lamp is a line source which can be divided into a number of point sources. These assumptions apparently caused little error. Our approach to testing the model involved the following features: (1) that no meter is available to measure 3 dimensional energy flux density near a distributed source, and (2) thus we calculated average dose rate in a volume of outer radius r and assumed that fit to the average over a range of outer radii and absorbances verified the calculation. The batch exposures enabled an unambiguous determination of exposure time. Calibration of the bioassay to the collimated beam and determination of lamp UV output enabled the use of units in mW/cm^2. Shadowing by the stirrers made use of very thin batch cylinder experiments dubious; however, the flowthrough injection method verified the model at distances close to the quartz sleeve.

Comparison to other methods of calculation used in other studies

One way to show differences in calculation methods is to calculate and compare dose rate profiles at the mid-length of the cylindrical apparatus used in our experiments in a fluid of .16 UV absorbance.

There are large differences between the PSS model and the radial path model, Equation 21.

$$I = I_0 \frac{r_0}{r} \exp\left(-a_e(r - r_0)\right) \qquad (21)$$

where I is the intensity (or dose rate) at radial distance r, I_0 is the intensity incident on the absorbing solution at radial distance r_0, and a_e is the absorption coefficient. This equation was used by Scheible and Bassel (1981), Haas and Sakellaropoulos (1979), Roeber and Hoot (1976), and in a modified manner, by Petrasek et al. (1980). It can be seen from Equation 21 that for the case of an infinite line source and no absorbance, the integral form of the point-source summation can be solved to yield an equation equivalent to the radial path model. However, for a line segment source and in the case of absorbing medium, the radial path model is not applicable. Examination of Equation 21 shows that the path length to which the absorption coefficient is applied for rays from the lamp reaching a point P, is the perpendicular or shortest possible path. However, rays reaching point P come from various points along the lamp and traverse varying path lengths through the absorbing medium. Thus the attenuation due to absorption will be underestimated by the equation. Equation 21 also does not consider end effects and requires a measurement or calculation of dose rate very near the lamp. Petrasek et al. made this measurement of I_0 with a Il-500 radiometer at the quartz wall. Several difficulties arise in making a measurement close to the lamp:

1) the probe does not properly measure 3 dimensional dose rate,

2) the outer edges of the probe sensing surface are further from the lamp axis than is the center of the probe, and

3) the probe sensing area does not fit against the quartz sleeve.

For comparison, a measurement was made with our Il-500 radiometer (Figure 33) and shows a value 57% lower than the PSS calculation.

Scheible and Bassel (1981) took another approach. They divided the rated UV output of the lamp by the surface area of the quartz sleeve to obtain an I_0 value (less 10% for absorption by the sleeve). This calculation gives an approximate value of the planar energy flux density at the sleeve surface averaged along the length. Since the tube surface is again normal to the axis of the lamp at all points, light coming from lamp segments further down the axis is "spread out" on the quartz surface according to the cosine law. Again, a 3 dimensional object at a point on the surface as shown in Figure 3 does not intercept the same amount of energy as a plane surface oriented normal to the lamp axis. These calculations are shown in Figure 34. Scheible and Bassel's I_0 calculation gives a value 37% lower than the PSS method and 35% lower than the PSS dose rate averaged along the length of the quartz sleeve. The planar dose rate was calculated using the PSS method by multiplying each point source contribution by the cosine of the angle of incidence normal to the axis. This planar dose rate was similar to Scheible and Bassel's value. The dose rate profiles show that, relative to the PSS calculation, Scheible and Bassel's procedure underestimates the I_0 value but also underestimates the attenuation over the absorbing fluid so that Scheible and Bassel's dose rate is 28% higher at 5 cm whereas it would be 103% higher if the same I_0 were used. Thus the average dose rate over 5 cm radius cylinder is coincidentally similar. These two differences tended to balance one another in their reactor calculations so that our point source summation model simulation of Scheible and Bassel's reactor and the values for average dose rate were not vastly different. The similarity was strictly coincidental though, because their two incorrect estimates happened to balance one another in that particular situation.

The average dose rate over a 5 cm radius by the method of Petrasek et al. yields a value 72% lower. Thus, their estimates of average dose rate in their reactors are probably much lower than the PSS model would give and consequently the dose-log survival curves would be very different. The difference may also explain the great difference in dose-survival curves for their two different units since only one used submerged lamps. Calculations according to the method of Severin (1976) are not shown, but Severin's basic equation omitted a term for the radial attenuation of rays from a line source and would yield vastly different values.

Multiple lamp systems

Averaging of dose rate values over the reactor volume used the basic method of Petrasek et al. except that our method averaged dose rates at points on a cross-sectional grid by computer rather than by isopleth planimetry. Our averaging included end and edge effects not included by the other methods. Also Scheible and Bassel's method included contributions from only the four surrounding lamps (our calculations showed that the total contri-

BEGIN FIRST LINE OF TEXT HERE
CENTER OF PAGE
TOP OF IMAGE AREA
DROPPED HEAD; BEGIN SECTIONS HERE
BEGIN LAST LINE OF TEXT
3/8"
BOTTOM OF IMAGE AREA; OUTSIDE DIMENSION FOR TABLES AND ILLUSTRATIONS
PAGE NUMBER
EPA Form 2350-4 (4-80)
(PREVIOUSLY CIN. EPA FORM 247)
☆ U.S. GOVERNMENT PRINTING OFFICE 1980-660-603
TYPING GUIDE SHEET

bution of the larger number of lamps further away were quite significant).

Extension of our calculations to multiple lamp systems makes the following main simplifications:

1) there is not reflection from the walls;

2) there is no refraction or reflection by the quartz sleeves;

3) scattered light continues on its original path;

4) shadowing by neighboring lamps is complete and that the neighboring lamp acts as a cylinder blocking a line source;

5) rays passing between the quartz sleeve and lamp from neighboring lamps is attenuated as if it were passing through the fluid.

Manufacturers tell us that under operating conditions, assumption #1 will be essentially true. Reflection and refraction by the sleeves will change the paths of some light rays, but the net effect is difficult to evaluate. The effect will be greater at very close lamp spacings. Scattering by particles is mainly narrow angle scattering which alters the light path only somewhat and affects only a small percentage of the light. Assumption #4 is an approximation based on our experiment, and assumption #5 may be shown to have a very minor effect on a small percentage of the light except at very close lamp spacings.

While we were able to evaluate the calculations for a single lamp system, time limitations prevented a bioassay in the multiple lamp reactors. However, averaging over the volume is a very straightforward assumption, blocking by neighboring lamps has been shown by experiment, and we believe the other assumptions would create only minor error except at very close lamp spacings. Testing of multiple lamp flowthrough units may be performed by a procedure illustrated in the small flowthrough tube, by injection of spores and separate collection of flow fractions as a function of injection time.

Exposure time and non-ideal flow

The second factor in dose calculations, exposure time, can lead to at least as much error in calculation as dose rate. In flowthrough reactors, neither the theoretical retention time nor the average retention time determined from dye studies can be used to predict the survival. Again, since survival is not linearly related to dose, the average dose is insufficient to predict the average survival. For an aliquot that enters the reactor at a specific time, dispersion will cause various fractions to be exposed to various doses. Survival in each of these fractions is a function of dose and can be calculated separately, weighted by the relative volume of the fraction and averaged to give the average survival in the reactor effluent. The following equations show how the titer of survivors in the reactor effluent may be predicted from (1) average dose rate (DR), (2) retention time distributions from dye studies and (3) a known dose-survival curve. For an aliquot of volume Vt entering the reactor at time t_0, the aliquot will exit in n fractions of volumes V_i at time t_i. Survival is a non-linear function (fn) of dose.

22) $\frac{N}{N_0} = \text{fn (dose)}$

where N_0 is the titer before irradiation and N is the titer of survivors after irradiation.

23) The dose of the i^{th} fraction = $(DR)(t_i)$

24) Survival in the i^{th} fraction = $\frac{N_i}{N_0} = \text{fn}[(DR)(t_i)]$

25) Thus the average dose = $\frac{\Sigma(V_i)(DR)(t_i)}{V_t}$

26) The average titer of survivors, $\bar{N} = N_0 \frac{\Sigma V_i(\text{fn}[(DR)(t_i)])}{V_t}$

It can be seen from this equation that if the dose survival curve were linear, the expression could be simplified such that the summation term would be equal to the average dose. However, our curves have been non-linear for effluent samples. Data from a dye study may be put in a form to use in this equation. The area under a curve of absorbance or concentration is set equal to V_t and may be thought of as a 1 ml aliquot entering the reactor. Then,

$$V_i = \frac{(\Delta t)(\text{relative concentration})}{V_t}$$

For a computer computation of the survival, the dose-log survival curve is most easily handled by finding an empirical equation to fit the function or by linear interpolation between several specified intervals.

The previous equations also suggest two methods for measuring dose rate by a bioassay when the titers are known by experiment.

1) One is the injection of the bioassay organism and separate collection of the fractions as a function of time from injection as demonstrated on the lab scale flowthrough reactor. The assayed dose rate can be calculated directly from this method.

2) Accurate dye studies are done. Then a test organism is mixed in the inflowing batch beforehand and the mixed out-flow titer is determined. Numerous values for DR may be used in Equation 26 along with the other data and the values for the effluent titer are plotted vs. the dose rate. Thus the dose rate may be read from the plot from the outflow titer. This approach does not require injection and collections of separate fractions of bacteria but requires an accurate dye study at exactly the same flow rate to which the test organisms are subject. This numerical solution of the equation could even utilize the native coliforms but the lack of dose response of coliforms at high dosages would make them less precise than cultured spores.

EPA Form 2350-4 (4-80)
(PREVIOUSLY EIN: EPA FORM 267)
U.S. GOVERNMENT PRINTING OFFICE 1980-960-639
TYPING GUIDE SHEET

The use of average dose rate in the Equations 22 through 27 depends on the assumption that each particle is exposed to the same average dose rate while traveling through the reactor. We assume that lamps will be distributed and flow will be turbulent such that this assumption will hold.

From our equations, we can also see that a curve of log survival vs. average dose, however calculated for a flowthrough reactor with non-ideal flow, is not a true log survival-dose curve. It can be useful for only that reactor with that specific flow distribution. Systematic changes in the shape of the flow distribution curve as average retention time increases, such as occurred in the Pure Water Systems unit, will also produce additional distortion of a log survival vs. average dose. Thus a plot of coliform density vs. ultraviolet dosage such as appears in Scheible and Bassel (1981) is likely to be useful only for their particular unit with its flow distribution since theoretical retention time was used to calculate dose. Their coliforms appear to be vastly more resistant than the ones tested in our study (Figure 2). This difference may, in large part, be due to the dispersion of flow in their unit and the effects on dose calculation. A curve of log survival vs. average dose is a valuable guide to operation of a particular unit as long as its ambiguities are understood. However, it cannot be used to compare with other units without going back through the corrections outlined above for the effect of dose rate and non-ideal flow.

LAMP SPACING AND EFFICIENT USE OF UV LIGHT

The calculations of average dose rate and average dose rate-volume product, as a function of fluid depth in the collimated beam apparatus, were shown as the simplest illustration of the effect of fluid depth on effective treatment of a volume of water. The relative tradeoffs between average dose rate and volume are summarized by the dose rate-volume product. This measure is the best one to compare the effectiveness of the dose rate regimes of different reactors and different designs. The calculations also show that the advantage of deeper fluid depth is reduced at greater absorbances. The calculations made for the single lamp cylindrical system show the same relationships apply in the cylindrical geometry. These calculations were shown to be valid by the bioassay tests. Figure 21 showed that a small proportion of the light penetrates beyond 5 or 6 cm; thus, obstructions beyond that radial distance would have little effect on efficiency. However, it showed that major obstructions within the radius will significantly affect the efficient use of the UV energy. The extension of these results to actual multiple lamp units is based on the assumption that little light is reflected from the walls of a unit which has been in use, and the fact that neighboring lamps block most light which strikes them. Since surrounding lamps will only intercept a portion of the light emitted from a central lamp, the effect is less marked than for closely spaced walls. Thus the advantage of a large matrix of lamps, such as that used in the Bergen County study, is that less light is lost to the walls compared to smaller units like the Pure Water Systems I-75 and Aquafine CSL-6. The simulations of dose rate in Scheible and Bassel's unit, however, showed that lamp spacing can exert a significant effect on efficient use of all the UV. The simulations were made for their unit rather than either of our small units in order to isolate more clearly the effects of lamp spacing and since the larger array is clearly a better design for large plants than a battery of small units. Some units such as the PWS I-75 unit use even more closely spaced lamps than the Bergen County reactor's 3.55 cm spacing and thus present a more marked reduction in efficient use of UV. However, factors related to flow distribution can be more important in controlling ultimate disinfection efficiency as was shown by our pilot plant studies. It is important that no particles consistently traverse areas of low dose rate. Also, designs which tend to attenuate the flow distribution curve should be avoided. Lamp spacing should take these hydraulic factors into account. Our calculations for the Bergen County reactor indicate that the lamps would interfere with each other less if every other row of lamps were staggered half the 3.55 cm distance between lamps and thus the dose rate-volume product would be improved somewhat. However, if the arrangement led to additional flow dispersion, the arrangement would be less effective.

Use of the concepts we have outlined to compare units is illustrated for the Aquafine CSL-6 and PWS I-75 in Table 20. The average dose rates were calculated by the PSS method for an absorbance of 0 and .17. The thin film PWS unit has a much higher dose rate because the lamps are more closely spaced and the difference is even greater at absorbance .17. However, a much smaller volume of fluid is being exposed in the PWS reactor and the dose rate-volume products of the reactors are very similar. However, the PWS unit uses 46% more lamp wattage and thus the dose rate-volume "efficiency" $[(\mathrm{mW/cm^2})(\mathrm{l})/\text{input wattage}]$ is 31% lower than that of the Aquafine unit. The economic significance of using lamp input wattage in the efficiency term is greater considering the cost of extra lamps and associated equipment than for the cost of power. The dose rate-volume product compares the effectiveness of the dose rate regimes of two reactors but does not take into account differences in non-ideal flow distributions. Given ideal flow, the dose rate-volume product will be proportional to the UV doses given by the two units at any given flow rate. However, the ultimate disinfection differences between the two units were determined by their differences in flow distribution. Even when operated at the same flow rate of 2.87 l/s, the dye peaks exited the Aquafine in 3 sec and the PWS in only 1.4 sec.

PROTECTION OF COLIFORMS BY PARTICLES OF VARIOUS SIZES AND THE EFFECTS OF FILTRATION

The experiment which compared the dose survival curves of samples from which various sizes of particles were removed showed directly that, at high UV doses, survival is largely determined by the protection afforded by particles. The curves of the three filtration treatments appeared to be similar until less than 1% of the coliforms remain. Thus only a small minority of the coliforms were afforded protection by particles. However, at the extreme levels of disinfection required to meet standards, less than .1 or .01% of the original coliforms remain and these appear to be much more

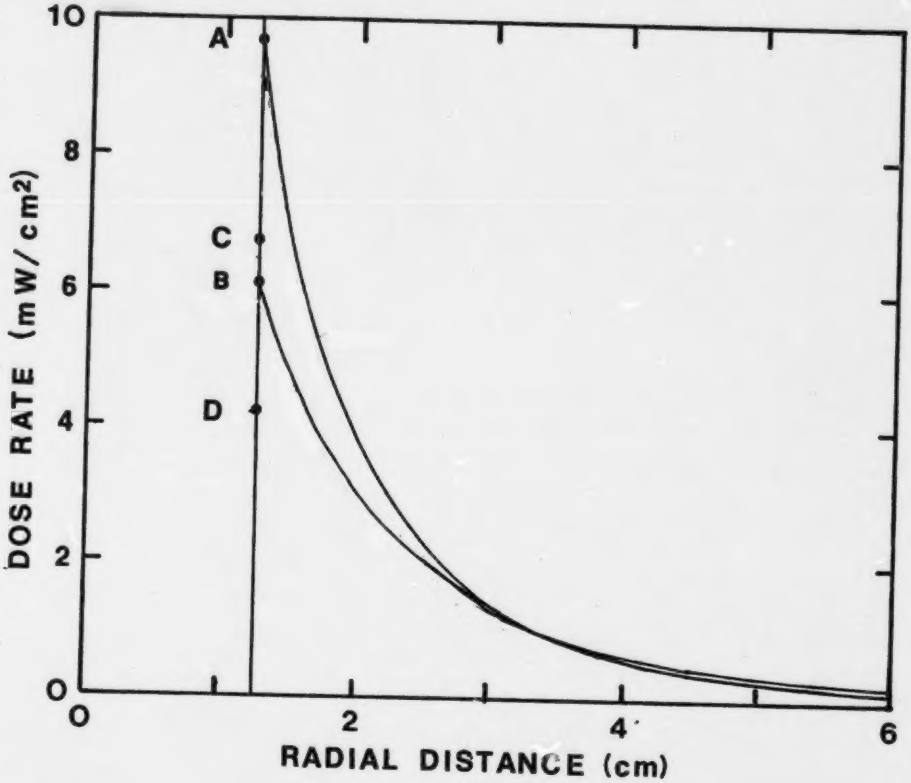

Fig. 34. Comparison of methods for calculation dose rate profiles. Curve A is from the point source summation method. Curve B is from the method used by Schieble and Bassel (1981). Point C is the calculated planar dose rate Point D is the radiometer reading at the radius of the quartz wall. Apparatus and output (35% voltage) as in Fig. 28.

Table 20. Comparison of Aquafine and Pure Water Systems units.

Characteristic	Aquafine	PWS
Number of lamps	6	14
Input watts/lamp	40	25
Effective volume (l)	11	5.82
Length of 1 lamp, effective (cm)	73.7	38.1
Total lamp lengths (cm)	442	533
UV output/cm lamp length (mW)	142	146
UV output, total (W)	62.3	77.8
Average retention time at 2.27 l/s (s)	4.63	2.42
Average retention time at 4.92 l/s (s)	2.32	1.20
Retention time of dye peak[1] (s)	3.0	1.4
Calculated average dose rate:		
absorbance = 0	23.2	39.1
absorbance = .17	9.7	18.5
Dose rate-volume product (mW/cm^2)(l)	107	107
Dose rate-volume "efficiency"[2] [(mW/cm^2)(l)/input wattage]	0.445	0.307

[1] At flow rate of 2.87 l/s.

[2] At absorbance = 0.17.

resistant than the majority. At doses of 15 to 17 mW/sec/cm^2 the particles which could not pass the 70 μ filter accounted for about half a log difference in survival. For the unfiltered sample, there was relatively little dose-response at survivals below -3 logs. The small volume used made it difficult to work below -4 logs survival, but it appears likely that a very large increase in dose to the unfiltered sample would have been necessary to achieve the same disinfection levels obtained by eliminating particles over about 70 μ diameter.

The numbers obtained in the coliform counts are colony forming units. Thus one particle may harbor many bacteria but form only one colony. It may be necessary to kill all the coliforms in the particle to prevent development of a colony.

Experiments of this sort may be performed with smaller increments of filter mesh size and the apparent resistances as a function of particle size could be predicted. A Coulter Counter could then be used on various effluent samples to determine particle size distributions and their survival curves could then be predicted.

These findings are consistent with those of Oliver and Carey (1976) in which ultrasonic treatment apparently broke particles and decreased the UV resistance of the remaining coliforms. Petrasek et al. (1980) also investigated this hypothesis, but their results were somewhat ambiguous.

The experiment also supports the idea that the greater disinfection observed in our dual media filtered pilot plant effluents was caused by removal of some of the suspended particles which harbored protected bacteria. The small differences between UV absorbance in the filtered and unfiltered effluents were not enough to produce a change in average dose rate within the units to account for the differences. The simulated average dose rate within the Aquafine unit as a function of UV absorbance is shown in Figure 35. If we make an approximate correction in the mean absorbances for scattering based on the relationship between turbidity, particulate absorbance and UV scattering in the bioassay experiments, the mean absorbances of the unfiltered and filtered effluent would be .163 and .154 respectively. These absorbances correspond to simulated average dose rates of 9.0 and 9.5 mW/cm^2 respectively. It can be seen from Figure 27 that large changes in dose are needed to produce much response at the low levels of survival. The changes in voltage resulted in an output at 60 V only .59 times that at 128 V and thus the same change in average dose rate. However, these changes usually evoked smaller changes in survival than did the filtration treatments (although response to voltage changes was sometimes inconsistent). The UV radiometer readings at the Aquafine reactor wall showed a larger % difference between the filtered and unfiltered treatment means but, this reading was taken at the reactor wall where the difference in dose rate will be greatest because it represents a greater path length than is reflected in the average dose rate. The PWS unit showed smaller differences between unfiltered and filtered survival. As shown in Figure 27, at the higher levels of survival, the relatively rare protected bacteria play less of a role in controlling survival. In view of this fact and the shape of the dose-survival curves, the greater the levels of disinfection required, the greater the potential effect of filtration on survival. Thus, in considering the relative costs of filtration vs. the costs of increased dosage, the tradeoffs will depend on the number of protected bacteria, the initial titer and disinfection goal.

The dual media filter probably removed varying particle sizes with varying efficiency but probably removed a relatively small percentage of the particles below 70 μ. However, the experimental data show that removal of the particles above 70 μ could account for much of the difference observed in the Aquafine filtration treatments. It must be remembered that the large resistant particles are only a very small percentage of the initial colony forming units (<.1%) and removal of these would probably be statistically undetectable in the unirradiated titers.

Simulation of average survival in a flowthrough reactor

As an example of a simulation of survival in a flowthrough reactor, we simulated runs with the Aquafine reactor. These simulations were then compared to the observed survival in the pilot plant results. The input needed for the model was:

Input:

1) coliform density of inflow (N_0)

2) average dose rate (either measured or calculated)

3) retention time distribution

4) dose-survival curve, (determined in a case where dose is determined accurately, as in the collimated beam apparatus)

Output:

6-1/2"

1) average survival and coliform density of outflow ($\bar{N}$)

The specific input data used were those for the average of the 9 runs for the Aquafine reactor unfiltered effluent at a flow rate of 4.92 ℓ/sec at both the 60 and 128 volt levels. The average dose rate was that calculated by the PSS model using the average absorbance (Figure 35) for each voltage level. The retention time distribution was shown in Figure 15 and was adjusted to the higher flow rate (4.92 ℓ/sec) by multiplying the x-asis by a constant factor. A dose-survival curve was determined in a collimated beam on a sample of Sandy Creek secondary effluent some time after the pilot plant experiments (Figure 36). The average density of survivors, $\bar{N}$, was calculated by computer using equations 22, 23, 24 and 26.

The average log survival predicted by the simulation corresponded reasonably well with that observed in the pilot plant experiments (Table 21). Some deviation should be expected, especially since the dose-survival curve was based on only one sample taken at a later date. Further research should involve simulation using dose-survival curves of samples taken simultaneously with full reactor runs.

Recommendations

We propose the following methods be used to compare different UV reactors. It is essential to separately evaluate the effects of dose rate and reactor volume from the effects of non-ideal flow. The dose rate-volume product is the best measure to compare reactors of different size and flow rates at a given absorbance. It is proportional to the effectiveness of the reactor under ideal flow conditions. In addition, the RTD show always be reported. There is no one measure to simultaneously consider the dose rate-

BEGIN LAST LINE OF TEXT
BOTTOM OF IMAGE AREA, OUTSIDE DIMENSION FOR TABLES AND ILLUSTRATIONS
3/8"

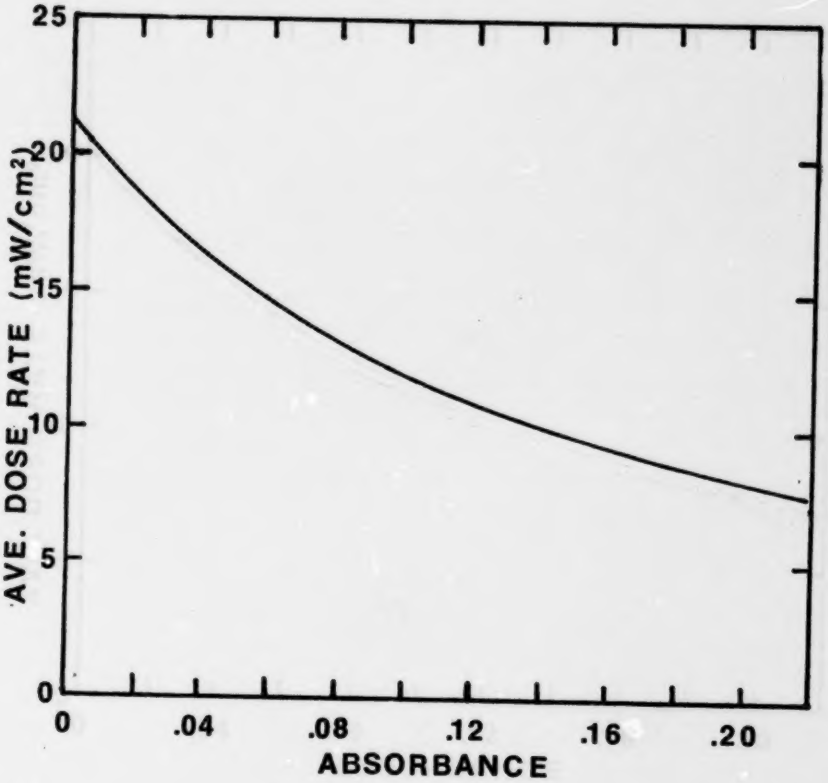

Fig. 35. Simulated average dose rate in Aquafine reactor as a function of absorbance of fluid.

volume product and the effects of non-ideal flow. However comparison may best be made by simulating the average survival using a standard dose-survival curve for coliforms such as that reported here. Reactors of different size could be compared by reporting the flow rate necessary to achieve a 3-log survival (for example) using the standard curve.

We recommend the following procedures be used in UV pilot or demonstration plant research so that results may be generalized within and between studies. Use of a UV radiometer to determine dose rate should be limited to a collimated beam. A radiometer detector situated in reactor wall cannot be used to estimate average dose rate without an accurate empirical determination. A newly installed reactor may undergo a series of calibration runs to prepare accurate dose data for continuous use. Accurate tracer studies

BEGIN LAST LINE OF TEXT
3/8''
BOTTOM OF IMAGE AREA; OUTSIDE DIMENSION FOR TABLES AND ILLUSTRATIONS

PAGE NUMBER
EPA-287 (Cin.)
(4-76)

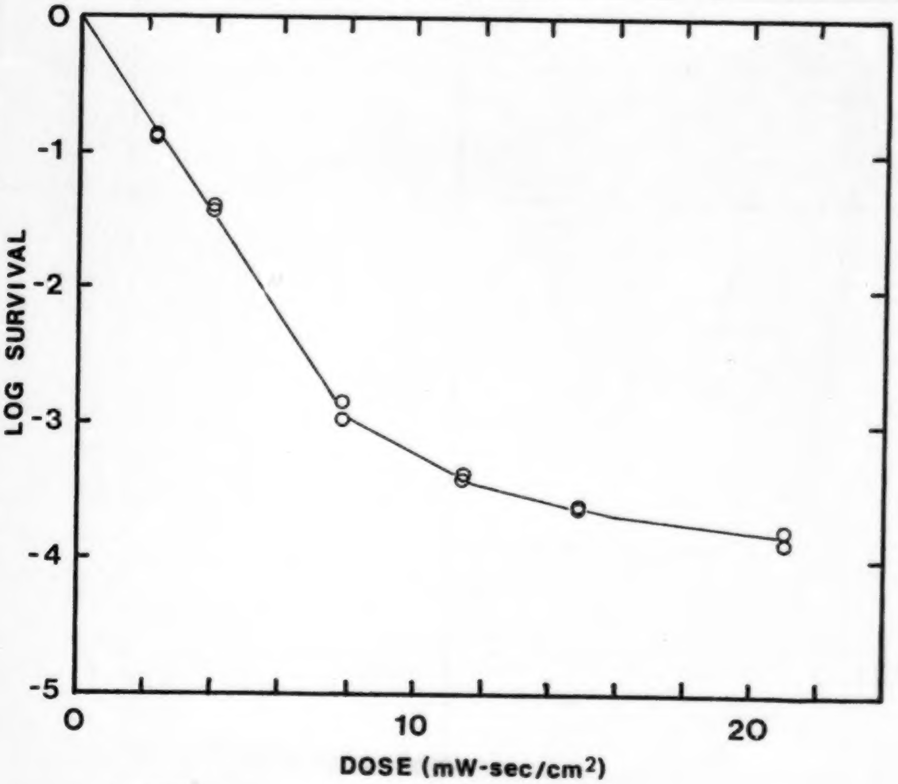

Fig. 36. Dose-survival curve for total coliforms in unfiltered Sandy Creek secondary effluent in a collimated beam.

Table 21. Observed vs. simulated survival(s) of total coliforms in a Sandy Creek 2° effluent

Lamp voltage	Avg. dose rate (mW/cm^2)	Simulated log S	Pilot plant log S
60	6.2	-3.26	-3.29(±.13)
128	9.7	-3.61	-3.69(±.16)

should be done to determine the RTD over the range of flow rates used. Accurate measurements of lamp output as a function of temperature should be performed. Injection bioassay measurements of dose rate should be made at different absorbances. The PSS calculations may be compared with the bioassay and used for interpolation. For continuous monitoring of average dose

BEGIN LAST LINE OF TEXT
BOTTOM OF IMAGE AREA: OUTSIDE DIMENSION FOR TABLES AND ILLUSTRATIONS
3/8"

EPA-287 (Cin.)
(4-76)

rate, empirical curves of average dose rate vs. relative radiometer readings at several points in the reactor for different absorbances may be use. Dose-survival curves on effluent samples should be determined accurately in a collimated beam for comparison with other studies. Curves of average survival vs. average dose under conditions of non-ideal flow can apply only to a particular situation.

If the disinfection of single coliform cells in wastewater under ideal flow conditions is considered as "ideal efficiency", then the results of this report show the following to be the chief factors limiting ideal efficiency in practice: (1) protection of cells inside particles, (2) flow dispersion and poor mixing across dose rate gradients, and (3) shadowing and absorption of UV light by walls within a reactor.

LITERATURE CITED

Aldrich, K. H. 1978. An evaluation of the use of the standard potassium ferrioxalate actinometer to measure dosages in ultraviolet disinfection. Master's thesis, University of North Carolina at Chapel Hill, December.

American Public Health Association. 1975. Standard Methods for the Examination of Water and Wastewater. 14th edition.

Antopol, S. C. and P. D. Ellner. 1979. Susceptibility of Legionella pneumophila to ultraviolet radiation. Applied Envr. Microbiol. 34: 347.

Arthur, J. W., R. W. Andrew, V. R. Mattson, D. T. Olson, G. E. Glass, B. J. Halligan, C. T. Walbridge. 1975. Comparative toxicity of sewage-effluent disinfection to freshwater aquatic life. Ecol. Res. Series, EPA-600/3-75-012.

Banin, A. and N. Lahav. 1968. Particle Size and optical properties of montmorillonite in suspension. Israel J. Chem. 6: 235.

Barrows, W. E. 1951. Light, photometry, and illuminating engineering. 3rd ed. McGraw-Hill, N.Y.

Baxendale, J. H. and N. K. Bridges. The photoreduction of some ferric compounds in aqueous solution. J. Phys. Chem. 59: 783 (1955).

Black, A. P. and S. A. Hannah. 1965. Measurement of low turbidities. J. A.W.W.A. 57: 901.

Bitton, G., Y. Henis and N. Lahav. 1972. Effect of several clay minerals and humic acid on the survival of Klebsiella aerogenes exposed to ultraviolet irradiation. Applied Microbiol. 23: 870.

Boardman, C. D. and O. J. Sproul. 1977. Protection of viruses during disinfection by adsorption to particulate matter. J. Water Poll. Control Fed. 49: 1857.

Bunch, R. L., E. F. Barth, and M. B. Ettinger. 1961. Organic materials in secondary effluents. J. Water Poll. Control Fed. 33:122.

Calkins, J. 1965. A determination of the absorption and scattering of visible and ultraviolet light by six species of protozoa. Applied Spectroscopy. 19: 15.

Carson, L. A. and N. J. Peterson. 1975. Photoreactivation of *Pseudomonas cepacia* after ultraviolet exposure: a potential source of contamination in ultraviolet-treated waters. J. Clinical Micro. 1: 462.

Chambers, C. W. and N. A. Clarke. 1966. Control of bacteria in non domestic water supplies. Adv. Appl. Microbiol. 8: 105.

Cortelyou, J. R., M. A. McWhinnie, M. S. Riddiford and J. E. Semrad. 1954. Effects of ultraviolet irradiation on large populations of certain waterbourne bacteria in motion. I. The development of adequate agitation to provide an effective exposure period. II. Some physical factors affecting the effectiveness of germicidal ultraviolet radiation. Appl. Microbiol. 2: 269, 267.

Cowan, D. O. and R. L. Drisko. 1976. Elements of Photochemistry. Plenum Press, New York.

Cramer, W. N., K. Kawata, and C. W. Kruse. 1976. Chlorination and iodination of Poliovirus and f_2. J.W.P.C.F. 49: 61.

Dean, R. B., S. Claesson, N. Gellerstedt and N. Bowen. 1967. An electron microscope study of colloids in wastewater. Environ. Sci. Tech. 1: 147.

Elliott, M. E. 1978. Studies on photoreactivation in ultraviolet disinfected secondary wastewater effluents. Master's thesis, University of North Carolina at Chapel Hill, December.

Flynn, M. P. 1979. The effects of turbidity on ultraviolet disinfection of secondary wastewaters. Master's thesis, University of North Carolina at Chapel Hill, December.

Frobisher, M. 1962. Fundamentals of Microbiology, 7th edition. W. B. Saunders Co.

Gates, F. L. 1929. A study of the bactericidal action of ultraviolet light. II. The effects of various environmental factors and conditions. J. Gen. Physiology 13: 249.

Gilcreas, F. W. and L. DeLalla. 1953. Application of ultraviolet ray sterilization to water treatment. J.N.E.W.W.A. 67: 130.

Grunau, J. A. 1978. The ultraviolet sensitivity of *Klebsiella pneumoniae* as a function of growth rate. F.E.M.S. Microbiology Letters 4: 47.

Haas, C. N. and G. P. Sakellaropoulos. 1979. Rational analysis of ultraviolet disinfection reactors. Proceedings National Conference on Environmental Engineering, Amer. Soc. Civil Engineers: 540.

Hatchard, C. A. and C. A. Parker. 1956. A new sensitive chemical actinometer. II. Potassium ferrioxalate as a standard chemical actinometer. Proc. Royal Soc. London A. 235: 518.

BEGIN LAST LINE OF TEXT
BOTTOM OF IMAGE AREA; OUTSIDE DIMENSION FOR TABLES AND ILLUSTRATIONS
3/8"

Heukelekian, H. and J. L. Balmat. 1959. Chemical composition of particulate fractions of domestic sewage. Sewage and Indust. Wastes 31: 413.

Hill, W. J., F. E. Hamlet and E. W. Akin. 1967. Survival of poliovirus in flowing turbid seawater treated with ultraviolet light. Appl. Micro. 15: 533.

Hill, W. J., Jr., F. E. Hamblet, and W. H. Benton. 1969. Inactivation of poliovirus type I by the Kelley-Purdy ultraviolet seawater treatment unit. Appl. Micro. 17: 1.

Hoathers, R. C. 1955. The penetration of ultra-violet radiation and its effects in waters. J. Inst. Water Engr. 9: 191.

Huff, C. B., H. F. Smith, W. D. Broing, and N. A. Clarke. 1965. Study of ultraviolet disinfection of water and factors in treatment efficiency. Public Health Reports 80: 695.

Hunter, J. V. and H. Heukelekian. 1965. The composition of domestic sewage fractions. J. Water Poll. Control Fed. 37: 1142.

Jacob, S. M. and J. S. Dranoff. 1970. Light intensity profiles in a perfectly mixed photoreactor. Am. Inst. Chem. Eng. J. 16: 359.

Jagger, J. H., T. Fossum and S. McCaul. 1975. Ultraviolet irradiation of suspensions of micro-organisms: possible error involved in the estimation of average fluence per cell. Photochem. Photobiol. 21: 379.

Jagger. 1967. Introduction to research in UV photobiology. Prentice-Hall, Inc., N. J.

Jepson, J. D. 1968. Some notes on ultraviolet disinfection of small rural water supplies. Water Treat. Exam. 3: 205.

Johnson, J. D., K. Aldrich, D. E. Francisco, T. Wolff and M. Elliott. 1978. UV disinfection of secondary effluent. In: Progress in Wastewater Disinfection Technology. Proceedings of the National Symposium, Cincinnati, Ohio. September 18-20. p. 108. U.S.E.P.A. 600/9-79-018.

Jolley, R. L., N. L. Lee, W. W. Pitt, Jr., M. S. Denton, J. E. Thompson, S. J. Hartmann and C. I. Mashni. 1979. Effects of chlorine, ozone, and ultraviolet light on nonvolatile organics in wastewater effluents. In: Progress in Wastewater Disinfection Technology. Proceedings of the National Symposium, Cincinnati, Ohio. September 18-20, 1978. U.S.E.P.A. 600/9-79-018.

Kase, K. R. and W. R. Nelson. 1978. Concepts of Radiation Dosimetry. Chapter 5. Pergamon Press, N. Y.

Kelley, C. B. 1961. Disinfection of seawater by ultraviolet radiation. Amer. J. Public Health. 15: 1670.

Koch, A. L. 1961. Some calculations on the turbidity of mitochondria and bacteria. Biochim. Biophys. Acta 51: 429.

Knapp, W. G. 1959. Modified 4,7-Diphenyl-1,10-Phenanthroline method sensitive to 1 ppb of iron in high purity water. Anal. Chem. 31: 1445.

Latimer, P. and C. A. H. Eubanks. 1962. Absorption spectrophotometry of turbid suspensions: A method of correcting for large systematic distortions. Arch. Biochem. Biophys. 98: 274-285.

Levinson, H. S., et al. 1972. Distribution and correlation of events during thermal inactivation of Bacillus megaterium spores. J. Bact. 108: 111.

Luckiesh, M. and L. L. Holladay. 1944. Disinfecting water by means of germicidal lamps. Gen. Electric Rev. 47: 45.

Luckiesh, M. and A. H. Taylor. 1946. Transmittance and reflectance of germicidal (λ 2537) energy. J. Opt. Soc. Amer. 36: 227.

Manka, J., M. Rebhun, A. Mandelbaum and A. Bortinger. 1974. Characterization of organics in secondary effluents. Envr. Sci. and Tech. 8 : 1017-1023.

Morowitz, H. J. 1950. Absorption effects in volume irradiation of microorganisms. Science 111: 229-230.

Morton, R. A. and R. H. Hayes. 1969. Changes in the ultraviolet sensitivity of Escherichia coli during growth in batch cultures. J. Bact. 97: 1374.

Morris, E. M. 1972. The practical use of ultraviolet radiation for disinfection purposes. Med. Lab. Technol. 29: 41.

Munikata, N. 1974. Ultraviolet sensitivity of Bacillus subtilis spores upon germination and outgrowth. J. Bact. 120: 59.

Oliver, B. G. and J. H. Carey. 1976. Ultraviolet disinfection: an alternative to chlorination. J.W.P.C.F. 48: 2619.

Oliver, B. G. and E. G. Cosgrove. 1975. The disinfection of sewage treatment plant effluents using ultraviolet light. Can. J. Chem. Engr. 53: 170.

Oster, G. and A. W. Pollister (eds.). Physical techniques in biological research. Vol. I, Optical techniques. Academic Press, Inc., New York.

Oster, G. 1948. The scattering of light and its applications to chemistry. Chem. Rev. 43: 319.

Petrasek, A. C., H. W. Wolf, S. E. Edmond, D. C. Andrews. 1980. Ultraviolet disinfection of municipal wastewater effluents. E.P.A.-600/2-80-102, 262 pp.

Piecuch, Peter. 1974. The chlorination controversy. J.Water Poll.Control Fed. 46:2637.

Powers, E. L., M. Cross, and C. J. Varga. 1974. A dose rate effect in the ultraviolet inactivation of bacterial spores. Photochem. Photobiol. 19: 273.

Presnell, M. W. and J. M. Cummins. 1972. Effectiveness of ultraviolet radiation units in the bacterial treatment of seawater. Water Res.: 1203.

Richert, D. A. and J. V. Hunter. 1967. Rapid fractionation and materials balance of solids fractions in wastewater and wastewater effluents. J. Water Poll. Control Fed. 39: 1475.

Richert, D. A. and J. V. Hunter. 1972. Colloidal matter in wastewaters and secondary effluents. J. Water Poll. Control Fed. 44: 134.

Rockwell, T. 1956. *Reactor Shielding Manual*. Van Nostrand, Princeton, N. J.

Roeber, J. A. and F. M. Hoot. 1975. Ultraviolet disinfection of activated sludge effluent discharging to shellfish waters. E.P.A. 600/2-75-060, 85 pp.

Rude, J. and T. Alper. 1972. Changes in UV survival curves of *Eschericia coli* B/r concomitant with changes in growth conditions. Photochem. Photobiol. 15: 51.

Scheible, O. K. and C. D. Bassell. 1979. Ultraviolet disinfection of a secondary wastewater treatment plant effluent. Project Summary E. P. A. 600/2-81-152.

Severin, B. F. 1978. Disinfection of municipal wastewater effluents with ultraviolet light. J. Water Poll. Control Fed. 52:2007.

Sharp, D. G. 1938. A quantitative method of determining the lethal effect of ultraviolet light on bacteria suspended in air. J. Bact. 35: 589.

Shibata, K., A. A. Benson and M. Calvin. 1954. The absorption spectra of suspensions of living micro-organisms. Biochim. et Biophys. Acta 15: 461.

Simons, J. P. 1971. Photochemistry and spectroscopy. John Wiley, N. Y.

Singer, M. and N. Nash. 1979. Ultraviolet disinfection of a step aeration effluent. J. Water Poll. Control Fed. 16: 9.

Standard Methods for the Examination of Water and Wastewater. 1975. 14th edition. A.P.H.A.-A.W.W.A.-W.P.C.F.

Stiff, F. R. 1971. The disinfection of industrial and potable water supplies using ultraviolet radiation. Chem. and Ind. 1: 116.

U. S. Environmental Protection Agency. 1974. Manual of methods for chemical analysis of water and wastes.

Ward, R. W. and G. M. DeGraeve. 1978. Residual toxicity of several disinfectants in domestic wastewater. J.W.P.C.F. 50: 46.

White, G. C. 1972. Handbook of Chlorination. Van Nostrand Reinhold Co., New York, N. Y. p. 697.

Westlake, D. F. 1965. Some problems in the measurements of radiation under water: a review. Photochem. Photobiol. 4: 849.

Witherell, L. E., R. Solomon and H. M. Stone. 1968. A demonstration project to determine the feasibility of using ozone and ultraviolet radiation disinfection for small community water systems. E.P.A. Report No. 68-03-2182.

Yip, R. W. and D. E. Konasewich. 1972. Ultraviolet sterilization of water -- its potential and limitations. Water and Poll. Control (Canada) 110: 6.

Zelle, M. R. and A. Hollaender. 1955. Effects of radiation on bacteria, pp. 365-430. I. Hollaender (ed.), Radiation Biology. Vol. 2, Ultraviolet and related radiations. McGraw-Hill, N. Y.